THE ANALYSIS OF SPATIAL-TEMPORAL DYNAMICS OF URBAN LANDSCAPE

STRUCTURE: A COMPARISON OF TWO PETROLEUM-ORIENTED CITIES

DISSERTATION

Presented to the Graduate Council of
Texas State University-San Marcos
in Partial Fulfillment
of the Requirements

for the Degree

Doctor of PHILOSOPHY

by

Junmei Tang, M.S.

San Marcos, Texas
May 2007

THE ANALYSIS OF SPATIAL-TEMPORAL DYNAMICS OF URBAN LANDSCAPE

STRUCTURE: A COMPARISON OF TWO PETROLEUM-ORIENTED CITIES

Committee Members Approved:

Le Wang, Ph.D., Chair

F. Benjamin Zhan, Ph.D.

Mark A. Fonstad, Ph.D.

Jiaguo Qi, Ph.D.

Approved:

J. Michael Willoughby
Dean of the Graduate College

TABLE OF CONTENTS

Page

LIST OF TABLES

LIST OF FIGURES

ABSTRACT

THE ANALYSIS OF SPATIAL-TEMPORAL DYNAMICS OF URBAN LANDSCAPE

STRUCTURE: A COMPARISON OF TWO ENERGY-ORIENTED CITIES

by

Junmei Tang, B.S., M.S.

Texas State University-San Marcos

May 2007

SUPERVISING PROFESSOR: LE WANG

This dissertation integrates remote sensing, spatial metrics, and urban modeling to map, compare, and model the urban process in two petroleum-oriented cities, Houston in the United States and Daqing in China. The primary objective of my research is to understand the relationships between the human behavior and natural environments under different socio-political contexts at a regional scale. Accordingly, there are two major research foci in this dissertation: 1) improving the accuracy of remote sensing classification in the highly fragmented urban landscapes, especially the human land use classes such as the residential area and the industrial/commercial area; and 2) testing the utility of sub-pixel information for a self-organized model towards a framework to

support and improve urban modeling. Although a variety of studies have focused on the

urban remote sensing and urban modeling, this research is the first investigation on the

relationship between sophisticated remote sensing techniques and urban process models

within socioeconomic dimensions. The results of this study provide evidences on the

threatened natural landscape and environment deterioration during the urbanization

processes in two petroleum-oriented cities and suggest that the utility of sub-pixel

techniques improves the accuracy of both mapping and modeling in urban research

through the cost effective satellite imagery.

CHAPTER I

INTRODUCTION

Problem Statement

Approximate 70% of the population in developed counties and 50% of the worldwide population live in urban areas. As a result of human behavior, the natural environmental in these areas have evolved into an urban landscape with modified ecological processes (IGBP 1988). These landscapes now represent one of the greatest challenges in environmental, economic, social, political, and cultural research. Urban landscape also provides numerous challenges for urban planners, civil engineers, environmentalists, sociologists, economists, and even remote sensing scientists (Mesev 2003).

Rapid urbanization, as the result of population growth and migration from rural to urban areas, has been recognized as a critical process in metropolitan areas. It changes both the structure and function of our cities (Frank 1999). Rapid urbanization also affects the climatology of cities and their surrounding areas (Orville et al. 2000). These changes have a direct, immediate, and significant impact on human settlements (Douglas 1994), ecological diversity (Grove and Burch 1997), energy flows (Breuste et al. 1998), and climatic conditions (Orville et al. 2000) from local to regional scales. The need to understand urban evolution and preserve the natural resources has culminated in

1

analyzing the urban process over a medium or long term (Ward et al. 2000). To analyze

the structure, function, and dynamics of urban systems, we need to link the landscape

pattern with its processes (Geoghegan et al. 1998). Current studies were seldom able to

ascertain how urban landscape patterns affected natural ecosystem processes. However,

the increasing awareness of the importance of sustainability in natural resources is

stimulating the improvement of current methods to better understand and quantify the

causes and consequences of urban landscape evolution (Turner 1987).

To understand and predict urban change processes, we need to monitor and

characterize their spatial landscape patterns by observing them at different states in time.

Essentially, it involves the ability to quantify the pattern change using multi-temporal

data sets (Singh 1989) and incorporate this information into appropriate landscape

models. In the early days, aerial or field surveys were commonly used to produce land

use maps to serve the planners' needs (Zhang et al. 2002). These aerial or field methods

are easy-to-use in describing land use / land cover processes through a detailed and

spatially-disaggregated way (Petit et al. 2001; Tang et al. 2005). However, these manual

interpretations are labor intensive, and unable to detect the spatial patterns at the

landscape scale and grasp changes that occurred over a long period of time (Nelson

1983).

Remote sensing data, in conjunction with geographic information systems (GIS),

has been recognized as an effective tool in quantitatively measuring landscape patterns

and their changes over a large area in a timely and cost-effective manner (Nelson 1983;

Singh 1989; Metzger and Muller 1996; Frohn 1998; Quattrochi and Luvall 1999; Roy

and Tomar 2001; Petit et al. 2001). Images from satellite sensors provide a large amount

of cost-effective, multi-spectral and multi-temporal data to monitor landscape processes and estimate biophysical characteristics of land surfaces (Weng 2002). GIS technology provides a flexible tool with which to store, analyze, and model the digital data for the detection of change and the development of model. Significant progress in acquiring remotely sensed data in a higher spatial resolution and developing the spatial geographic process model using GIS technique has widened our research on the process, driving-forces, and impacts of urbanization.

Although remote sensing has been widely applied in providing the knowledge of where, how much, and what kind of landscape change has occurred, considerable uncertainty continues to exist in the quality and scope of spatial data for landscape models. There is still a large research gap between the sophisticated remote sensing, GIS techniques, and landscape process modeling. In particular, we need more standardized methods for incorporating high quality remote sensing data into the urban process model, not only for the further analyses of urban pattern and dynamics, but also for finding a better way to determine the parameters in the model's development, calibration, and validation. Thus, there is an urgent need for us to determine the potential of spatial data and find an innovative method to incorporate this potential into a real landscape dynamic model.

<div align="center">Study Objectives and Research Design</div>

This dissertation is the first systematic study of urban landscape dynamics in two petroleum-oriented cities, Houston, Texas in the United States, and Daqing, Heilongjiang in China. Although these two cities have a similar domain industry and economic history,

they developed under different socio-political contexts. Building on my pre-dissertation research, I will investigate the landscape structure, urban growth, and environmental change along with the fast-growing petroleum industry.

The general objective in this dissertation is to combine remote sensing, GIS, and landscape ecology models to compare the landscape pattern in these cities and predict their future patterns. The lack of high quality data on a large scale has limited the application of landscape process models for urban forecast. Moreover, the accuracy of such models depends both on the data source and on the defined relevant parameters. Specifically, after comparing Houston and Daqing, I will develop a new sub-pixel classification to analyze the internal structure in Houston and apply the sub-pixel results into a fuzzy logic Cellular Automaton (CA) model. In order to verify this new model, I will also develop a traditional CA model based on the hard classification and compare the hard model results with the soft model results.

The general framework in this research is threefold (Figure 1). First, I will conduct a multi-temporal landscape classification with satellite imageries in Daqing and Houston. With that information, I will perform an in-depth quantitative urban analysis based on the landscape ecology method to link the physical pattern change with the urban growth drivers. The sub-pixel classification will be developed specifically for Houston since it has a more heterogeneous pattern than Daqing. Lastly, I will predict the future landscape pattern in these two cities. Based on the fuzzy logic laws, I also develope and calibrate the spatiotemporal model through the fuzzy data source from remote sensing. Theoretically, the urban pattern / process analysis will provide complementary

information regarding the ecological function of urban landscape and consummate the analysis on the spatial-temporal modeling.
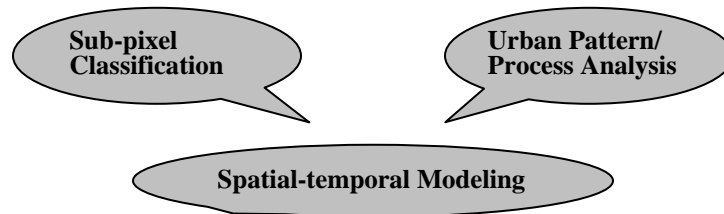
Fig. 1. General framework of this research

Specifically, my research will focus on three critical questions:

o What are the current landscape patterns of Houston and Daqing? In what particular ways did the landscapes in these cities change during the urbanization? What factors have caused them difference from each other given their similar nature of petroleum-based cities?

o What are the future patterns of these two cities? What are the major human drivers shaping these two cities, and could they be incorporated into the urban dynamics models?

o How can I incorporate a finer sub-pixel classification in the cell-based model, and will this incorporation really improve the accuracy in the landscape model?

My hypothesis is that both cities are experiencing environmental deterioration during the urban sprawl, and the development of petroleum industry is still the dominant factor in steering urban landscape dynamics. We will test the following hypotheses:

o Theoretically, urban patterns in these two cities have experienced significant changes over the last two decades. Specifically, natural landscapes were

substituted gradually by human landscapes due to the urban sprawl. As a refinery center, Houston does not have the oil field in its urban area. Thess different economic modes in these two cities lead to different change types and manners during their urbanization.

o Technically, the sub-pixel classification will improve not only the pattern analysis in urban areas, but also the capability of urban landscape models. Through incorporating sub-pixel information into the cell-based model, we can derive a more sophisticated urban landscape process model.

The general framework of this dissertation follows the structure of Figure 1. Chapter II focuses on the review and discussion of theoretical background, and Chapter III introduces the study sites and data preprocessing. Chapters IV, V, and VI represent the cores of this dissertation. They correspond to the three sections in Figure 1, reflecting three individual research tasks accomplished within this research. Chapter VII includes the summary and potential research.

Contribution and Significance of This Research

We will investigate spatial and temporal patterns of urban landscape change through synthesizing remotely sensed data with both landscape ecology methods and urban dynamic models. The direct beneficiaries of this research will include two distinct groups: (1) resource managers at the local, regional and state levels of government, and (2) urban planners who want better urban planning in broader social and economic settings.

The primary significance of this research falls into three aspects:

o This research is the first systematic comparison of landscape dynamics in two petroleum-based cities. My research will provide a better understanding of the relationship between urban morphology and human behavior and a better conceptual and scientific framework to quantify the interaction between human and social environments on a regional scale.

o This research also provides an advanced soft classification for urban areas. The primary significance of this research lies in identifying the heterogeneous urban landscapes under the pixel level. It offers additional scientific evidence to the ongoing remotely sensed analysis on the urban growth and environmental quality monitor.

o More significantly, it provides a geographically referenced model using the sub-pixel information which is derived from the soft classification. My research attempts to standardize methods in incorporating sub-pixel information into a cell-based landscape process model and to find a better way to determine the parameters in the model's development, calibration, and validation. This will provide a bridge study between the advanced remote sensing techniques and landscape process model.

CHAPTER II

THEORETICAL CONSIDERATIONS AND LITERATURE REVIEW

In general, urban area can be described as a physical concentration of people and buildings in a wide variety of social, economic, political and cultural contexts (Herbert and Thomas 1982). Not surprisingly, many current pressing social, political, and economic problems are associated with cities and their growth. Traditionally, geographers have been concerned with long-term issues on spatial topics such as the spatial layout of transport facilities, the location of industry or service activities, and the interactions of environment and society (Herbert and Johnston 1979). That is, the concern of urban geographers is the space organization within the urban context.

Traditional Urban Geography and its Emphases

The first urban study was developed in the late nineteenth and early twentieth centuries, the years social science first formed. This overlay provided the context for geographers' emerging interest in cities (Berry and Frank 1970). Early urban studies were mostly descriptive and centered on physical appearances and subjective impressions of urban places. The most influential research was the early theory on city location, such as Cooley (1894) and Weber (1899), who touched on the importance of urban centers for urban development, especially for the route way and the transportation system. Hassert

(1907) and Blanchard (1917) pioneered the study on the site and situation of towns and cities, emphasizing that the urban character was the response to local physical conditions.

With more complex urban structures appearing in the early twentieth century, some cities, of course, displayed neither a rank-size nor a primary pattern. Urban researchers tried to find the reason for differences among cities, asking whether the classification of internal urban structure could be associated with the urban size. These questions have stimulated the research on the urban pattern and function (Johnston 1984). Haig (1926) noted that house payments and the accessibility of transportation could be involved in a bidding process determining the occupancy and the use of urban land. Crowe (1938) used town studies as an example of objects' classification upon the urban landscape, rather than upon people and movement.

Stepping into the early 1960s, interests in urban geography shifted significantly toward the social aspect of cities (Herbert and Thomas 1982). Associated with the increasing influence of spatial analysis, this shift gave quantification and model-building a new and vigorous platform. The typical research at that time included the classification of settlements (Smith 1965), examination of urban population sizes (Berry and Garrison 1958), and analysis of population densities within cities (Berry, Simmons, and Tennant 1963). These studies focused on the internal urban structure or the gradient land value and land use types (Yeates 1965).

A further development within urban geography was the interest in spatial imageries and cognitive mapping. The key reference of the early image study is Boulding's (1956) work on images of urban life and society which has become central to many later geographical works. Given the external socialization condition and the

internal value, Boulding (1956) defined the image as a picture that carries reference

points for actors' behavior. For many urban geographers, images formed the link

between the phenomena and the behavioral environment (Herbert and Thomas 1982).

However, technical procedures were still limited in representing detailed urban

distributions though images and maps have served largely to qualify spatial entities such

as urban structure and its neighborhoods.

To date, many works by urban geographers relate to the sophisticated description

of *patterns, processes, and responses* of cities. The study of urban patterns remains a

traditional concern in urban geography, while the process and response further investigate

what and how patterns will appear in the future (Herbert and Thomas 1982). Spatial

analysis, quantitative measurement, and modeling, with the essential geographers'

descriptive methods, gradually broadened their research fields. Some important efforts in

understanding and representing urban spatial structures and dynamics have been triggered

by the fields of urban modeling and remote sensing. This research agenda will be

discussed in following sections.

Urban Pattern, Process, and Response

Classic Theories and Models

Geographic research in interpreting and analyzing internal differentiations of

cities within the last century has resulted in developing a variety of classic urban theories.

According to the economic base of urbanization, we can divide early urban development

theory into three aspects: *trade, location, and staple* (Berry and Frank 1970).

Early movements of goods among nations and regions made cities grow in different ways. Urban geographers found that the difference in urban structure was caused by special products. Ohlin (1933) assumed that qualities and functions of the production in one region are identical, attributing relative advantages of productivity to different "factor endowments" in the urban development. Heckscher (1949), on the other hand, tried to find regional differences in the function of productions based on this theory. The above two studies provided a satisfactory basis to explain the difference among regions, however, they failed to account for effects of urban changes. Other theories must be sought out to provide more general frameworks for the urban growth.

The *location theory* was developed out of a need to explain and predict locations of urban entities by rationalizing the "survival of the fittest" theory. The most popular work is the *central place theory*, proposed by German economists / geographers Walter Christaller and August Lösch. Christaller (1933) first developed this theory based on the size and distribution of settlements in the southern area of Germany with an assumption that both entrepreneurs and consumers made rational decisions in minimizing transport costs. Thus, urban structure is characterized by the business type, the maximum distance from a customer to the grocery store, and the threshold volume to operate the business. The ideal urban pattern predicted in this theory is a hierarchical spatial system of nesting hinterlands on a hexagonal frame. Lösch (1954) studied a more complex example with a consideration on the assumptions about the business type.

The *staple (export) theory* was developed for problems existing in settlements of undeveloped regions. In this theory, size and function of a city were affected by a given industry and the land use characteristic of this industry. Other land use types, such as

retail shops and service centers, were secondary since they existed only to serve workers

employed in staple industries (Fox and Kumar 1966). Thompson (1965) argued that the

growth rate in a large city is self-sustained and the urban hierarchical structure will be

filtered down from the center to the periphery by exploiting new industry staples. Thus,

according to the staple theory, cities are developed continually from new staple industries

accompanying the "filtering down" and "diffusing outward" of older staple industries.

One characteristic of modern cities is their high level of internal differentiations.

A number of models have been developed by urban geographers to understand urban

spatial structures. Thünen (1826) first developed a basic analytical model between

markets, productions, and distances to analyze agricultural land use patterns in Germany.

The earliest urban spatial model, *concentric-zonal model*, was proposed by Burgess from

an ecologist's view. Founded on economic bases of land values and bid-rents, Burgess

(1925) suggested a five-zone arrangement of land use as concentric circles in Chicago

(Figure 2A). These zones began with the city center, namely Central Business District

(CBD), as zone 1. This zone was surrounded by concentric rings of commercial and

residential land uses, which were also known as transition or gray zones (zone 2) between

the commercial core and residential communities. Following the transitional zone is the

zone of working-men's homes (zone 3) consisting of older residential buildings for low-

income working-class families, and then the residential zone (zone 4) occupying newer

and more spacious dwellings for middle-class families. Finally, the commuter's zone

(zone 5) lies beyond the continuous built-up areas of the city. Although this model is

crude and unrefined, it provided an empirical framework to test the urban spatial structure

and a detailed example to study land use areas within a city.
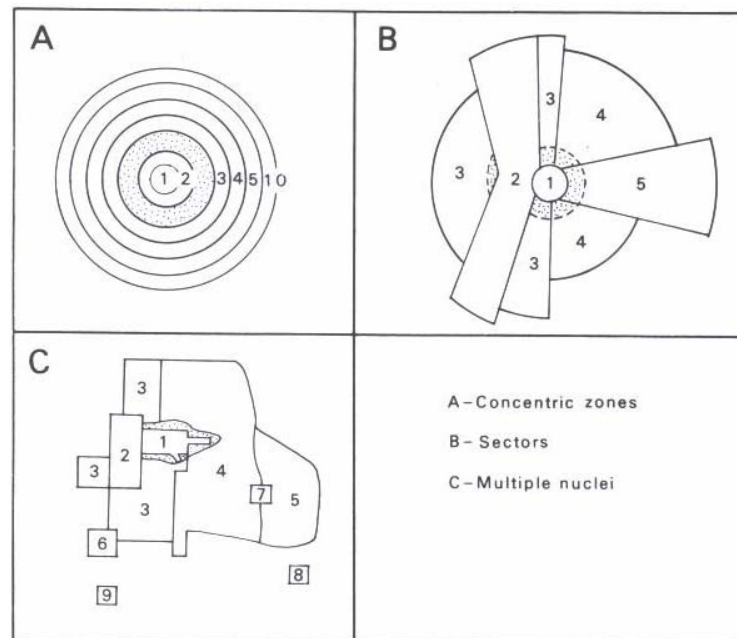
Fig. 2. Three classic spatial city models: A. concentric-zonal model (Burgess 1925); B. sector model (Hoyt 1939); and C. multiple nuclei model (Harris and Ullman 1945)

The *sector model* of urban land use was formulated by a land economist Hoyt in 1939 (Figure 2B). Through the rental and other data in block level for 142 American cities, Hoyt (1939) argued that residential areas were not aligned concentrically along the city center, but rather were distributed in a sector fashion along major roadways from the CBD. This model is normally regarded as the second classic model of urban spatial growth since it considered specific characteristics, location, and dynamics of different urban land use categories. Hoyt's view of cities is partial, constrained by his narrow observation on housing characteristics, particularly in rent, with little consideration for the occupants.

The third classic model, termed as *multiple nuclei model*, was developed by two geographers, Harris and Ullman (1945). Its main distinctive quality was its abandonment

of CBD as a sole focal point, replacing it by a number of discrete nuclei around which individual land uses were geared (Herbert and Thomas 1982). This model has no generalized spatial form since the location of nuclei may depend on the unique location and function.

In general, merits of these classic spatial models are their basic structure concepts, especially the zone and sector. These concepts continue to have useful roles in organizing city structure and testing some general theories in urban geography. Whatever the detail-functional characteristic of a city, its internal spatial structure will be organized around the concentration of employment opportunities, service facilities, and their associated land uses (Herbert and Thomas 1982). Moreover, it is not necessarily contradictory to use these spatial models in one city to measure different areas or aspects. This complementary idea is more practical in real cities.

The urban growth during the 1950s - 1970s generated a significant research contribution and raised compelling questions regarding more detailed urban infrastructures. Given the complex structure and function of a city in the real world, early classic models became unrealistic for representing and predicting urban patterns and dynamics. This prompted the need for a more spatially explicit model with more detailed spatial data.

Sensing Urban Landscapes Remotely

Remote sensing is the science and art of obtaining information from an object, area, or phenomena through the analysis of data acquired by a device that is not in contact with the object, area, or phenomena (Lillesand, Kiefer, and Chipman 2004).

Given the diverse assemblage of materials in urban landscapes and recent developments in sensors and computing technology, the application of remote sensing as a tool for mapping and monitoring urban areas increased greatly. However, the operational potential of urban remote sensing will depend on the capacity of remote sensing to capture objects in urban areas and how to interpret urban areas by remote sensing, namely, *data demands for mapping urban areas* and *attempts to enhance urban classifications*.

Data Demands for Mapping Urban Areas

From the historical remote sensing perspective, the first use of remote sensing in urban areas dates back to 1858, when Gaspard Felix Tournachon (also known as "Nadar") used a camera carried aloft by a balloon to study the city of Paris (Forster 1983). His "bird-eye" photograph of the village of Petit Bicetre is the world's first aerial photograph, in which houses can be clearly seen from approximately 260 feet.

Since then, especially after the Second World War, the increasing awareness of image potential for identifying and classifying urban spaces brought about a dramatic development of remote sensing in urban areas. Until the early seventies, aerial photography, in both black-and-white and multi-spectral bands, was still the mainstream in urban remote sensing. Green (1957) applied the interpreted data from the black-and-white aerial photography to extract socio-economic parameters for cities. Wellar (1968) used nine spectral bands of a large scale aerial photography to evaluate the quality of houses and neighborhood environment. More recently, Collins and El-Beik (1971) further extended the use of aerial photographs to real world problems through acquiring the

information in urban land use of Leeds, Great Britain. Indeed, this form of remote sensing is still extensively used today. Notwithstanding, the aerial photograph is easy-to-use in describing the land cover / land use information of urban areas, they are high in cost and not available in digital formats (Yagoub 2004). Moreover, such images are labor intensive and unable to discover spatial patterns at the landscape scale and grasp changes that occurred over a long time frame.

The 70s and early 80s saw a gradual shift of urban remote sensing from aerial photograph to digital, multispectral images, particularly those acquired by earth-orbiting satellite sensors (Donnay, Barnsley, and Longley 2001) because of their widespread availabilities and high frequency in updating with low costs. The land use study on the boundary region of Texas and New Mexico is a typical urban analysis performed by MacPhail and Campbell (1970) using spacecraft photographies from Gemini 4, Apollo 6, and Apollo 9. This trend of applying satellite remote sensing data, especially in the urban land use/land cover classification, was reinforced with the first generation of satellite sensors, notably the Landsat Multispectral Scanning System (MSS). This gave further impetus by a number of second generation devices, such as Landsat Thematic Mapper (TM) and SPOT High Resolution Visible (HRV). The earliest research using Landsat data in urban areas was reported by Erb (1974) to detect land use classes through both unsupervised and supervised clustering techniques. Using satellite data, Cater et al. (1977) classified the urban land use into a more detailed system: large building, strip cluster development, single-family residential area, and multiple-family trailer court.

The development of non-photographic remote sensing systems, such as thermal infrared and their application to urban area has generally paralleled to that of advanced

photographic techniques in spatial resolution. The most commonly used thermal remote sensing data in urban area includes infrared bands on Landsat TM 4, 5 and 7, Advanced Very High Resolution Radiometer (AVHRR) on the National Oceanic and Atmospheric Administration (NOAA), Thermal Infrared (TIR) subsystems under the Advanced Spaceborne Thermal Emission and Reflection Radiometer (ASTER) spaceborne sensor. Instead of detecting the urban structure, thermal infrared bands are mostly applied to detect the thermal attribution on the presence of a urban heat island (Quattrochi and Ridd 1994; Chrysoulakis and Cartalis 2002).

Hyperspectral remote sensing is another important data source for urban observation, providing a large amount of contiguous spectral detail. Hepner et al. (1998) used the Airborne Visible Near Infrared Imaging Spectrometer (AVIRIS) to compare the spectra of different urban land cover types. Herold et al. (2004) developed a spectral library to identify urban land cover using AVIRIS on Santa Barbara and Goleta. Another popular hyperspectral sensor carried on satellite is MODerate resolution Imaging Spectroradiometer (MODIS) with enhanced spectral mapping capabilities. It has shown an improved capability in assessing the net primary productivity in urban areas at a continental scale (Tang and Zhang 2002). Usually, MODIS can be used in conjunction with the ASTER sensor to monitor the earth at moderate or coarse spatial resolution since both of them are equipped on the Terra satellite.

Generally, all former satellite data were initially used to analyze regional urban systems or big cities on a large scale. Experience has shown that the satellite data is not accurate for the urban classification due to the complex mixture and erratic spatial arrangement in urban areas. It makes the individual pixel into a mixture of several

materials. As early as 1982, Welch (1982) pointed out that high spatial resolution image, at least 5-meter or higher, was required to improve urban classification. With the advent of the third generations of satellite sensors, it is likely to stimulate the urban development in a detailed way (Aplin, Atkinson, and Curran1997; Ganas, Lagios and Tzannetos 2002; Puissant, Hirsch, and Weber 2005). These satellite images include IKONOS images with a 1-meter spatial resolution panchromatic band and 4-meter spatial resolution multispectral bands, and QuickBird images with a 0.6-meter panchromatic band and 2.4-meter multispectral bands. Moreover, the Light Detection and Ranging (LIDAR) sensor provided a new source of data that captured three dimensions of urban surfaces (Zhou et al. 2004). Many studies have demonstrated LIDAR's potential in different kinds of urban studies, especially in extracting buildings, roads and other surface features (Priestnall, Jaafar and Duncan 2000; Gamba and Houshmand 2002). These studies are considered to be the beginning of a new era of urban remote sensing in civilian spaces (Tanaka and Sugimura 2001).

The use of high or very high spatial resolution images, however, brought some unexpected problems. Cushnie (1987) found that increasing the spatial resolution will not increase the classification accuracy in some cases. This might be caused by the increase of spectral variability in both inter-class and intra-class due to the reduction of mixed pixels. Moreover, if the spatial resolution is too fine, remote sensing image captures much more spatial variation than the requirement for a specific application. This will result in the "information overload" and "salt and pepper" in the image classification result. Thus, enhancing the urban classification becomes necessary after appropriate remote sensing images have been acquired.

Attempts to Improve the Urban Classification

Traditional urban feature identification and classification are performed through visual interpretation and analysis of aerial photographs based on the tone, color, texture, contexture, and spatial configuration of urban land cover features on the images (Forster 1983). This early manual interpretation is labor intensive and relies on the interpreters' knowledge of both images and specific urban locations.

The increasing availability of digital remote sensing data stimulates researchers to improve the results of automatic and semi-automatic urban classification. One challenge in these automatic classifications is bridging the knowledge of human visual interpretation with digital image processing techniques. A key issue is to fully explore and evaluate the *textural*, *spatial*, *and contextural* information provided by digital remote sensing images.

Texture is a fundamental characteristic of images and is often crucial in targeting discrimination (Woodcock and Strahler 1987). The essential feature of texture methods is the inhomogeneity of urban landscapes that produces distinct textural characteristics between different classes (Shaban and Dikshit 2001). Galloway (1975) calculated various gray levels among rows of the satellite images to obtain the textural information. Haralick (1979) presented the first co-occurrence matrix as a second-order statistical index to describe textures of different materials in urban areas. Marceau et al. (1990) applied the gray-level co-occurrence matrix method for land cover classification using SPOT imagery. More recently, Myint (2003) applied a higher order statistical index of image texture in order to classify the urban area using fractal geometry.

Contexture methods will consider additional information from spatial neighbors around the classified pixel (Cortijo and Blanca 1998). There are three general approaches used to incorporate spectral properties of surrounding pixels in the image classification, including pre-classification spatial feature extraction (Gong and Howarth 1990; Xu et al. 2003), post-classification processing (Gurney 1981), and direct contextural classification (Harris 1985; Cortijo and Blanca 1998). Given the combination of spectral and contextual information, the contextual classifier offers the potential to increase the richness of information in the spatial data set.

Other ancillary GIS data are found as valuable referenced information in the urban remote sensing classification. Zhang et al. (2002) combined road density with spectral information from the multi-temporal Landsat TM data to detect the built-up land change in Beijing, China. Zha, Gao and Ni (2003) used the normalized difference built-up index in mapping urban areas from the TM imagery. Generally speaking, methods of combing the ancillary GIS data with the original spectral data in the image are particularly numerous. Besides the most commonly used unsupervised methods and supervised methods, other classifiers include the neural classification (Seto and Liu 2003), kernel classification (Kontoes et al. 2000), expert system classifier (Stefanov et al. 2001), and hybrid approach (Lo and Choi 2004). Theoretically, the major limitation of such a per-pixel classifier for urban landscape is that it assumed each pixel to be pure (Gong and Howarth 1989; Foody and Arora 1996), which is inherently unable to represent varying combinations of land covers below the pixel resolution (Small 2004).

An alternative to this conventional "hard" classification is required to map multiple class memberships at the pixel level (Foody and Cox 1994; Foody 1996; Foody

1997). Wang (1990) incorporated the "fuzzy mean" and "fuzzy variance" to do a

discriminant analysis in the traditional MLC. Foody (1992) proposed the initial "fuzzy"

c-means algorithm in the unsupervised classification. Spectral mixture analysis (SMA) is

another widely-used method to decompose mixed pixels in urban areas. More detailed

information about fuzzy classification and SMA will be introduced in Chapter V.

This mixed-pixel problem is ameliorated when the very high spatial resolution

images ($< 5m$) are used to map urban areas. In these digital images, the man-made

structures, in contrast to natural environments, have been identified as one or few objects

with distinct and straight boundaries (Couclelis 1992). This characteristic brought the

object-based perspective to urban analysis. Recent development of object-oriented

classification has taken advantage of detailed spatial information from the very high

spatial resolution data. This classification usually segments images based on the

aggregate information from both spectral and shape characteristics of adjacent image

objects. In this method, images are segmented into homogenous objects to reduce the

spectral variety within segments. Further image classification is based on the spectral

characteristic of these homogenous objects, i.e. the mean spectral reflectance.

Additionally, other information, such as the spatial relationship, contextual

information, and elevation threshold, can be incorporated into the object-based

classification. Johnson (1994) first provided a segment-based land use classification for

the SPOT satellite data based on the object characteristics of contextual images. Barnsley

and Barr (1997) further developed the object-based idea in image analysis and presented

a complex graph-based system to recognize the detailed urban land use pattern.

Ecognition, one of the most popular commercial object-based softwares, classifies the

image based on the attributes of segmented image objects rather than on the attributes of individual pixels.

In conclusion, urban remote sensing is concerned with obtaining and interpreting physical properties of urban surfaces. The traditional remote sensing emphasizes technical aspects of data assembly and physical image classification with less attention to the cross-discipline study and application-oriented research. In terms of urban spatial analyses, Longley, Barnsley, and Donnay (2001), for example, described the inherent vagueness and ambiguity in urban structures associated with apparently discrete urban functions. There is still a lot of resistance, especially among social scientists, against using remote sensing in urban studies. Given this situation, the statistic or quantitative analysis on urban landscape maps in certain social circumstances will be our next research objective.

Spatiotemporal Urban Analysis

The emerging agenda in urban remote sensing calls for a new orientation in the related research on urban areas. Recently, most urban studies have shifted from the simple interpretation of urban arrangements toward the quantitative measurement of urban spatial structures, mainly in *urban characterization* and *urban modeling*.

Urban Characterization

Traditional urban analyzers interpret urban land use from historical, social or economic data based on the interpreters' knowledge of city history and city environment (Herold, Goldstein, and Clarke 2003). Right now, most urban landscape studies have been directed toward the quantitative measurements on the spatial structure of urban environments through the urban landscape map classified from the remotely sensed data. Batty and Longley (1988) first employed the fractal method to describe urban land use structures. Mesev et al. (1995) demonstrated the capability of fractal indices in detecting urban land use density to describe structures and changes in urban morphology from remote sensing data. Barnsley and Barr (1997) tested a graph-based pattern recognition method to infer broad categories of urban land use from remote sensing data. Brivio and Zilioli (2001) applied the semi-variogram to explore urban spatial patterns in Landsat TM images of urban areas. All these studies indicated that the quantitative technique is necessary to better characterize the urban spatial pattern.

Understanding the dynamics in spaito-temporal urban patterns is another primary objective in urban characterization. Many techniques have been developed to detect the urban dynamics during past few decades (Singh 1989; Zhang et al. 2002) based on different study purposes. Most detection methods can be grouped into the spectrum-based method and the post-classification method. The spectrum-based method assumes that the significant changes in image pixel values are caused by the changes on the ground instead of interference from atmospheric and other system variations (Singh 1989). This method compares the multi-temporal image using map algebra, such as image difference (Yeh and Li 1997) or image regression (Yuan and Elvidge 1998), and detects the change area

using a given threshold. Alternatively, the post-classification technique applies the traditional classification methods to the registered multi-temporal image datasets, and then labels the change and non-change areas (Zhang et al. 2002) after comparing these two images.

Both the spectrum-based method and the post-classification method have their own advantages and disadvantages. First, the spectrum-based method is straightforward and widely used in natural landscape 'change detection. However, it is impossible to capture the small change in a heterogeneous urban landscape which has various land use/cover types. Secondly, it only describes the change area without finding out the "from" and "to" information. Moreover, this method is time-consuming because it requires higher accuracy requirements on the registration, training, and cluster labeling of individual images. For the post-classification method, it is easy to identify and locate the change, but the detection error comes from not only the image registration but also the image classification.

Although many quantitative methods have been applied in providing the knowledge of what, where, and how much landscape change has occurred, researchers still face a fundamental problem in providing an effective dynamic spatial model to describe the former urban landscape pattern and assess the future urban landscape pattern. Thus, there is an urgent need for us to explore the potential of new spatial data and provide innovative methods to improve current urban spatiotemporal models.

Urban Modeling

Although several descriptive and analytical models of urban land use were developed before 1950, the real urban growth model began to arise in the 1960s and faded in the early 1970s, since the models fail to monitor the real cities. Currently, urban models are always built in mathematical terms with identified driving factors. These factors, such as human activity, one of the most active factors, determine spatial structures of cities.

After 1990, especially in recent years, updated computers can support a larger spatial database for GIS analysis. Incorporating high quality data, more sophisticated models were developed with the capability of prediction. Batty and Longley (1989) introduced a diffusion limited aggregation (DLA) model to predict urban growth. In this growth model, a cluster developed from a seed site by the accretion of randomly walking particles across a simulation space. In the late 1990s, various spatial models were developed due to the availability of remote sensing data on a large scale, such as UrbanSim model (Waddell 2002), Markov chain model (Stewart 1994), LUCAS model (Berry et al. 1996), CLUE model (De Koning 1999), CA model (Batty and Xie 1994), and Agent-based model (Liebrand et al. 1998). The detailed review of these spatial explicit models can be found in Table 1.

TABLE 1 DETAILED COMPARISON OF URBAN LANDSCAPE MODELS

	Model Name	Developer	Purpose	Variables	Strengths	Weakness
Vector-based	UrbanSim	Waddell 2002	Predict land use, physical development, the movement and location of businesses and households	Socioeconomic, environmental parameters	Simulate the interaction between urban activities and the natural environment	Deterministic model
	What if	Klosterman 1999	Determine what will happen in land use patterns in the future if policy choices are made	Natural conditions, urban infrastructure,	Fully operational model in adapting particular data sets and policy concerns	Lack of a firm theoretical basis
	Area Base	Lichtenberg, 1985	Project the proportions of land use using hedonic rent theory and acreage allocation model	Based on Palmquist's hedonic rent theory and acreage allocation model (Lichtenberg, 1985)	Easy to incorporate available socioeconomic data, such as age, income, population, and rent	Long-term prediction is not good
	Markov	Bell, 1974	Characterize the land use/land cover change	Multi-temporal change, transition probabilities	Mathematically compact, easy to implement	Does not account for spatial context
Grid-based	CA	Batty and Xie 1994	Model the spatial structure of urban land use over time	Landscape maps, environmental factors in neighborhood	The spatial factor and ecological aspects are easily to be incorporated	Face challenge in incorporating human decision making
	LUCAS	Berry et al. 1996	Simulate the landscape change with socioeconomic information and its environmental impacts	Socioeconomic variables, such as transportation network, ownership, population density etc.	Flexible and interactive computing environment	The patch size is no sense due to the pixel-based method
	LTM	Pijanowski et al. 1997	Analyze the land use change and predict land use pattern	Landscape maps, social, political, and environmental factors	Can be applied to multiple scales using a moving scalable window metric	Suppose all the variables constant
	CLUE	DeKoning 1999	Predict future land use	Biophysical drivers and human drivers	Covers a wide variety of biophysical and human factors and ranges multiple spatio-temporal scales	No social or political factors
Grid/Vector	Agent-based	Liebrand et al., 1988	Represent a wide variety of entities and its activities	A simulated environment, entities under human decision making	Flexibility, and successful in replicating human decision	Difficult to develop and control

In terms of the methods to represent the model object, there are vector based

models and grid based models (Herold 2004). Vector based models use the thematic map

as the input data for the model and the spatial objects are usually defined as homogenous

land units. *UrbanSim* is one of land use simulation models for the growth government,

regional land use, and transportation planning in the states of Hawaii, Oregon and Utah

(Waddell 2002). Within the context of urban infrastructure and governmental policy,

UrbanSim represents zonal structure in the urban area to monitor the market behaviors of

households, business, and land developers. Theoretically, *UrbanSim* is an object-oriented

model.

What if model (Klosterman 1999) begins with uniform analysis zones or

homogeneous land units generated from the GIS software. Through applying the

governmental policies and land use demands, this model derives the aggregating value of

the regional condition on the land units. *What if* model projects future land use patterns

by balancing the supply, demand, and land sustainable at different locations.

Area Base model is a vector based model used in resource assessments to predict

the availability of farm and forest land. Transformed from the regional model (Palmquist,

1989), *Area Base* model allocates the proportions of a given land use to predefined land

use categories using Lichtenberg's (1985) acreage allocation method.

Another vector-based model is *Markov* model which predicts future landscape

patterns based on the spatial transition probability. Although Markov model is a typical

spatial transition model, early Markovian analysis is a descriptive tool to predict land use

change on a local or regional scale (Bell 1974; Bourne 1976). Actually, the Markov

model is not a strict vector-based model, it is based on the statistical results from the

thematic map. Lopez et al. (2001) used Markov chain to simulate the relationships among a set of urban and social variables in predicting land use/cover change in the urban fringe of Morelia city, Mexico. Weng (2002) demonstrated that the integration of satellite remote sensing and GIS techniques into the stochastic urban modeling was an effective approach for analyzing the direction, rate, and spatial pattern of landscape change in Zhujiang Delta of China.

Mathematically, most vector-based models rely on some static equations and this characteristic provides the potential in integrating the GIS information into the model entities. The major drawbacks of such models are the poor handling in dynamic entities and poor representation of external variables, e.g. the spatial information and socio-economic factors.

The models developed on grid have more advantage in solving these problems than the vector ones. Land-Use Change Analysis System (*LUCAS*) is a grid-based model which integrates socioeconomic and ecological variables in the multilayered, gridded maps (Berry et al. 1996). This model consists of three subject modules: socieconomics, which derives the transition probability from the function of socioeconomic driving variables; landscape change, which predicts the landscape maps from the socieconomical module; and environmental impacts, which estimates the impacts of selected environmental variables from the landscape maps from second modules.

Land Transformation Model (*LTM*) (Pijanowski et al. 1997) applied the spatial rules to land use transitions for each location in the processed spatial layer or grid. It is easy to quantify the contribution of different spatial variable because of its format. In order to aggregate the land use change and change drivers, this model adopted the similar

method with the Conversion of Land Use and its Effects (*CLUE*) model (DeKoning et al. 1999). Both of them apply the variable values in grid format to create a series of future land uses over the time.

Agent-based model (Liebrand, Nowark, and Hegselmann, 1988) is a complex behavior model which used both vector data and raster data. Usually, the raster data is the agents' environment, and the agents, in turn, act on the simulated environment. This model can be applied to a wide variety of simulations, including moving cars, animals, people, or even organizations.

In conclusion, a reliable urban growth model should have following capabilities:

o Providing an appropriate theoretical and technical framework for urban growth

o Understanding and describing the historical dynamics of urban structures

o Anticipating and predicting future changes or trends of urban developments

o Exploring and incorporating different economical, social, and political parameters to monitor the urban growth.

Current Research Challenge: Combining the Remote Sensing with Urban Research

Based on the literature review in urban research, the following assumptions can be made for current research in urban remote sensing and urban modeling:

o Over the past half century, rapid urbanization has exhibited an extreme impact on the environment and climate change in both developing and developed countries on local, regional and global scales. Research in geography, especially in urban geography, has performed the shift from traditional descriptions to quantitative measurements.

o Remote sensing, in conjunction with geographic information systems (GIS), has been recognized as an effective tool in detecting urban landscape patterns and its processes. More satellite images with high spatial and spectral resolutions are becoming more available in urban studies.

o An important agenda in the availability of remote sensing data asks for a new orientation in related image analysis methods and pattern recognition techniques. Given different image sources, appropriate classification methods and enough ancillary information are important in producing detailed spatial data for urban research.

o More sophisticated urban dynamics models are needed to support the exploration of urban landscape changes under a variety of natural and social scenarios.

The nature and pace of development in urban remote sensing was, and remains, very impressive, but detailed interpretation of urban areas needs more exploration besides the conventional urban classification of spectral reflectance. Most research on remote sensing focused on technical issues of data assembly and physical classification, in which the socio-economic factors were always ignored. Moreover, what and how advanced remote sensing techniques make progress in measuring urban morphology and predicting future urban patterns are still interesting topics. If this can be accomplished, remote sensing will certainly play an important role in urban research, not only for interpreting urban forms, but also for understanding their functions.

CHAPTER III

STUDY AREA AND DATA PREPARING

<u>Study Area</u>

This research was conducted in two petroleum-oriented cities: Houston, Texas in the United States and Daqing, Heilongjiang in China. In order to make Houston and Daqing comparable, two smaller areas were subset from the original images, covering around 1,200 km^2 of the major metropolitan areas in both Houston and Daqing.

Houston, Texas in the United States

Houston, seat of Harris County, Texas, lies largely in the northern portion of the Gulf coastal plain, a 40- to 50-mile-wide swath along the Texas Gulf Coast, 50 miles from the Gulf of Mexico (Moser 1998). Centered at 95°22' W longitude and 29°46' N latitude, the city has a total area of 1,558 km^2 and a total population of 2.02 million in 2006, according to the United States Census Bureau. The city of Houston has undergone significant growth in the last decade and is the fourth largest city in the United States.

(1) Physical Environment of Houston

The geology of Houston developed from the erosion of the Rocky Mountains, whose stream deposit consists of a series of sands and clays from decayed organic material. Over time, this material was transformed into oil and natural gas (Moser
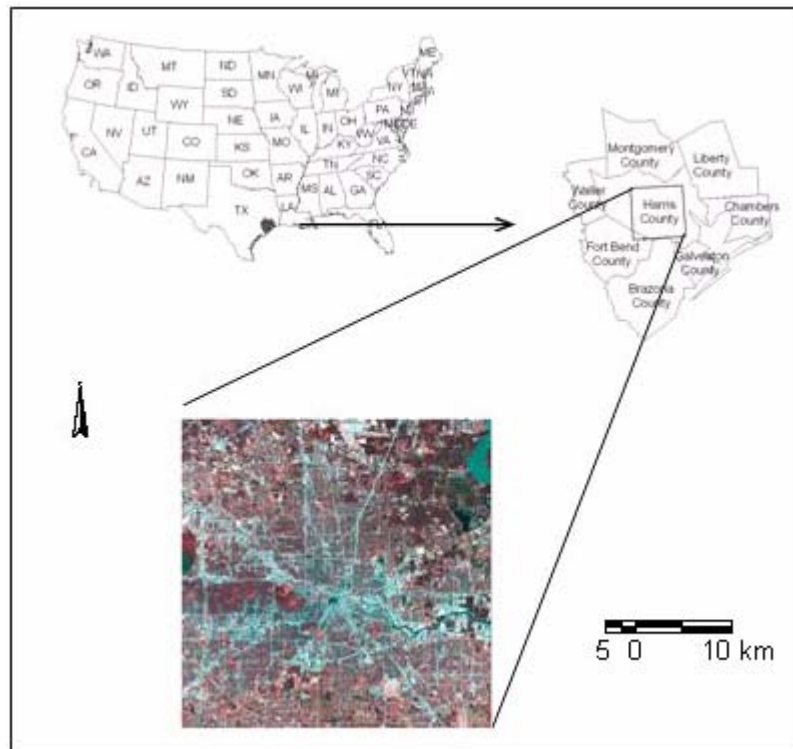
Fig. 3. Study area of Houston, Texas in the United States

Fig. 4. The major six landscape classes in Houston

1998). During the last century, subsidence in Houston has caused significant impact on flood control, utility distribution, and water supply as a result of the withdrawal of oil or gas and other minerals.

The climate of Houston is classified as humid subtropical. Houston has a temperate climate all year round due to the proximity to the Gulf of Mexico, though the humidity in summer makes the city feel hotter than the actual temperature. Mean annual precipitation in Houston is 43 inches and the mean temperature ranges from 45°F in winter to 93°F in summer, varying seasonally between a hot, humid summer and a cool, dry winter (Texas State Historical Association 2002). Located on the upper Gulf coastal plain (Figure 3), Houston has a rather low elevation, with the highest elevation in the area at 27 meters and elevation rises approximately 0.2 meters per meter inland (Houston city and meeting planners guide 2004). The metropolitan area is located in the Gulf costal plains biome, and its main vegetation is classified as temperate grassland. Under this particular natural environment, a variety of landscape types were generated in this region:

the northern and eastern portions of the study area are largely forested and the southern and western portions are predominantly prairie grassland, while coastal areas are prairie and sand. Totally, the Houston region contains over 110 tree species, with the dominant native species being oaks and pines. The major distinct ecosystems in the Houston area include saltwater marsh, prairie, swamps, and upland pine / hardwood. However, in the city itself, there is relatively little canopy coverage, especially in downtown areas. Figure 4 shows the major landscape types in Houston.

(2) Economic-social Status of Houston

Although nowadays more frequently referred to as the Space City, Houston was founded in 1836 as the Bayou City on the banks of Buffalo Bayou. Historically, Houston was first developed as a cotton and lumber market in the early nineteenth century. The discovery of oil at the Spindletop oilfield in 1901, and later at Humble and Goose Creek in 1905 and 1906, respectively, dramatically changed the Houston economy in the twentieth century. These discoveries made it the largest city in Texas as of 1930 and the fourth largest city in United States since 1990 (Texas State Historical Association 2002). Until recently, the economy of Houston was still focused on the exploration and production of oil and natural gas, even though oil production continues to slide after the early 1980s. Although the government tried to diversify its economy (Key to the city 2001), the city's unchallenged role as an international center of oil technology, headquarters for a number of the world's largest energy companies, and a strong refining and petrochemical manufacturing base should shore up the local economy of Houston in the near future.

Different from other large cities in the United States, Houston did not adopt city zoning laws in its urban planning. Lacking city zoning has led to an abundance of urban sprawl in Houston, resulting in a relatively large metropolitan area and low population density. Land developers inspired the spread of Houston when they built suburbs such as Pasadena (1892), Houston Heights (1892), Deer Park (1892), Bellaire (1911), West University Place (1919), and River Oaks (1922-24). Basically, the heavy industries concentrated in the area of the ship channel and subdivisions controlled construction along the banks of Buffalo Bayou.
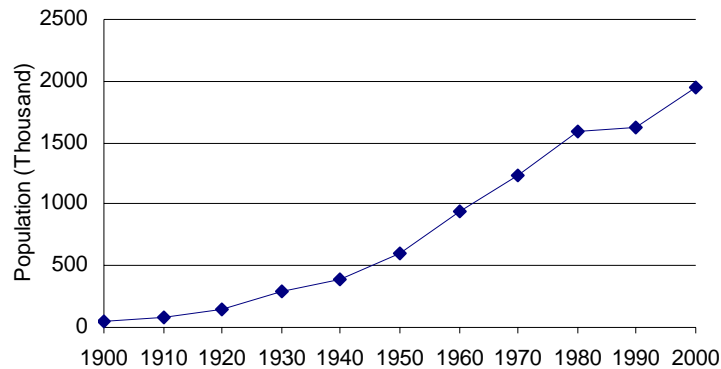
Fig. 5. The growth of population in Houston from 1900 to 2000

With the rapid economic development in the last century, the population in Houston has undergone a dramatic growth since the last century, from 45,000 in 1900 to 1.95 million in 2003 (Figure 4). As one of the most developed cities, Houston's population increased in one of the fastest growth rates in the United States.

Daqing, Heilongjiang Province in China

Daqing lies in the middle of Songlen Plain of Heilongjiang Province in the northeast of China, located about 159 kilometers from the city of Haerbing and 139

kilometers from the city of Qiqihaer. Centered at 124°15' E longitude and 46°20' N

latitude, the study area covers four major urban areas, Shaertu district, Ranghulu district,

Longfeng district, and Honggang district (Figure 6). Daqing, the energy capital of China,

maintains a variety of landscape types due to its unique geology and climate

environment. The typical land use types include agriculture, urban or build-up, grass,

saline or barren land, water, wetland, and woodland (Figure 7).
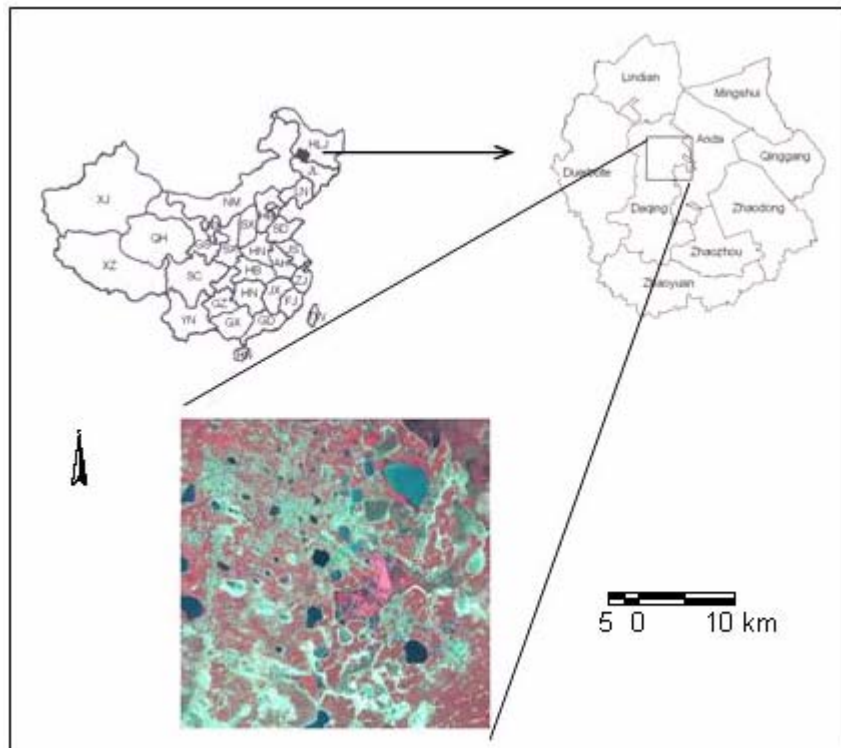
Fig. 6. Study area of Daqing, Heilongjiang Province, China
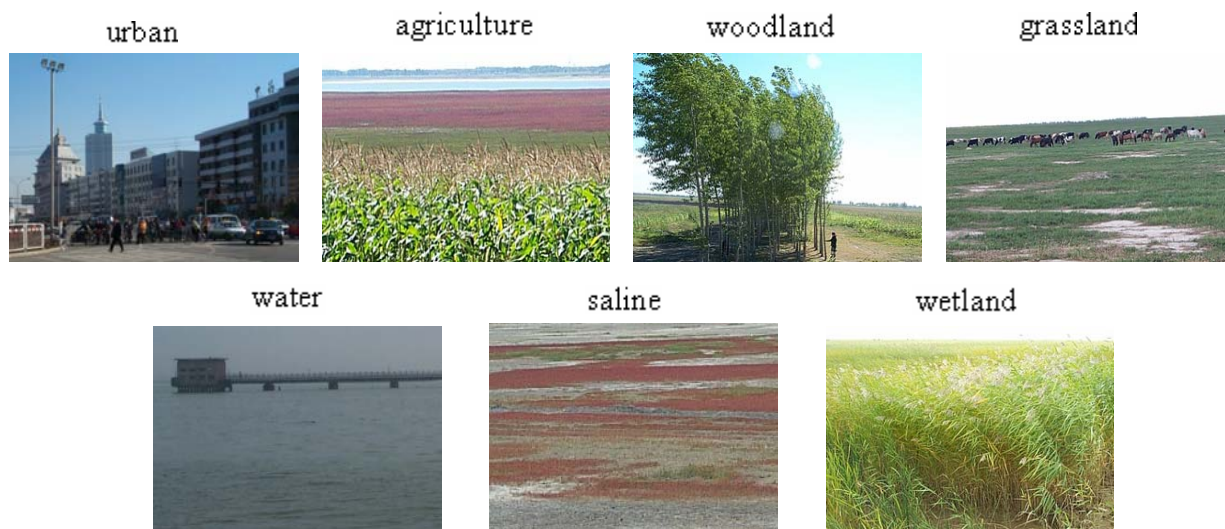
Fig. 7. The major seven landscape classes in Daqing

(1) Physical Environment of Daqing

The study area shows typical characteristics of the large-scale Mesozoic and Cenozoic land sediment basin. After long geotectonic movements, Daqing ends up with a unique geological structure for the storage of oil. Since the elevation ranges from 126-165 meters, the study area is a relatively flat plain and the elevation difference ranges from 10-39 meters.

Located in the edge of the North Temperate Zone, the Daqing area is affected by both cold monsoons from Mongolia and warm monsoons from the near North Pacific Ocean. Mean annual precipitation is 17 inches and the rainy seasons are summer and autumn, varying seasonally between a hot, wet summer and a cool, dry winter. The average temperature in Daqing is $36 - 40°$ F, with $-3 - 7°$F during January and $73 - 74°$ F during July (Statistic Bureau of Daqing 2001).

Daqing also has plenty of surface water, such as natural lakes and man-made reservoirs. The major soil in the Daqing region is chernozem, covering almost 33% of the

whole Daqing area. Herbage is the major vegetation in Daqing, mainly as meadow, halophyte, and swamp. With the great development of Daqing in recent years, a large area of wildwood has been cultured into farmlands or woodlands around the farmland.

(2) Economic-social Status of Daqing

Daqing, once a rural area, has become the largest oil production base in China since the oil was found in 1959. Although Daqing is now diversifying its energy-oriented economy, petroleum and petrochemical industries are still the main backbones of its economy. In 2000, 99.9% of petroleum and 100% of gas in Heilongjiang province were produced in Daqing, which are 53.0 million ton and 2.3 billion m^3 respectively. The continual construction of the oil field has spoiled the original landscape pattern over the last 50 years. The reduction of swamp, grassland, and forest has resulted in the deterioration and desertification of Daqing, potentially affecting its future landscape pattern, regional environment, and climate.

With the fast economic development, the population of Daqing has grown greatly during the last 50 years, increasing from 150,000 in 1960 to 1.2 million in 2000 (Figure 8a, Statistic Bureau of Daqing 2001). The major population is distributed in the Ranghulu district (39.53%), which is the old industry center in Daqing (Figure 8b).
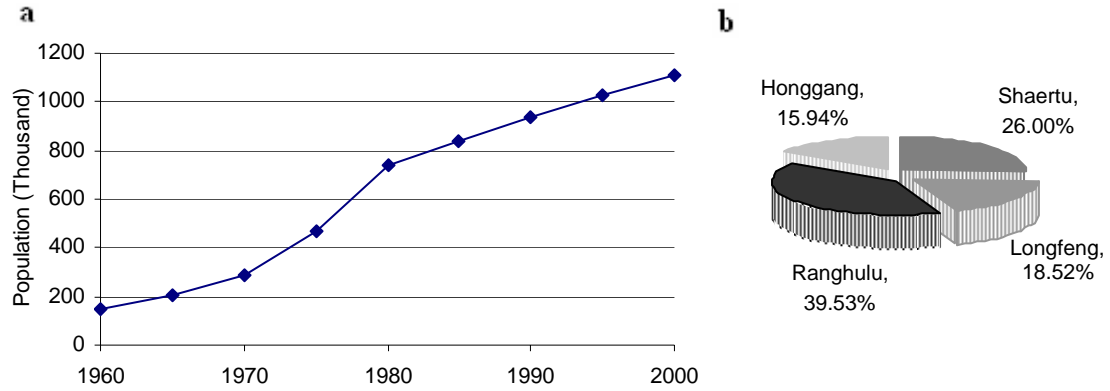
Fig. 8. a: The growth of population in Daqing from 1960 to 2000; b: the distribution between the major city district: Ranghulu district, Shaertu district, Longfeng district, and Honggang district

Data and Preprocessing

Multi-temporal Landsat MSS/TM/ETM

In order to study the urban dynamics in Houston and Daqing, two sets of Landsat MSS/TM/ETM satellite images were chosen. Table 1 describes the characteristics of these images. All images were geometric rectified into the UTM map projection, WGS 84, Zone 51, on a SUN workstation using ERDAS[TM] Software. Fifty to seventy ground control points (GCP) were chosen in this rectification given the size of study area. They were evenly distributed throughout the whole study area, and most of them were laid on the distinguishably discerned objects, for example, the intersections of roads, aqueducts, or the fence tree around the agriculture. The registration procedure achieved an accuracy of less than 0.5 pixels Root Mean Square Error (RMSE) for both Houston and Daqing.

TABLE 2 CHARACTERISTICS OF USED SATELLITE REMOTE SENSING IMAGES

Study area	Sensors	Dates	Data characteristics
Houston	Landsat Multispectral Scanner (MSS)	10/1/1976	4 spectral bands, 60 m spatial resolution
	Landsat Thematic Mapper (TM)	12/8/1990	7 spectral bands, 30m spatial resolution
	Landsat Enhanced Thematic Mapper (ETM)	11/9/2000 1/2/2003	8 spectral bands, 15m spatial resolution
Daqing	Landsat Multispectral Scanner (MSS)	8/23/1979	4 spectral bands, 60 m spatial resolution
	Landsat Thematic Mapper (TM)	7/20/1990	7 spectral bands, 30m spatial resolution
	Landsat Enhanced Thematic Mapper (ETM)	6/21/2000 8/11/2001	8 spectral bands, 15m spatial resolution

IKONOS Data

Considering the scene size and the availability of our data source, six scenes IKONOS images, including one panchromatic band at 1-meter spatial resolution and four multispectral bands at 4-meter spatial resolution, were used to study the downtown area of Houston. The specific IKONOS image characteristics are shown in Table 2. These IKONOS remote sensing datasets were acquired in January 2002 with initial geo-rectification completed. All images were additional geometric corrected to the same projection with the satellite images. This was done by standard polynomial transformation with fifty ground control point (GCP).

TABLE 3 CHARACTERISTICS OF THE IKONOS DATA

Source Image ID	Scene ID	Acquisition Date	Collection Azimuth	Collection Elevation	Sun Angle Azimuth	Sun Angle Elevation
740	702	1/2/2002	128.52 deg	83.65 deg	158.83 deg	34.25 deg
	703	1/2/2002	128.52 deg	83.65 deg	158.83 deg	34.25 deg
741	805	1/2/2002	181.01 deg	66.89 deg	159.10 deg	34.30 deg
	806	1/2/2002	181.01 deg	66.89 deg	159.10 deg	34.30 deg
980	501	12/14/2002	279.63 deg	85.19 deg	164.22 deg	35.25 deg
	502	12/14/2002	279.63 deg	85.19 deg	164.22 deg	35.25 deg

Since the IKONOS were acquired on different dates with varying atmospheric and illumination conditions, it is necessary to conduct image-to-image radiometric normalization between the image 980 to image 740 and 741 (Table 3). To perform this normalization, we applied a histogram matching the adjacent scenes using the Radiometric Enhance function in ERDAS Software. Then, we mosaic all six scenes into one image to cover our study area in Houston.

Ancillary Digital Data

Other reference data used in this research are: (1) a soil thematic map at the scale of 1:100,000 from Committee for Agricultural Development Planning of Daqing in 1980's; (2) vegetation thematic map of Daqing at the scale of 1:750,000 from the Geography Institution of Changchun, Chinese Academic Science in 1973; (3) district map at the scale of 1:100,000 from Daqing land bureau in 1999; (4) land use map at the scale of 1:100,000 from Daqing land management bureau in 1994; (5) social and economic statistical data for Houston from the United States Census Bureau and for Daqing from Daqing's Statistic Bureau.

CHAPTER IV

PATTERN AND DYNAMICS ANALYSIS OF URBAN LANDSCAPE

Introduction

The magnitude and intensity of urbanization are of grave concern. It changes both the extent and density of urban areas (Wikipedia 2006). The limited understanding of urban landscape changes and trends, however, often results in an incomplete assessment of the urbanization and impedes the comprehensive planning for future urban developments. To make an intelligent urban planning, planners need a comprehensive and extensive knowledge about the causes, chronology, and effects of these processes.

Many spatial techniques have been developed to detect the landscape change. As mentioned in Chapter II, post-classification methods begin the analysis with the classification of multi-temporal images; from this, changes are detected through comparing the classification results directly or the indices of classification results. Landscape metrics technique is one of most commonly used methods to detect landscape change on the classified maps. This technique derives various spatial indices to summarize the spatial pattern at each given time, and then compares the result of spatial indices to detect the spatial pattern changes over different times (Singh 1989; Jensen 1996; Zhao et al. 1996; Zheng et al. 1997; Macleod and Congalton 1998; Miller et al. 1998; Mas 1999; Roy and Tomar 2001; Yang and Lo 2002). Different from the direct comparison of two classified maps, the landscape metrics technique is advantageous in

capturing inherent spatial structures of landscape pattern and biophysical characteristics of these spatial dynamics.

Within the landscape metrics technique, a variety of landscape metrics have been proposed to characterize the spatial configuration for either the individual landscape classes or the whole landscape base (Patton 1975; Forman and Gordron 1986; Gardner et al. 1987; Schumaker 1996; Chuvieco 1999; Imbernon and Branthomme 2001). For instance, patch size and patch shape indices have been widely used to convey meaningful information on the biophysically changed phenomena associated with patch fragmentation at a large scale (Viedma and Melia1999; Fuller 2001). These configuration indices vary as a function of patch shapes and usually correlate with the basic parameter of individual patches, such as the area, perimeter, or perimeter-area ratio, but perform poorly in reflecting the spatial location of patches within the landscape (Imbernon and Branthomme 2001).

Based on the information theory, O'Neill et al. (1988) first developed the dominance and contagion indices to capture major features of spatial patterns throughout the eastern United States. According to Gustafson and Parker (1992), the proximity index quantifies the spatial context of patches in relation to their neighbors; specifically, the nearest-neighbor distance index distinguishes the isolated distribution of small patches from the complex cluster configuration of larger patches (Turner 1989). These indices reflected the spatial heterogeneity by quantifying the spatial structures and organization within the landscape. The above two groups of indices, patch-based and heterogeneity-based, reflect two aspects of the same spatial pattern, and complement each other. Although the choice of indices relies on the emphasis of a specific research, it is preferred

to adopt both groups of indices when speculating on a spatial pattern (Turner and Gardner 1990) because the landscape pattern possesses both homogeneous and heterogeneous attributes.

The objective of this chapter has two folds: 1) to analyze and interpret the landscape pattern as well as its change in both Houston and Daqing during the last twenty years using the classified maps from satellite images, and 2) to explore the inter-linkage between landscape change, economic development, and land management. To enable a comprehensive investigation and comparison of the complex and heterogeneous landscape in Houston and Daqing, I chose a set of landscape indices with inter-complementary ecological meanings. Lastly, these indices are analyzed to effectively examine both current landscape patterns and retrospective change processes to monitor ongoing changes.

Data and Methodology

Data and Preprocessing

The images used for two study areas run across three decades through from the 1970s to 2000 (Table 1). For each city, I conduct a histogram match between the images so that the distribution of brightness values between the resultant images in different years is as close as possible (Richards 1993).

TABLE 4 CLASSIFICATION SYSTEMS AND DEFINITIONS OF TRAINING SAMPLES

	Landscape type	training samples using color composite (bands 4, 5, 3)
Houston	Residential	Rectilinear shape with brown, gray, and dark blue
	Industrial or commercial	Bigger and brighter than the residential roof, usually in brown, white, and gray
	Grassland	Light red and regular shape
	Woodland	Dark red and distributes along northeast of Houston
	Barren or soil	White or yellow and distributes along the river or grassland
	Water	Smooth, cyan, blue, and sometimes black
Daqing	Urban	Intensively used by the building, and shows in the image as mixed pixels of light blue
	Agriculture	primarily for the production of rice and fiber, shows in the image as light or dark red, green with stripe texture
	Grassland	Mixed pixels of red, white, and light green
	Woodland	Dark red and distributes along northeast of Daqing
	Wetland	Identified on higher elevations, Regular shape, red or dark red
	Saline	White or light, most near to the water
	Water	Irregular shape, ultramarine

Gained from the long-term field knowledge of geology, geography, vegetation and land use in Houston and Daqing, I set up two sets of classification schemes. These classification schemes are listed and described in Table 3. Considering the requirement of traditional Maximum Likelihood Classification and the size of the study area, I chose a separate set of training and test samples for the images at each year. The ancillary data mentioned in Chapter III, including soil thematic map, vegetation map, and land use map were overlaid on the image to help to select the training samples. The selection of training and test samples was guided by the characteristic description of each class (Table 3). Landscape maps for Houston and Daqing from the 70's to 2000 were produced using

a traditional maximum likelihood classification (MLC). The number of training and test

samples and the classification accuracy are shown in Table 4.

TABLE 5 THE ACCURACY ASSESSMENT OF LANDSCAPE MAPS FROM LANDSAT IMAGES BY MAXIMAM LIKLIHOOD CLASSIFICATION

Houston	Train sample			Test sample			User Accuracy (%)			Producer Accuracy (%)		
	76	**90**	**2000**	**76**	**90**	**2000**	**76**	**90**	**2000**	**76**	**90**	**2000**
Residential	79	324	1215	78	313	1312	91.72	98.01	99.72	97.79	94.25	100.00
Industrial or commercial	73	320	1112	65	296	1218	82.67	85.85	80.23	95.75	90.20	100.00
Grassland	74	270	1259	69	302	1216	95.12	90.72	99.99	84.48	94.69	99.89
Woodland	75	338	1200	78	308	1140	99.68	100.00	100.00	100.00	100.00	99.79
Barren or soil	80	343	1192	79	272	1172	88.77	82.84	98.99	80.06	81.87	70.47
Water	75	304	1243	63	287	1102	98.39	100.00	100.00	99.19	97.39	99.47

Overall accuracy (%):92.58(1979); 94.45(1990); 96.19(2000)
Kappa: 0.92(1979); 0.93(1990); 0.95(2000)

Daqing	Train sample			Test sample			User Accuracy (%)			Producer Accuracy (%)		
	79	**90**	**2000**	**79**	**90**	**2000**	**79**	**90**	**2000**	**79**	**90**	**2000**
Urban	72	276	1216	75	278	1142	88.60	99.23	100.00	96.40	98.85	90.67
Agriculture	68	275	1128	77	283	1220	72.83	90.25	77.88	61.22	85.49	91.88
Grassland	74	296	1132	83	326	1216	76.18	91.90	85.50	84.30	92.99	66.14
Woodland	74	268	1172	69	285	1116	87.16	87.08	92.11	83.77	87.08	84.39
Wetland	78	282	1204	71	282	1118	83.60	93.63	88.55	87.55	93.63	96.93
Saline	76	285	1158	77	308	1208	97.50	99.61	87.21	99.41	99.61	100.00
Water	78	294	1152	71	278	1164	99.36	99.64	100.00	92.81	99.64	100.00

Overall accuracy (%):86.41(1979); 93.07(1990); 89.90(2000)
Kappa:0.84 (1979); 0.92(1990); 0.88(2000)

Indices to Measure Patch Attributes

(1) Patch Size Coefficient Variation (PSCOV):

(4.1)
$$PSCOV = PSSD \big/ MPS$$

(4.2)
$$MPS = \frac{\sum\limits_{i=1}^{m}[a_i]}{m} \; ; PSSD = \sqrt{\frac{\sum\limits_{i=1}^{m}[a_i - MPS]^2}{m}} \left(\frac{1}{1000}\right)$$

where a_i is the patch size, m is the total number for ith landscape, and MPS is the mean

patch size.

PSCOV is one of the typical indices to indicate the distribution of area among the

patches by finding out the area difference among patches within one landscape class.

Basically, the class with a large PSCOV (or PSSD) is less uniform than that with a small

PSCOV (or PSSD) (Chuvieco 1999), i.e., if the landscape class is dominated by several

big patches, both PSCOV and PSSD values would be large.

(2) Landscape Shape Index (LSI):

The first index to characterize landscape shape is the Edge Density (ED), a simple

ratio between the perimeter and area.

(4.3)
$$ED = \frac{P_i}{A_i}$$

Since the simple ratio is usually affected by the patch size, I used the modified

perimeter – area ratio here to imply the shape of landscape (Patton 1975; Schumaker

1996).

(4.4)
$$LSI = P_i \big/ 2\sqrt{\pi A_i}$$

Where P_i and A_i are the perimeter and area of the ith landscape. As a modified index of ED, LSI attains its minimum value when the shape of patches is completely regular, such as a circle, and it increases when the patch turns to be more complex (Schumaker 1996; O'Neill et al. 1999; Fuller 2001).

(3) Area-Weighted Mean Patch Fractal Dimension (AWMPFD):

Fractal dimension, with its value ranging from 1 to 2 for a 2-dimensional landscape (Mandelbrot 1967), is another modified shape index to indicate the patch shape in the landscape ecology. It is usually built on the linear regression between the logarithms of perimeter and area (De Cola 1989).

To acquire a normalized fractal dimension, I calculated the area-weighted mean patch fractal dimension using the following equation:

$$(4.5) \qquad AEMPED = \sum_{i=1}^{m} \left[\frac{2\ln(0.25 p_i)}{\ln(a_i)} \left(\frac{a_i}{A} \right) \right]$$

Where p_i and a_i are perimeter and area of each patch within one landscape class; A is the total area for one landscape class. Theoretically, The AWMPFD of the highly convoluted perimeter will approach closer to 2 than the simple perimeter due to an increasing complexity in the patch shape (De cola and Lam 1993; Schumaker 1996; Olsen et al. 1999; Read and Lam 2002).

Indices to Measure Spatial Heterogeneity

(1) Shannon's Diversity Index (SHDI):

$$(4.6) \qquad SHDI = -\sum_{i=1}^{m} \left[P_i \ln(P_i) \right]$$

The Shannon Diversity Index measures the landscape diversity using two components: the number of different patch types, m, and the proportional area distribution, P_i, among patch types. Furthermore, the other two indices will be calculated followed by the diversity index to measure the dominance and evenness. They are: Patch Dominance and Patch Evenness (PD and PE):

(4.7)
$$PD = H_{max} + \sum_{i=1}^{m} \left[P_i \ln(P_i) \right]$$

(4.8)
$$PE = \frac{H}{H_{max}}; \quad H_{max} = \ln(m)$$

Where H is the shannon's diversity index and m is the number of patch of ith landscape class; P_i is the probability of ith class in the landscape. In this study, I used the ratio between the area of ith class and the total landscape area to denote P_i. Indices of landscape diversity, dominance, and evenness have been widely used to indicate the size and distribution of patches in the landscape (O'Neill et al. 1988; Viedma and Meliâ 1999).

(2) Contagion Index (CONT):

CONT index developed by O'Neill et al. (1988) quantifies both the composition and configuration of the landscape (Li and Reynolds 1993):

(4.9)
$$CONT = 1 + \sum_{i=1}^{m} \sum_{j=1}^{n} P_{ij} \ln\left(P_{ij}\right) / 2\ln(n)$$
$$P_{ij} = P_i P_{j/i}, P_{j/i} = m_{ij} / m_i$$

Where the P_{ij} is the probability that a patch of ith landscape is found adjacent to a patch of jth landscape, while m is the patch number within one landscape category and n is the number of landscape categories. P_i is the probability that a randomly chosen polygon

belongs to patch type *i*, and $P_{j/i}$ is the conditional probability. In this study, I set this

conditional probability as the ratio of *i* adjacent to *j*. A large CONT reflects the clumping

of large contiguous patches while a small CONT value reflects a landscape that is

dissected into small patches (O'Neill et al. 1988; Turner 1990; Li and Reynolds 1993;

Griffith et al. 2002).

(3) Proximity Index (PI):

In landscape ecology, nearest-neighbor distance is defined as the distance from a

patch to the nearest neighboring patch of the same type, based on edge-to-edge distance.

Mean Nearest-Neighbor Distance (MMND), Nearest-Neighbor Standard Deviation

(NNSD), and Nearest-Neighbor Index (NNI) were chosen to calculate in this study as

follows:

$$(4.10) \qquad MNND = \frac{\sum_{i=1}^{m} h_i}{m}; \quad NNSD = \sqrt{\frac{\sum_{i=1}^{m}(h_i - MNND)^2}{m}}$$

$$(4.11) \qquad NNI = MNND \Big/ ENND; \quad ENND = \frac{1}{2\sqrt{n/a}}$$

Where h_j is distance from each patch to its nearest neighbor, and *m* is the total number of

nearest neighbor to this patch, *n* and *a* are the number and area of this class. ENND is the

expected value of MNND in random. The NNI ranges between 0 and 1, and the less NNI,

the landscape is less random and more clumped. The proximity indices measure both the

degree of patch isolation and the degree of fragmentation of the corresponding patch type

within the specified neighborhood of the focal patch (Gustafson and Parker 1992).

(4) Fragment Indices (FI):

I chose the Total Core Area (TCA), Core Area Percent of Landscape (CAPL), and Mean Core Area per Patch (MCA) to denote the landscape fragmentation:

(4.12) $$TCA = \sum_{i=1}^{m} a_i^c; \quad CAPL = \frac{\sum_{i=1}^{m} a_i^c}{A}; \quad MCA = \frac{\sum_{i=1}^{m} a_i^c}{m}$$

Where a_i^c is the core area, the interior habitat as an undisturbed area in the ecological meaning; A is the total class area, m is the number of patch.

To identify the core area of each patch, we smoothed the sharp edge and calculated the core area within each patch. These edge-to-interior indices provide fragmentation information of the class, i.e., the higher the ratio between core area and total area is, the less fragmented this class would be (FRAGSTATS * ARC 2004). To summarize, two categories of landscape indices were chosen from perspectives of the patch attributes and spatial heterogeneity. The patch-based indices consist of PSCOV, LSI, and AWMPFD with aims to measure the area distribution and the shape of landscape among the patches. Regarding the spatial heterogeneity-based indices, I chose SHDI to describe the landscape diversity, CI to measure the composition and configuration of landscape, PI to denote the degree of isolation, and FI to measure the landscape fragmentation.

Results and Discussions

Quantitative Description of Landscape Dynamics

Figure 9 is landscape maps of Houston in 1976, 1990 and 2000, and Daqing in 1979, 1990 and 2000, respectively. In Houston (Figure 9A), most of the industrial / commercial areas are distributed in the downtown area or along the major roads. The central business district (CBD) is surrounded by the concentric rings of residential area, which spread greatly during 1976 – 2000. Residential buildings are surrounded by the grassland and woodland. This pattern can be attributed to the regional characteristics of Houston's neighborhoods. Located in the coastal biome of the gulf plains, the vegetation of Houston is classified as temperate grassland. Prevailing winds from south and southeast bring enough moisture from the Gulf of Mexico, which provides a favorable environment for the woodland in the northeastern Houston.
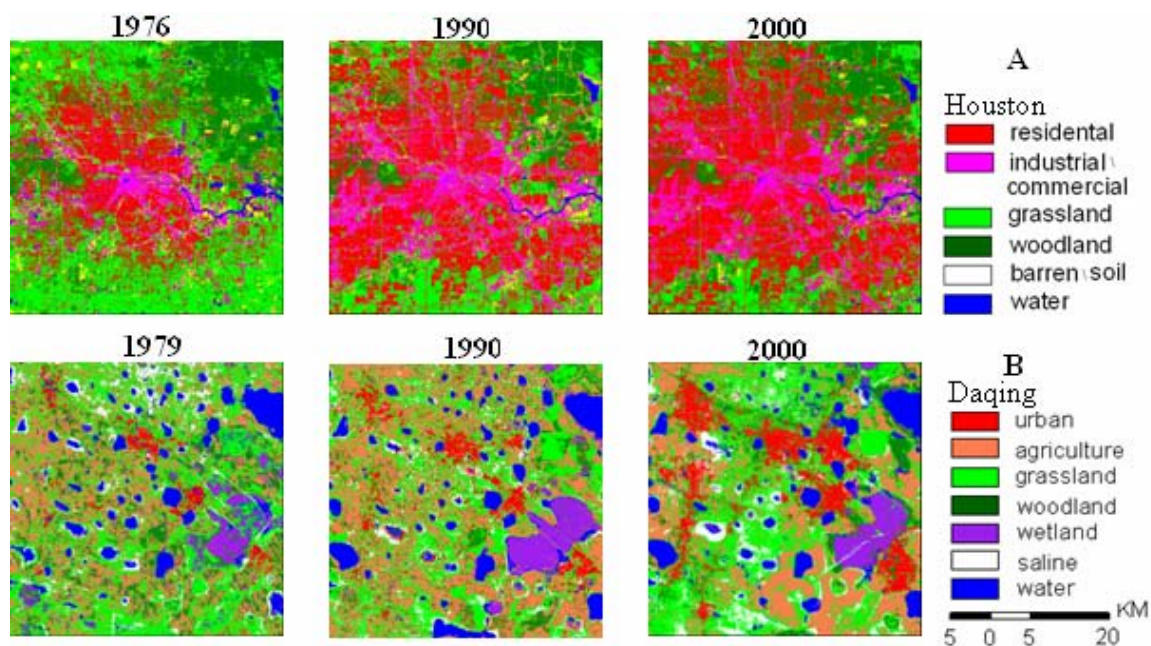
Fig. 9. The landscape maps of Houston and Daqing

Figure 9B is the landscape map of Daqing in 1979, 1990, and 2000. It reveals a north-south distribution throughout the whole study area. Most of the agriculture is distributed in the southeast and northwest of the study area, while the city itself lies along the railway line between the city of Haerbin and Qiqihaer. Most lakes distribute in the middle part of the study area, with the grassland and saline distributing around them.

Grassland was the dominant class in Houston, which occupied 511.34 km^2 and 41.61% of the whole study area in 1976 (Figure 9, Table 5). The residential area became the dominant class after the 1980s, occupying 479.78 km^2 (39.07%) in 1990 and 564.43 km^2 (45.97%) in 2000, respectively. The expansion of residential areas occupied a mass of grassland and woodland in the suburban area of Houston. Similar to Houston, the dominant class of Daqing is also grassland, occupying 432.67 km^2 and 35.21% of the whole study area with a large mean patch area (0.16 km^2/per patch) in 1979 (Table 5). As a part of alluvial Songnen plain, a mass of grassland in Daqing was cultivated into agriculture in the eastern area due to the fertile soil and sufficient rain conditions there. From 1990, agriculture became the dominant class, occupying 383.19 km^2 (32.82%) in 1990 and 419.63 km^2 (34.18%) in 2000, respectively.

Although grassland is the dominant class in both Houston and Daqing, it experienced a rapid decreasing in the mean patch area in these two cites. In Houston, it decreased from 0.12 km^2/ per patch to 0.01 km^2/ per patch in 1990 and 2000. In Daqing, the mean patch area of grassland decreased from 0.16 km^2/ per patch in 1979 to 0.03 km^2/ per patch in 1990 and 0.02 km^2/ per patch in 2000. This is in accordance with the fragmentation process caused by urban sprawl. Woodland, similar with the grassland, experienced the fragmentation process from the 1970s to 2000, in both Houston and

Daqing. It is interesting to find other impervious surfaces, i.e. residential or industrial /

commercial area had a decreasing average area though their total area increased. This

implies that new buildings are likely to be constructed sporadically far away from the

original building instead of just beside them. Although the water landscape does not own

a large area in Daqing, its average patch area is larger than other classes (0.08 km^2/ per

patch in 1979; 0.10 km^2/ per patch in 1990; and 0.07 km^2/ per patch in 2000). The reason

is obvious because water is found as lakes in Daqing and lakes are always naturally

continuous in space.

TABLE 6 THE ANALYSIS OF AREA CHANGE IN HOUSTON AND DAQING

Houston	Area (km^2)			Patch #			% Area			Average Area (km^2)		
	1976	1990	2000	1976	1990	2000	1976	1990	2000	1976	1990	2000
Residential	312.47	479.78	564.43	6401	16689	18712	25.43	39.07	45.97	0.05	0.03	0.03
Industrial / commercial	93.50	228.58	198.21	2282	12402	12286	7.61	18.62	16.14	0.04	0.02	0.02
Grassland	511.34	287.53	235.89	4416	19693	22052	41.61	23.42	19.21	0.12	0.01	0.01
Woodland	209.68	140.32	184.70	3325	4003	15048	17.06	11.43	15.04	0.06	0.04	0.01
Barren / soil	70.13	81.98	32.72	4404	19751	12364	5.71	6.68	2.66	0.02	0.00	0.00
Water	31.73	9.67	11.85	1655	722	1133	2.58	0.79	0.97	0.02	0.01	0.01
Daqing	Area (km^2)			Patch #			% Area			Average Area (km^2)		
	1979	1990	2000	1979	1990	2000	1979	1990	2000	1979	1990	2000
Urban	33.38	79.55	148.07	464	6333	5352	2.72	6.47	12.06	0.07	0.01	0.03
Agriculture	362.90	403.33	419.63	6544	12912	14409	29.53	32.82	34.18	0.06	0.03	0.03
Grassland	432.67	383.19	285.93	2757	11134	16400	35.21	31.18	23.29	0.16	0.03	0.02
Woodland	141.00	85.61	97.06	3334	11321	8297	11.47	6.97	7.91	0.04	0.01	0.01
wetland	70.18	72.05	62.90	1847	1771	3359	5.71	5.86	5.12	0.04	0.04	0.02
saline	76.27	89.21	102.19	1570	10421	8929	6.21	7.26	8.32	0.05	0.01	0.01
water	112.45	115.92	112.02	1499	1220	1700	9.15	9.43	9.12	0.08	0.10	0.07

Over the past 20 years, our study areas have experienced tremendous changes. The total change area in Houston between 1976 – 1990 and 1990 – 2000 are 629.48 km^2 and 262.49 km^2 and the percentage are 51.22% and 21.38%, respectively. As indicated in Figure 10A, the most significant change in Houston appears to be the spread of residential and build-up, and the loss of grassland. The total change area in Daqing between 1979 – 1990 and 1990 – 2000 are 209.74 km^2 and 219.55 km^2 and the percentage are 17.07% and 17.87%, respectively (Figure 10B). Compared with Houston, Daqing has a smaller change area. Only three classes have obvious changes: urban and agriculture increased, and grassland decreased.
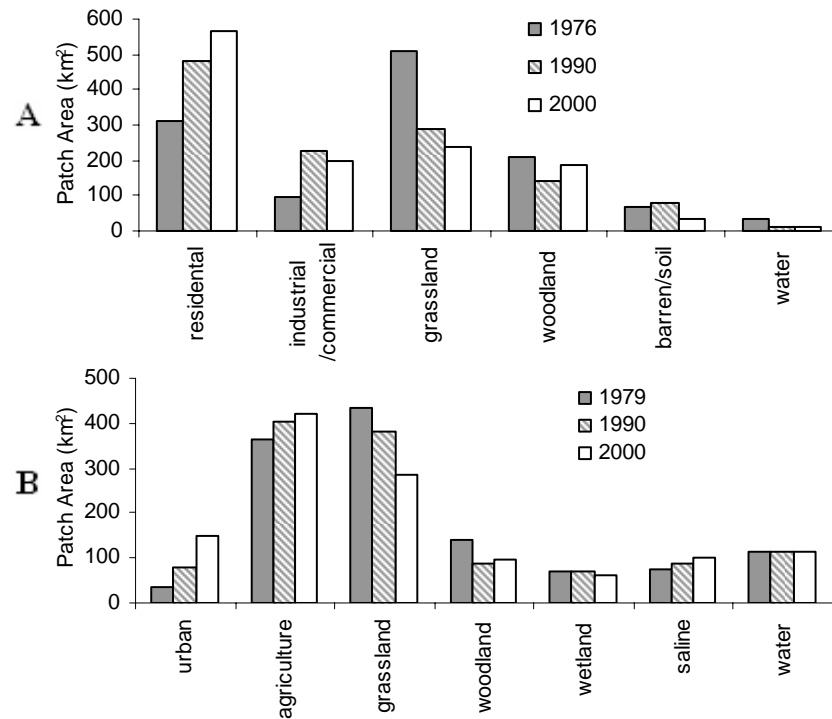
Fig. 10. Comparison of area change in Houston (A) and Daqing (B)

TABLE 7 THE DESCENDING SORT OF THE MAIN CHANGE OF HOUSTON AND DAQING

Transform Type (Houston)	1976-1990		Transform Type (Houston)	1990-2000	
	Change Area(km²)	% area		Change Area(km²)	% area
Grassland to Residential	204.22	16.74	Industrial /commercial to Residential	69.17	5.67
Grassland to Industrial /commercial	51.94	4.26	Grassland to Residential	68.70	5.63
Residential to Industrial / commercial	49.45	4.05	Grassland to Woodland	44.84	3.68
Woodland to Grassland	40.75	3.34	Residential to Grassland	35.80	2.93
Grassland to Barren / soil	39.30	3.22	Residential to Woodland	32.05	2.63
Transform Type (Daqing)	1976-1990		Transform Type (Daqing)	1990-2000	
	Change Area(km²)	% area		Change Area(km²)	% area
Grassland to Agriculture	124.06	10.10	Grassland to Agriculture	135.04	10.99
Agriculture to Grassland	117.24	9.54	Agriculture to Grassland	76.04	6.19
Woodland to Agriculture	63.94	5.20	Urban to Grassland	66.75	5.43
Woodland to Grassland	38.58	3.14	Woodland to Agriculture	38.94	3.17
Grassland to Saline	35.75	2.91	Saline to Grassland	36.55	2.97

Table 6 shows the descending sort of main changes in Houston and Daqing. This analysis of change landscape provides not only the "from" and "to" information, but also the quantity of the conversion area. The major changes can be summarized as follows:

o A Mass of grassland was converted to human-disturbed landscapes in both Houston and Daqing. Although this conversion was slowed down in Houston and some agriculture converted back to grassland in Daqing, grassland was ranked as

first in decreasing classes due to urban expansion during the last two decades for these two cities.

o The human-disturbed landscape, especially the impervious surface in urban area increased greatly during these two decades. In Houston, the residential area kept increasing while the industrial / commercial area decreased from 18.60% in 1990 to 16.13% in 2000. Most of the decreasing area in industrial / commercial is transformed to residential (69.17 km^2), which made the residential area increase. In Daqing, both urban and agriculture, experienced obvious increase during 1979 – 2000. Most of urban is transformed from grassland (26.42 km^2) and agriculture (20.73 km^2) and most cultivated land is converted from grassland (124.06 km^2) and woodland (63.94 km^2).

o Woodland experienced a significant decrease during the first period in both Houston and Daqing. During the second period, both Houston and Daqing have slightly increased in woodland. In Daqing, most woodland was transferred from agriculture (26.00 km^2) and grassland (28.96 km^2). The increase of woodland in Houston might be caused by newly planted trees around the new houses in southern and northern Houston.

o A general trend of landscape change was revealed: grassland was taken over by impervious surface due to the urban sprawl. Some of woodland was degraded into grassland, and trees were planted sporadically around the residential area, resulting in a more fragmented landscape.

Landscape Metrics Analysis of Dynamics

We applied the chosen landscape metrics to characterize the change of patch attribute and spatial heterogeneity in each class throughout Houston and Daqing. Table 7 and 8 show the changes of these indices in both Houston and Daqing. In this research, we analyzed the landscape in three major groups: (1) human-disturbed landscapes, including agriculture and urban area; (2) vegetation, including grassland and woodland; and (3) other barren surface, including the soil around the vegetation and barren area around the building.

TABLE 8 PATCH ATTRIBUTE INDICES OF HOUSTON AND DAQING

Houston	PSD			ED			LSI			AWMPFD		
	1976	1990	2000	1976	1990	2000	1976	1990	2000	1976	1990	2000
residential	166.70	94.56	245.60	61.80	125.32	144.30	107.40	175.89	186.84	1.28	1.34	1.42
industrial / commercial	44.25	98.88	42.70	19.44	71.52	59.27	61.68	145.35	130.54	1.18	1.32	1.26
grassland	405.97	25.91	19.43	74.78	91.13	84.42	102.42	165.54	168.82	1.34	1.24	1.22
woodland	162.22	40.09	21.27	26.69	25.68	54.94	57.16	66.84	124.28	1.22	1.19	1.19
barren / soil	4.64	2.61	1.51	21.10	48.50	22.48	77.63	165.43	120.61	1.10	1.14	1.12
water	22.46	17.77	14.18	7.53	2.41	3.46	41.06	23.67	30.83	1.13	1.20	1.20
Daqing	PSD			ED			LSI			AWMPFD		
	1979	1990	2000	1979	1990	2000	1979	1990	2000	1979	1990	2000
urban	44.39	15.35	68.82	5.06	27.63	35.88	26.96	97.14	90.48	1.19	1.23	1.32
agriculture	143.48	74.01	221.04	77.67	113.08	124.32	125.79	173.26	186.79	1.28	1.35	1.41
grassland	233.07	131.00	41.40	73.57	121.06	69.08	109.25	190.22	126.06	1.32	1.32	1.27
woodland	15.97	7.25	11.53	29.25	38.09	35.86	75.82	126.58	112.02	1.15	1.18	1.20
wetland	49.01	92.31	71.01	12.46	10.20	12.88	45.83	36.95	49.99	1.17	1.24	1.24
saline	24.80	8.25	14.65	14.51	37.08	36.94	51.22	120.65	112.37	1.15	1.19	1.22
water	69.00	78.43	65.02	9.99	8.43	12.19	29.17	24.16	35.72	1.09	1.09	1.12

In Houston, the PSD of residential area decreased in the first period and then increased in the second period (Table 7). A possible explanation is that more irregular-shaped residential areas appeared, not sprawling out from original buildings, but

gradually nibbling at the grassland around the urban area. The increasing of other patch attribute indices also indicates the residential area became more irregular. All the patch indices of industrial/commercial area in Houston increased in the first period and then decreased in the second period. This might because few industrial or commercial buildings were constructed in Houston due to the collapse of Houston's energy industry in the severe economic recession since the mid-1980s.

In Daqing, human-disturbed landscapes have a very similar trend with Houston. Both urban and agriculture have an increasing trend in ED, LSI, and AWMPFD. For all the landscape types, the Houston's residential and Daqing's agriculture have an identical trend in the patch attribute indices. This also indicates that the new small patches in them always appeared far away from original patches, instead of sprawled from them.

Grassland and woodland have different trends in our study areas, indicating different manners of conversion in these two classes. Since most of woodland is distributed in the northeastern corner of Houston, the edge of woodland was likely to be replaced by the impervious surface due to the urban sprawl during 1976 – 1990. At the same time, the grassland was fragmented into small pieces. During 1990 – 2000, more grassland was fragmented into pieces and then replaced by the impervious surface. Thus, PSD and AWMPFD, in both grassland and woodland, kept on decreasing during 1976 – 2000 with an increasing LSI.

It is also interesting to analyze different trends of grassland in Daqing and Houston. Although both of them have a decreasing patch area and increasing patch number, the LSI and AWMPFD indicated different locations of change areas. For Houston, most of grassland was updated by new residential buildings sprawling from the

central business district. In Daqing, the grassland was always cultivated into agriculture

far away from the urban; that is, the replacement always happened in the middle area of

grassland.

TABLE 9 SPATIAL HETEROGENEITY INDICES OF HOUSTON AND DAQING

Houston	SHDI			CONT			MNND			CAPL		
	1976	1990	2000	1976	1990	2000	1976	1990	2000	1976	1990	2000
residential	0.35	0.37	0.36	0.54	0.63	0.78	1.49	0.70	0.44	7.87	11.41	11.15
industrial / commercial	0.20	0.31	0.29	0.61	0.67	0.84	2.05	0.91	0.60	2.03	3.13	2.73
grassland	0.36	0.34	0.32	0.56	0.64	0.80	1.42	0.80	0.61	17.17	5.21	3.36
woodland	0.30	0.25	0.28	0.73	0.82	0.84	1.88	1.12	0.69	9.11	5.16	4.69
barren / soil	0.16	0.18	0.10	0.44	0.44	0.68	1.84	0.92	0.87	0.77	0.27	0.13
water	0.09	0.04	0.04	0.58	0.79	0.87	2.90	2.51	1.81	0.75	0.33	0.33
Daqing	SHDI			CONT			MNND			CPLI		
	1976	1990	2000	1976	1990	2000	1976	1990	2000	1976	1990	2000
urban	0.10	0.18	0.26	0.73	0.67	0.75	2.94	1.07	0.97	1.13	1.10	3.35
agriculture	0.36	0.37	0.37	0.47	0.64	0.59	1.37	0.76	0.76	7.33	6.70	5.86
grassland	0.37	0.36	0.34	0.54	0.60	0.71	1.37	0.71	0.85	11.31	5.33	8.28
woodland	0.25	0.19	0.20	0.59	0.58	0.63	1.84	0.92	1.01	3.09	0.75	1.15
wetland	0.16	0.17	0.15	0.67	0.87	0.80	2.55	1.36	1.22	2.28	3.16	2.62
saline	0.17	0.19	0.21	0.65	0.61	0.64	2.19	0.92	1.02	1.84	0.93	1.29
water	0.22	0.22	0.22	0.83	0.93	0.89	2.70	1.63	1.26	6.26	7.10	6.03

The result of spatial characterization indices suggests that these indices, as the

indicators of relation between the patches, provide complementary information to those

shape characterization indices (Table 8). In Houston, the CONT and MNND showed an

identical trend in all landscape types. This trend implies that all classes have a more

clustered pattern, with less mixture with other classes. Residential and

industrial/commercial have the same trend in the CAPL, which increased first and then

decreased. This might be caused by the planting of trees around new residential buildings,

which brought meandering edges to these impervious surfaces. The decreasing CAPL, in

both grassland and woodland, implies a more fragmented landscape associated with vegetation.

In Daqing, both urban and agriculture have an increasing SHDI and decreasing MNND. While in the CAPL, urban decreased lightly first (1.13 in 1979 and 1.10 in 1990) and increased greatly (3.35 in 2000) in the second period. Agriculture kept on decreasing in CAPL during 1979 – 2000. This different trend in urban and agriculture also denotes different conversion manners in them. Since new agriculture patches were always small, the CAPL and MNND kept on decreasing. More and more small urban patches were connected with original large ones during the second period, the CPLI of urban increased greatly during the second period though the MNND kept decreasing. As a typical decreasing landscape, grassland had a slight increase during the second period in the MNND and CAPL. The MNND and CAPL of grassland in Houston are different from those in Daqing. These different trends imply that the transformation of grassland in Houston always happened from the boundary area to the core area. Similarly, the MNND and CAPL of woodland in Daqing have a same change trend: decreased greatly in the first period and increased slightly in the second period. On the contrary, direct replacement of forest patches along the boundary dragged both the MNND and CPLI down in Houston.

Conclusion

The quantitative analysis of landscape pattern using multi-temporal Landsat images enabled us to characterize the internal structure of landscape, compare landscape classes, and monitor the landscape dynamics throughout both Houston and Daqing. This

study explored the potential of satellite remote sensing and GIS-related techniques in producing accurate landscape maps and statistical analysis of the landscape pattern.

Petroleum is the major economic source in Houston and Daqing. Agriculture is another economic support in Daqing due to its historical development. Although Houston has a similar physical environment as Daqing, it has no farmland around the city centre. Therefore, Daqing has an obvious trend in cultivating grassland into agriculture as well as the urban sprawl.

Landscape dynamics throughout the study area were estimated based on the analysis of multi-temporal maps. Obviously, Houston is a concentric-zonal pattern based on one central business district (CBD) while Daqing is a multiple-nuclei pattern in its expansion. This analysis indicated that during the first period, Houston experienced more change than Daqing due to the energy industry boom. Daqing kept expanding in the second period, while the sprawl of Houston slowed down from the 1990s due to the decline of petroleum production. Based on the derived indices, a general trend of landscape change was revealed: Houston experienced the urban expansion by gradually replacing the grassland around the suburban area during the first 10 years, whereas a mass of grassland and woodland was cultivated and taken over by agriculture and urban in Daqing.

This study also revealed that spatial indices built on the classified vectors were useful to detect landscape pattern and its changes. The patch attribute indices, PSD, ED, LSI, and AWMPFD, were found to be effective in the identification and description of the shapes of landscape types. The SHDI revealed the patch diversity associated with the proportion of landscape classes; CONT measured the degree of contiguity and

homogeneity by revealing the clumping trend of patches for each class; MNND reflected underlying natural processes or human-caused disturbance patterns, while CAPL measured the degree of fragmentation by the area of interior habitat. All these spatial heterogeneity indices have a great potential in providing useful information about the overall spatial pattern of the landscape. With incorporating more and more biophysical or social-economic factors in this research, the spatial statistics methods will demonstrate its unique role in the quantitative analysis of landscape pattern.

Current research results can be further improved from the following three aspects. First, ecological, social, political, and economic factors should be incorporated in the analysis of change detection. The added awareness of the landscape context from these factors will assist us in making objective statements about the changes in time series. Second, based on this analysis, we can found the urban area, especially the residential area, is major landscape type in Houston study area while the agriculture and grassland are two major landscapes in Daqing. Obviously, Houston is much more heterogonous than Daqing which requires a more sophisticated sub-pixel classification method for Houston. Third, the emphasis of this study is to assess landscape complexity and its dynamic process in the past and current time. In this dissertation, landscape metrics were calculated either on class or on landscape. This prevented us to apply these results into a cell-based model, such as the Cellular Automata model in the later study. A natural future is to develop a set of cell-based metrics for the further model application.

CHAPTER V

IMPROVING URBAN LANDSCAPE CLASSIFICATION

Introduction

Understanding the extent, distribution, and evolution of urban landscape is critical in analyzing and explaining its structure. Such information plays a vital role in predicting future urban landscape patterns and guiding the direction of urban planning for satisfying both environmental and socioeconomic sustainability. Moderate resolution satellite images such as Thematic Mapper (TM), provide a distinctive opportunity to capture urban landscapes over a large area in a timely and cost-effective manner (Yang and Lo 2002; Song 2005). Traditional per-pixel methods, nevertheless, are inadequate in classifying urban landscape from the moderate satellite imagery due to the presence of many mixed land cover categories in each pixel, as a result of the rapid alternation of artificial and natural objects within a small distance in a typical urban setting (Mesev et al. 2001; Small 2003; Lu and Weng 2004). Treating each individual pixel as a pure class, as has been assumed in such per-pixel classifiers, prevents the representation of varying land cover and use information below the inherited pixel resolution (Gong and Howarth, 1989; Foody and Arora 1996, Small 2004).

Instead of assigning only one class per pixel, sub-pixel classification approaches quantify multiple class memberships for each pixel (Foody and Cox 1994; Foody 1996;

Foody 1997; Myint 2003). Spectral mixture analysis (SMA) represents a widely-used method for tackling the decomposition of mixed pixels. The Linear SMA has so far been the most popular approach in the SMA family methods given its simple mathematical form. It has been adopted to generate fractions of urban physical constituents according to the spectral variability inherited in either multi- or hyperspectral imagery (Settle and Drake 1993; Tompkins et al. 1997; Small 2001; Wu and Murray 2003; Lu and Weng 2004). For the purpose of standardization, Ridd (1995) proposed the vegetation-impervious surface-soil (VIS) model to parameterize the biophysical composition of urban environment as vegetation, impervious surface, and soil. This model was later adopted as a scheme for choosing appropriate endmembers in the linear SMA (Madhavan et al. 2001; Phinn et al. 2002). Small (2001) conducted a spectral unmixing to characterize the pattern of New York City through three modified endmembers: vegetation, low albedo, and high albedo. Wu and Murray (2003) separated the impervious endmember as the low albedo and high albedo to accommodate four endmembers in the VIS model. Lu and Weng (2004) included the shade endmember in the spectral mixture analysis for Indianapolis, Indiana.

One critical problem encountered in the application of Linear SMA is that the number of endmembers has to be kept at a fairly limited size since it is constrained by the number of available bands offered by the remotely sensed imagery (Radeloff et al. 1999). Moreover, the impervious surface in the VIS model is not appropriate to be treated as one endmember given that the presence of various components are not unusual (Wu and Murray 2003; Lu and Meng 2004). A number of approaches have been made to address this question by either modifying the endmembers or altering from a simple Linear SMA

to a nonlinear function. Examples of these methods include iterative spectral unmixing (Meer 1999; Theseira 2002); endmember bundles approach (Bosdogianni et al. 1997; Bateson et al. 2000); neural network (Foody et al. 1997; Carpenter et al. 1999; Linderman et al. 2004); mixture discriminant analysis (Ju et al. 2003); and Bayesian spectral unmixing (Song 2005).

Fuzzy classification is another robust method which provides class memberships at the pixel level. After Zadeh (1965) introduced the fuzzy set concept in 1965 to describe imprecision, the fuzzy set concept was then widely applied to sub-pixel image analysis. Fuzzy C-Means (FCM) algorithm (Bezdek et al. 1984; Foody 1992), Fuzzy-Maximum Likelihood Classification (Wang 1990), and Neuro-Fuzzy (Carpenter et al. 1999), are three prevalent approaches in this category. Based on an iterative optimization of clustering, Fuzzy C-Means limits its application when the priori knowledge of the number of cluster and local optima are not enough (Bandyopadhyay 2005) before classification. Fuzzy-Maximum Likelihood Classification and Neuro-Fuzzy are two supervised soft classifications by softening the output of traditional Maximum Likelihood Classification and Neural Network Classification. Typically, these two methods need to identify the training samples to characterize the classes in the image. However, inability to account for mixed pixels when collecting information from the training samples, as a general practice when the aforementioned methods were applied, has circumvented the implementation of a "fully" fuzzy classification (Zhang and Foody 2001). Therefore, it is critical to choose proper endmembers and solve the mixed pixel problem for the fuzzy training data in order to perform an accurate supervised soft classification in urban areas.

In this study, I focus on the development, implementation, and evaluation of a new Fuzzy-SMA model based on the fuzzy supervised classification, along with the linear SMA, to improve the urban landscape classification accuracy. Considering both the availability of data and the practicability of results, I only apply this sub-pixel classification to Houston since Daqing is much more homogenous than Houston. Particularly, endmember signatures of training samples are not treated as constants, but rather represented by the probability density using the linear SMA. In order to examine the effectiveness of this new method, we compare the fraction images from our Fuzzy-SMA model with the fraction images that were derived from the linear SMA and maximum likelihood classification (MLC) methods.

Data Preparation

A subset image from Landsat 7 ETM+ (path 25, row 39) acquired on January 2, 2003 was employed in this study. For the sake of reducing atmospheric distortion, the digital number (DN) at each band was first converted to the normalized at-sensor reflectance using the method that was introduced in Markham and Barker (1987) (Figure 11; ENVI 2000). Figure 12 shows the normalized reflectance for each representative class. The Minimum Noise Fraction (MNF) transformation was then applied to remove the correlation that existed among six bands (the thermal band was excluded since it has a different spatial resolution) (ENVI 2000) (Figure 12). A bundle of IKONOS image, comprising a 1-meter panchromatic and 4-meter multispectral images, that were acquired on January 2, 2002, were adopted as references for choosing the training samples for different endmembers as well as the test samples of known fractions from land ETM+.
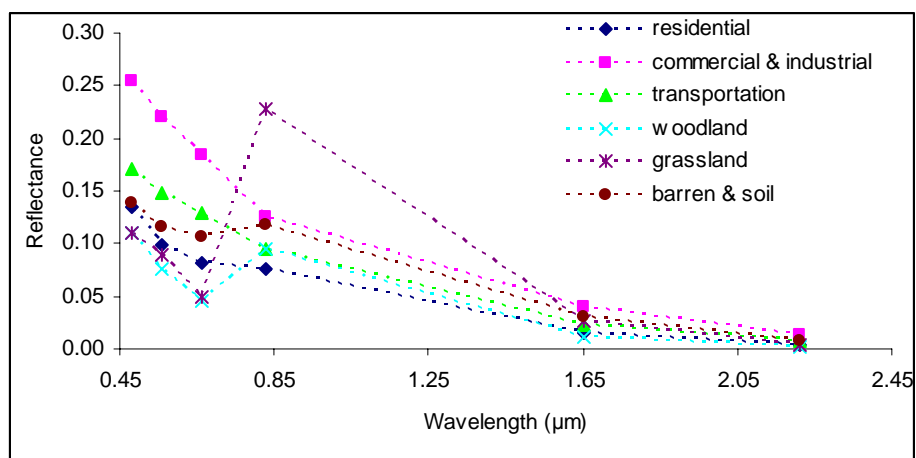
Fig. 11. Normalized at-sensor reflectance for the representative urban LULC wavelength
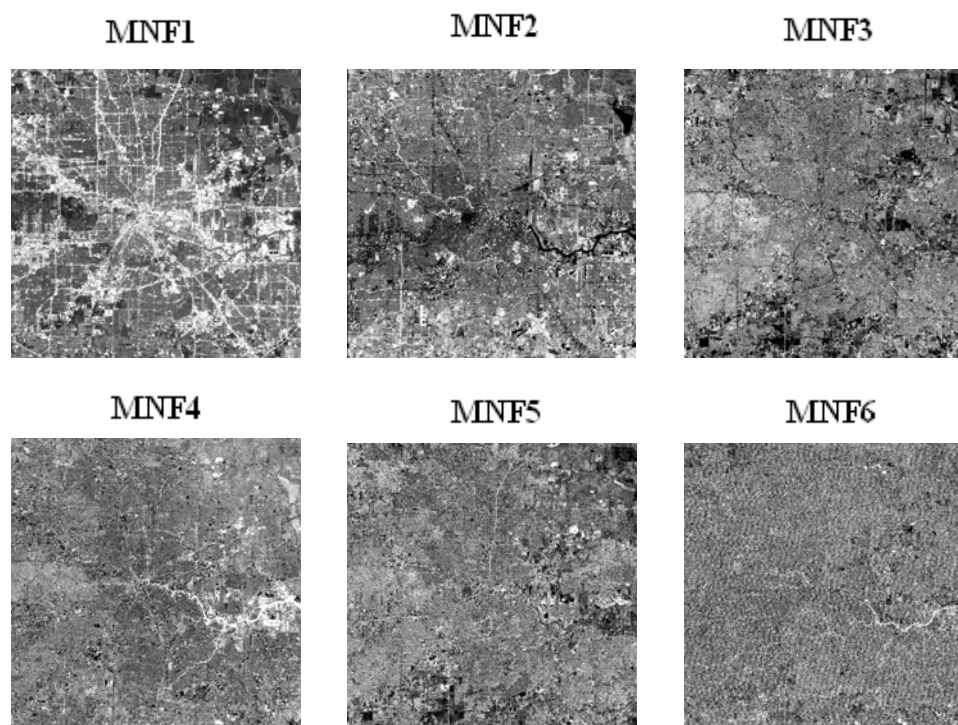
Fig. 12. MNF components of ETM+ image

<u>Methodology</u>

     A systematic framework of our model is presented in Figure 13. Three sets of proportion maps were derived using linear SMA, Partial-Fuzzy, and Fuzzy-SMA, respectively. The major difference between the Partial-Fuzzy and Fuzzy-SMA lies in the training spectrum among landscape classes. In the Fuzzy-SMA, we applied the linear SMA to obtain the fuzzy mean and fuzzy covariance matrix instead of treating them as constants. Based on these statistical measures, we derived the fractions of urban images using the fuzzy set theory. The following sections will describe the fuzzy logic and SMA in detail.
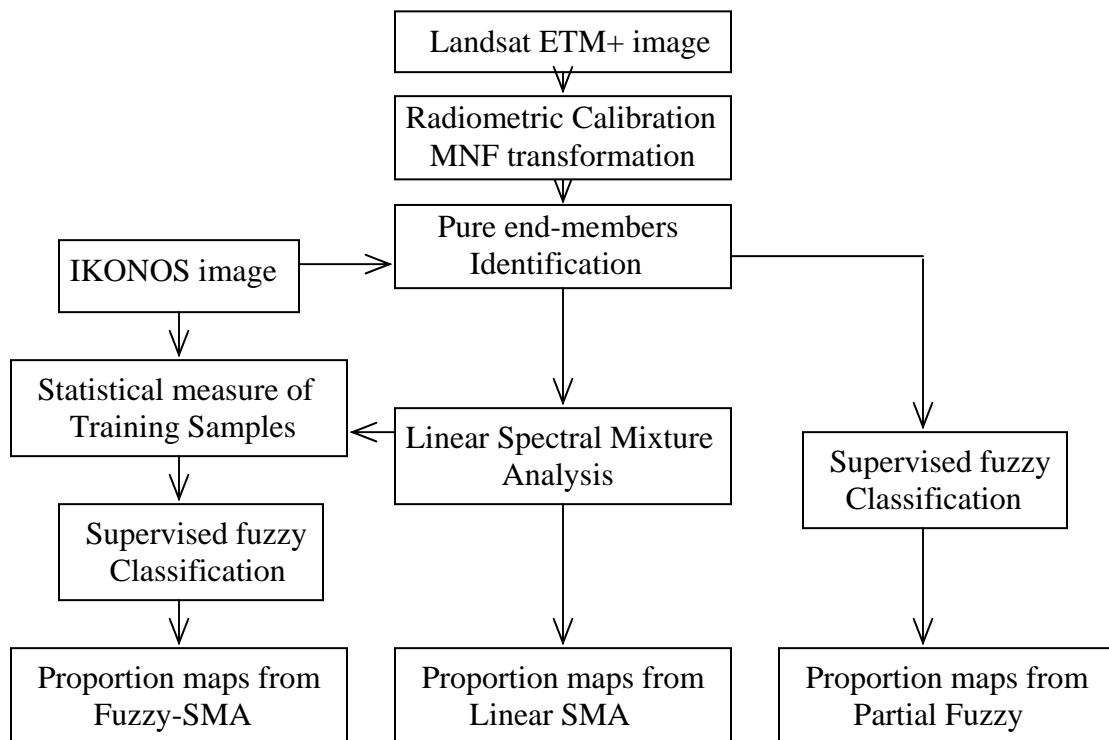
Fig. 13. Flowchart for the Fuzzy-SMA model. Note: IKONOS image is used to select pure endmembers and training samples, as well as check the resultant proportion maps from three sub-pixel classification models

Fully-fuzzy Supervised Classifier and its Training Data

Conventional discriminant analysis is a widely used classifier in the classification of remotely sensed data. This method allocates each pixel to the class which has the highest posteriori probability of membership (Foody 1996; Richards and Jia 1999). Without considering the prior probability, the posteriori probability, also named as discriminant function, is expressed as:

(5.1) $$g_i(x) = -\ln|\Sigma_i| - (x - m_{bi})^t \Sigma_i^{-1}(x - m_{bi})$$

Where x is the b-dimension pixel vector for b bands; m_i and Σ_i are the mean vector and variance-covariance matrix of training samples of class i respectively (Richards and Jia 1999).

To implement a fully-fuzzy supervised classification, we derived the fuzzy mean and fuzzy variance matrix (Wang 1990) from training samples in addition to "soften" the output of conventional "hard" classifiers by the fuzzy classifier. The fuzzy mean m_i^* and fuzzy variance matrix Σ_i^* can be derived from:

(5.2) $$m_i^* = \frac{\sum_{i=1}^{M} f(x_i)x_i}{\sum_{i=1}^{M} f(x_i)}$$

and

(5.3) $$\Sigma_i^* = \frac{\sum_{i=1}^{M} f(x_i)(x_i - m_i^*)(x_i - m_i^*)^T}{\sum_{i=1}^{M} f(x_i)}$$

Where x_i is the pixel spectral vector of the training samples of class i, M is the total

number of training samples; and $f(x_i)$ is the membership function of class i.

Training samples for six classes, including residential area, commercial or

industrial area, transportation, woodland, grassland, barren or soil, were selected from the

Landsat ETM+ image by referencing to the IKONOS image. Water was masked out

before the analysis since it occupies only a small area in the study area. Samples for each

class come from thirty training plots and each training plot covering 90×90 m^2 on the

ground. Due to the mixture of membership in each training plot, it is important to identify

the proportions of endmembers in these training plots before an accurate fuzzy mean and

fuzzy variance matrix can be derived. For example, Wang (1990) estimated the

endmembers' fractions from training plots with manual interpretation from aerial

photography. However, the inaccurate estimation of fuzzy mean vector and fuzzy

variance matrix through manual digitization often leads to poor classification results. In

this research, we applied the Spectral Mixture Analysis (SMA) to identify the fraction

membership of the training sample.

Spectral Mixture Analysis

Spectral mixture analysis (SMA) aims to map the fractions of landscape classes

within mixed pixels using an inverse lease square devolution method and spectra of pure

endmembers (Shimabukuro and Smith 1991; Gilabert, Garcia-Haro, and Melia 2000). In

this study, we employ a modified constrained least square method for the linear spectral

unmixing analysis using the following expression:

(5.4) $$R_n = \sum_{e=1}^{E} R_{n,e} f_e + \varepsilon_n \quad with \sum_{e=1}^{E} f_e = 1 \, and \, \, 0 \le f_e \le 1$$

Where R_n is the normalized spectral reflectance of the mixed pixel for each band n; f_e is

the fraction of endmember e; E is the total number of endmembers; $R_{n,e}$ denotes the

normalized spectral reflectance of endmember e within a pure pixel on band n; and ε_i is

the residual error.

The choice of spectral reflectance for endmembers is critical for the spectral

mixture analysis. An optical approach for selecting endmembers is to use laboratory-

based spectra from the field. However, substantial problems exist in accounting for the

atmospheric conditions when upscaling the field spectral value to the level that can be

employed with the satellite sensor data (Settle and Drake 1993; Wu and Murray 2003).

Alternatively, the endmembers' spectra can be obtained by locating pure pixels on the

same image (Bateson et al. 2000; Lu and Weng 2004). In our study, the endmember for

each class is carefully selected from the representative homogenous pixel, i.e. having a

full membership to the specified class and zero membership to the other classes. To

ensure the purity of the chosen pixel from the ETM+ image, the high spatial resolution

IKONOS image was employed as a reference image. The clear delineation of feature

spaces among the six classes in the first three Principle components (Figure 14) suggests

that the reflectance spectra of the ETM+ image could be represented by a six-endmember

linear mixing model.
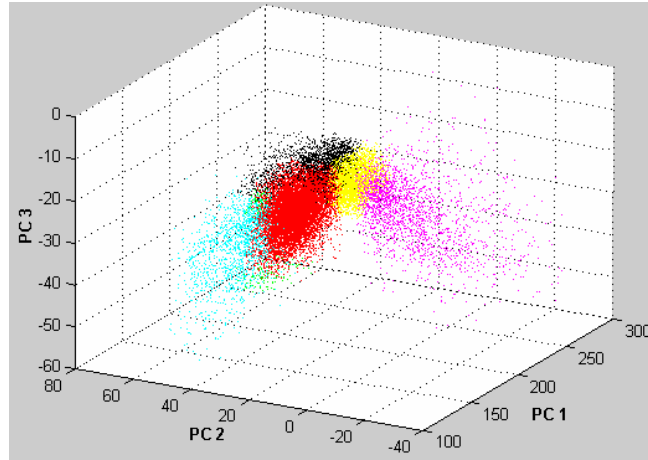
Fig. 14. Feature space representation of the first three principle components. Red: residential; Magenta: commercial or industrial; Yellow: transportation; Green: woodland; Cyan: grassland; Black: barren or soil

Accuracy Assessment

The accuracy assessment is an essential step for landscape mapping from remotely sensed data (Foody 2002). An independent set of test samples was chosen for this evaluation. Considering the statistical requirement and the size of our study area, we randomly selected 200 sample plots at the size of 90×90 m^2 from the IKONOS image using the ERDAS Imagine accuracy assessment module (Figure 15). For each sample unit, its actual land use types were acquired through digitizing the IKONOS image (Figure 16b). The actual fractions of each landscape class in sample units were obtained through dividing the class area by the total area of one sample plot.
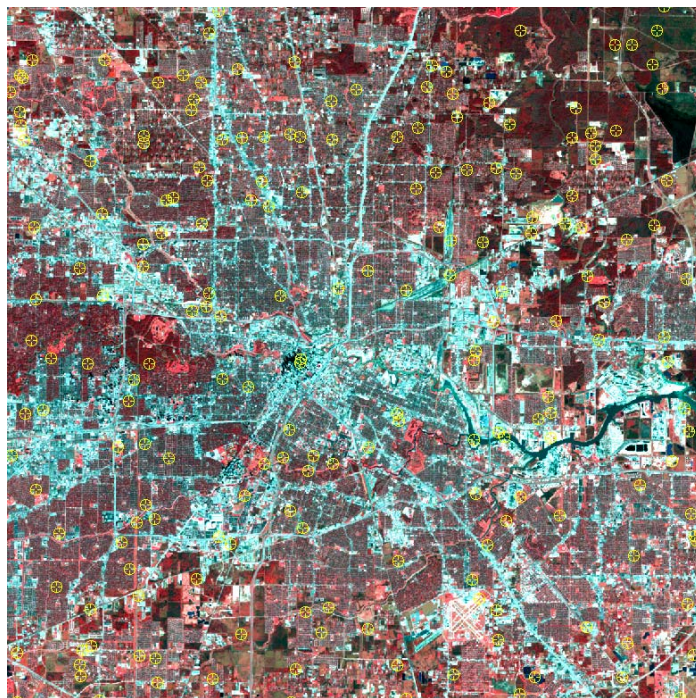
Fig. 15. Random test points distribution in the study area
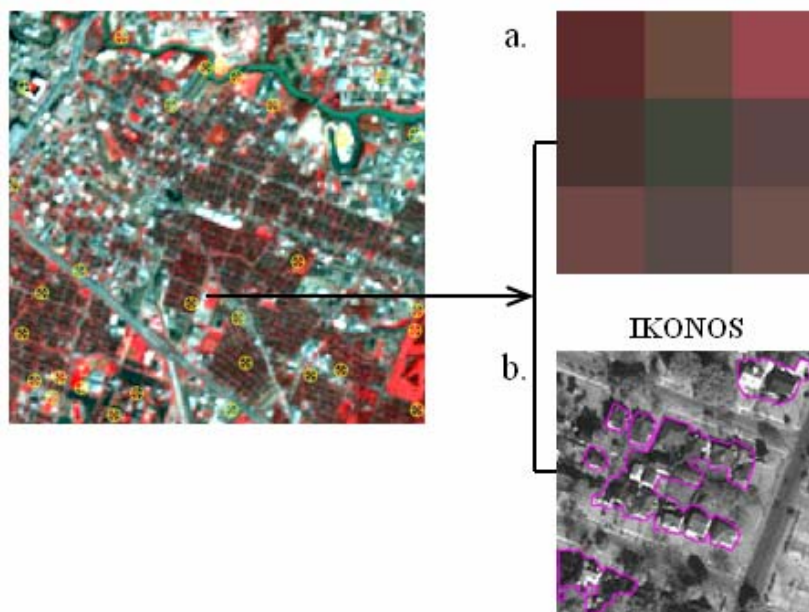
Fig. 16. The sample fraction validation using IKONOS, (a) one test plot in ETM; (b) corresponding IKONOS test plot, the magenta line is used to digitize the residential area in this unit

As stated by Foody (1996), conventional confusion matrix is inappropriate for the fuzzy classification evaluation since multiple memberships exist with each pixel. In this research, we adopt two accuracy assessment methods to evaluate the accuracy of urban composition of each land class. The first method is the mean absolute error (MAE) (Willmolt and Matsuura 2006) defined as follows:

$$(5.5) \qquad MAE_i(^1P, {}^2P) = \frac{\sum\limits_{n=1}^{N} \left| {}^1P_i - {}^2P_i \right|}{N}$$

$$(5.6) \qquad Total\_MAE = \sum\limits_{i=1}^{J} MAE_i$$

Where ^1P_i is the estimated land use composition fraction from the classification and ^2P_i is the "actual" land use composition fraction digitized from IKONOS for class i in the test simple n; N is the total number of test samples and J represents the number of categories.

The generalized cross-tabulation matrix as introduced by Pontius JR and Cheuk (2006) was also adopted to further analyze the disagreement between the estimated results and reference maps. Specifically, a composite operator was used to calculate the entries in the cross-tabulation matrix through:

(5.7)

$$P_{i,j} = \begin{cases} MIN(^1P_i, {}^2P_i) & if \ i = j \\ or \\ [^1P_i - MIN(^1P_i, {}^2P_i)] \times [(^2P_j - MIN(^1P_j, {}^2P_j)) / (\sum\limits_{j=1}^{J} (^2P_j - MIN(^1P_j, {}^2P_j)))] & if \ i \neq j \end{cases}$$

Where $P_{i,j}$ is the estimated entry in the cross-tabulation matrix for class i and class j.

Once all entries were filled, overall accuracy and Kappa values were calculated in the same manner as that was applied in the traditional hard classification. Further details about the accuracy assessment in soft classification can be found in Pontius and Cheuk (2006).

Results and Discussions

Figure 17 is the classified image of downtown Houston from the supervised MLC method in 2003. Different from the landscape maps created in Chapter IV, this map also classified the transportation area out from the images. It reveals the *central-zonal* spatial pattern throughout the whole study area. Most industrial or commercial area is located in the central business district (CBD) or distributed along the major road or the Buffalo Bayou. High-density residential areas are found around the CBD, especially around the highway I45 and the Buffalo Bayou in the southern study area. The woodland is mainly seen in the northeastern area of Houston. Grassland is mainly distributed in the southern part, mostly around the Houston International Airport. Although the supervised classification result describes the overall urban land use pattern, it could not provide a realistic or accurate measurement on urban pattern since it neglected the relative abundance of surface materials within a pixel.
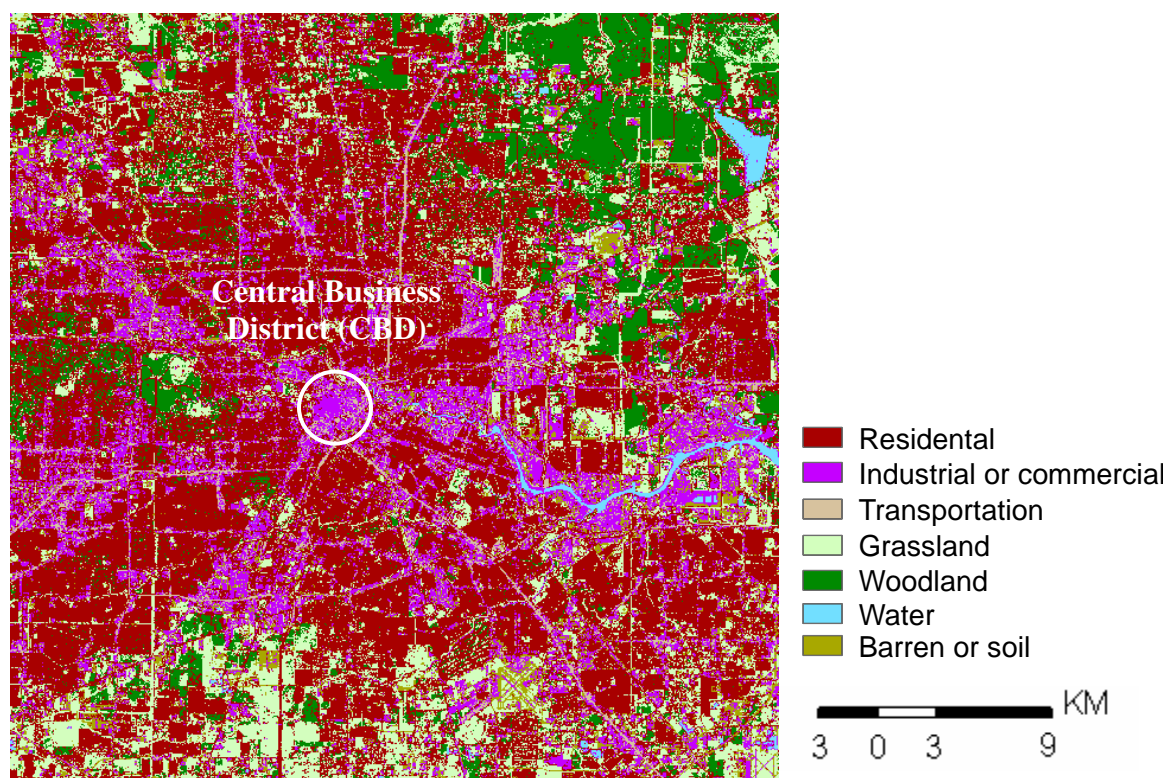
Fig. 17. Classified images generated from the MLC method

Conversely, a richer amount of land use information has been derived by the "soft" classification. Figure 18 illustrates six fraction images unmixed from the ETM+ image using the Linear SMA model. We used the gray level to designate the percentage of a specific class that a pixel contains. Therefore, a brighter pixel means a higher fraction. It is noticeable that the fraction images of all classes have a similar gray level. These results may be attributed to the spectral similarity among the six classes. The most obvious misinterpretation is the confusion between transportation and commercial/industrial area in the central part of the study area. Therefore, the Linear SMA would result in substantial misinterpretation due to the spectral similarity among classes.
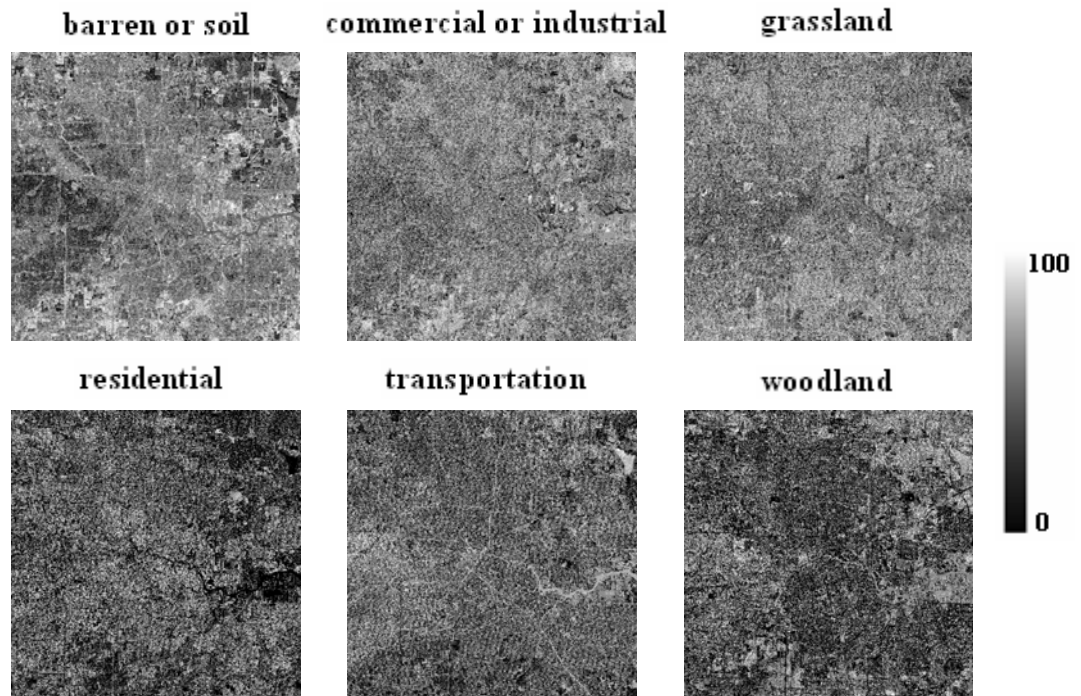
Fig. 18. Fraction images generated from the SMA model

The fraction images derived from the Partial-Fuzzy method (Figure 19) present a more obvious pattern than the Linear SMA. Particularly, fractions of the commercial/industrial area and the residential area have been refined. The bright pixels in the two fraction images correspond well to the known impervious area within the original ETM+ image. Moreover, the woodland fraction image concurs with the field woodland distribution: i.e., almost zero in the CBD and ranging between 60-80% in the residential areas.
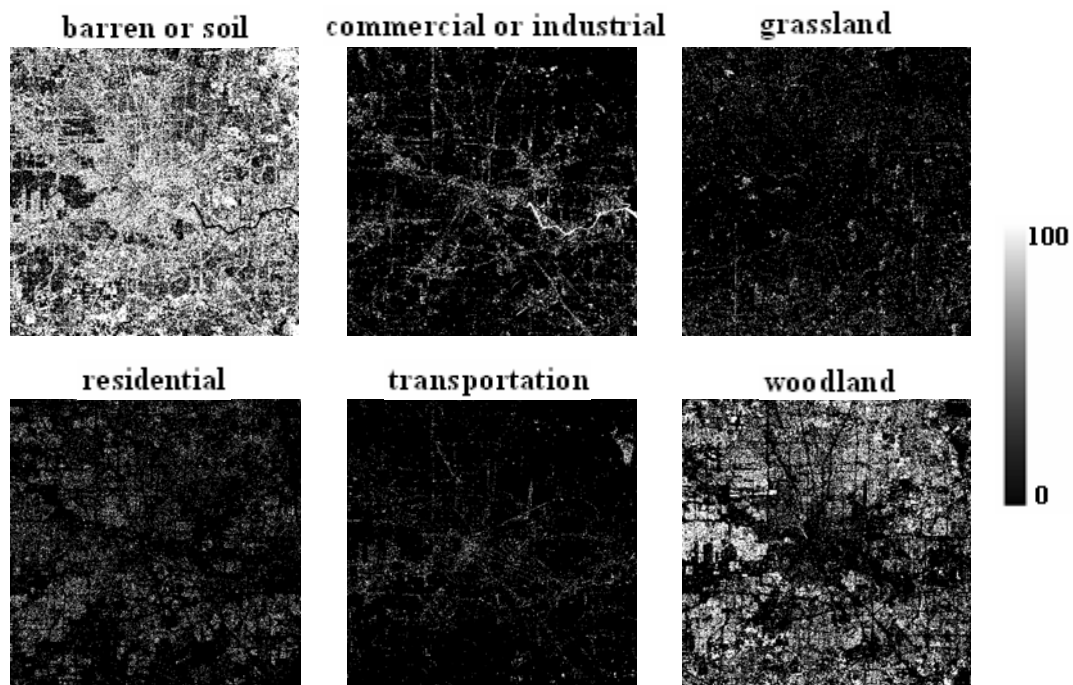
Fig. 19. Fraction images generated from the Partial Fuzzy model

The fraction images from the Fuzzy-SMA model achieved a remarkable improvement compared to both Linear SMA and Partial-Fuzzy methods. In Figure 20, the brightest spot, as an indicator of high proportion for the commercial/industrial fraction image, is located in the central area of the study area. The residential fraction is near zero in the high-density commercial or industrial area, while gradually increased to 10%-50% in the transition zone between the industrial area and residential area, and approach 90% in the high-density residential area. The transportation fraction image is also consistent with its actual distribution, showing an interlaced pattern. Most grassland is located in the southeastern corner and almost tops at 100% in the park area. The woodland has the least fraction in the central area of Houston, ranging between 10% and 30%. The brightest spot of the woodland is found in the known woodland area, the northeastern area of Houston. The fact that Fuzzy-SMA performed better than the Linear SMA can be attributed to the incorporation of fuzzy mean and fuzzy variance, with which the spectral overlaps between the endmembers has been significantly reduced.
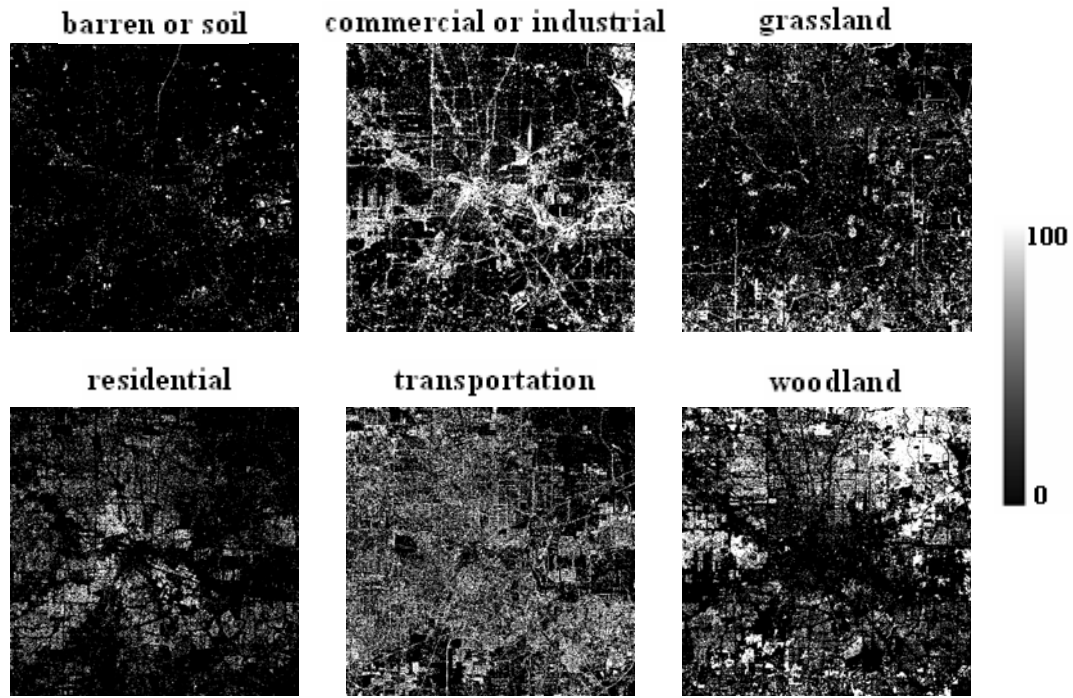
Fig. 20. Fraction images generated from the Fuzzy-SMA model

Table 9 shows the accuracy indices (MAE) and the cross-tabulation matrix for the Fuzzy-SMA, Partial-Fuzzy, Linear SMA, and MLC. In Table 9, a smaller indice denotes a better classification result. From this table we can easily find that the Fuzzy-SMA performed better than the other two methods since it has the smallest MAE (0.35). A detailed examination with the MAE shows that Fuzzy-SMA performed well with the impervious surface, e.g. the commercial or industrial area (0.06), residential area (0.05), and transportation area (0.09). The best fraction is associated with the barren/soil, having the smallest MAE (0.01). A possible explanation could be that most of the training samples for barren/soil are mixed with vegetation, especially for the "fragmentized" grassland. The Fuzzy-SMA accounts for the fractions in dealing with the training samples, thus reduces the signature confusion between the vegetation and soil.

TABLE 10 COMPARISONS OF MAE FOR THE FUZZY-SMA, PARTIAL-FUZZY, LINEAR SMA AND MAXIMUM LIKLIHOOD CLASSIFICATION

	Accuracy Assessment	residential	commercial or industrial	transportation	grassland	woodland	barren or soil	**overall**
	MLC	0.48	0.08	0.25	0.17	0.12	0.04	1.15
	Linear SMA	0.15	0.17	0.20	0.17	0.13	0.14	0.96
MAE	Partial-Fuzzy	0.13	0.10	0.28	0.17	0.14	0.46	1.27
	Fuzzy-SMA	0.05	0.06	0.09	0.06	0.08	0.01	0.35

Table 10 shows the cross-tabulation matrix for the MLC, Linear SMA, Partial-Fuzzy, and Fuzzy-SMA. The diagonal numbers in the matrix were underlined to highlight the agreement between the classified results and empirical map. Obviously, Fuzzy-SMA showed an obvious improvement in the results with the highest overall accuracy (82.11%) and Kappa (77.33%). Specifically, Fuzzy-SMA has the highest agreement in the commercial / industrial area (11.63%), transportation (26.83%), and woodland (16.40%).

TABLE 11 THE CROSS-TABULATION MATRIX FOR THE MLC, LINEAR SMA, PARTIAL-FUZZY, AND FUZZY-SMA

		EMPIRCIAL MAP					
		residential	commercial or industrial	transportation	grassland	woodland	barren or soil
	residential	17.77	3.73	20.30	8.77	15.90	0.70
		11.84	**1.71**	**3.86**	**1.83**	**1.51**	**0.11**
		9.15	*0.25*	*2.28*	*1.37*	*0.66*	*0.01*
C		***16.17***	***0.07***	***0.37***	***1.35***	***1.09***	***0.09***
L	commercial	0.13	6.20	1.48	0.38	0.29	0.54
A	or industrial	**2.05**	**5.26**	**3.30**	**1.71**	**3.69**	**0.03**
S		*0.01*	*3.51*	*0.89*	*0.35*	*0.09*	*0.00*
S		***0.45***	***11.63***	***1.78***	***2.19***	***0.92***	***0.26***
I	transportation	0.00	1.53	6.02	0.64	0.13	0.17
F		**0.23**	**0.70**	**12.12**	**0.72**	**1.33**	**0.13**
I		*0.01*	*0.37*	*1.39*	*0.10*	*0.02*	*0.00*
E		***0.98***	***0.26***	***26.83***	***2.81***	***1.98***	***0.47***
D	grassland	0.03	0.01	0.34	6.73	1.07	0.15
		1.20	**0.98**	**2.32**	**10.36**	**2.18**	**0.04**
R		*0.07*	*0.03*	*0.44*	*4.04*	*0.22*	*0.00*
E		***0.10***	***0.00***	***0.03***	***10.07***	***0.71***	***0.14***
S	woodland	0.00	0.00	0.00	0.00	3.48	0.00
U		**0.73**	**1.61**	**2.32**	**0.64**	**9.35**	**0.13**
L		*2.05*	*0.40*	*4.52*	*4.31*	*14.68*	*0.11*
T		***0.31***	***0.01***	***0.40***	***0.85***	***16.40***	***0.10***
	barren or soil	0.05	0.63	1.27	0.77	0.24	0.57
		1.96	**1.82**	**5.52**	**1.96**	**3.07**	**1.71**
		6.77	*7.53*	*19.85*	*7.08*	*5.41*	*2.04*
		0.00	***0.06***	***0.00***	***0.07***	***0.03***	***1.02***

Overall Accuracy: MLC (40.77); Linear-SMA (50.65); Partial-Fuzzy (34.81); Fuzzy-SMA (82.11)
Kappa: MLC (27.85); Linear-SMA (40.82); Partial-Fuzzy (26.76); Fuzzy-SMA (77.33)

Note: The MLC gives the upper number in normal font, the Linear SMA gives the second number in bond, the Partial-Fuzzy gives the third number in italics, and the Fuzzy-SMA gives the fourth number in bond and italics.

Further analysis on the cross-tabulation matrix suggests that there are still some drawbacks with the sub-pixel classification methods. In the cross-tabulation matrix, the improvement from the MLC to the Linear-SMA mainly can be found in the transportation (from 6.02% to 12.12%), grassland (from 6.73% to12.36%), and barren/soil (from 0.57% to 1.71%). These classes usually have a distinct spectral

characteristic. Other classes, such as the residential and commercial/industrial, due to the

spectral confusion, obtained even worse results with the Linear-SMA.

A regression analysis was carried out between the actual class fractions and

estimated fractions for the three models (Figures 21-24). The distance that the test

samples deviate from the standard line (y=x) was then used to assess the closeness

between the actual proportions and estimated proportions of each class. The total distance

($\sum D$) for each class was also shown in each plot. The closer the test samples to the line

y = x, the better the estimated result will be. In the regression relationships observed in

the MLC model (Figure 21), a number of fractions of landscape classes are estimated as

either 0 or 1, especially for the commercial or industrial and transportation, which

indicates that the conventional "hard" MLC approaches are ineffective for mapping urban

internal structures, especially when using the coarse resolution image.

Fig. 21. Regression relationships for the 30 test samples between the estimated fraction using MLC and the "actual" fraction digitized from the IKONOS image

In contrast to the MLC method, the Linear SMA has largely alleviated the

extreme situation of having either 0% or 100% fractions. A much clear correlation can be

discerned between the estimated and actual fractions (Figure 22). However, the

regression line thus formed shift way from the standard line. As previously discussed,

such situation may be a result of the spectral similarity among urban landscape classes.

Although many researchers have found the SMA is an effective approach in

characterizing urban landscape (Lu and Weng 2004; Wu 2004), few endmembers (e.g.

three or four surface covers) were usually the cases in their studies. When more

endmembers were designated in urban area, this method will easily reach its limit due to

the spectral closeness and overlap. The correlation between the estimated fraction using the Partial-Fuzzy and actual fraction from the IKONOS is shown in Figure 23. Although the Partial-Fuzzy has an improvement over the MLC, most classes still have zero fractions in several test plots. Therefore, we can conclude that from the MLC to the Partial-Fuzzy method, there is some, but not enough, improvement for the urban landscape classification.
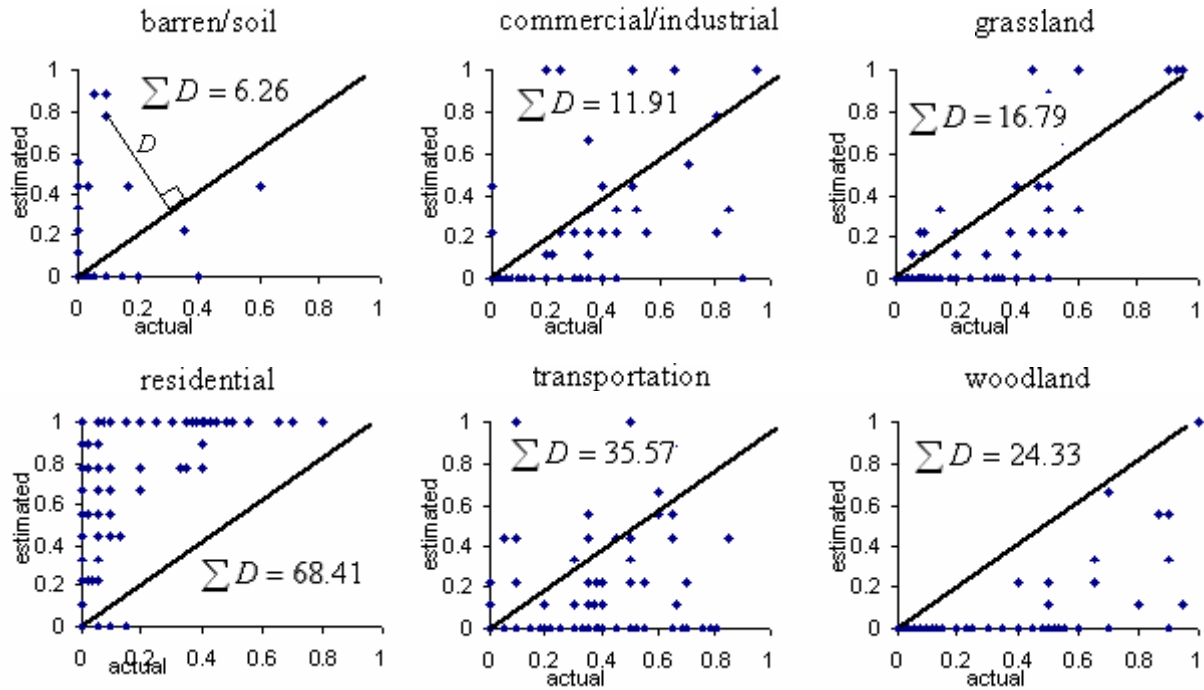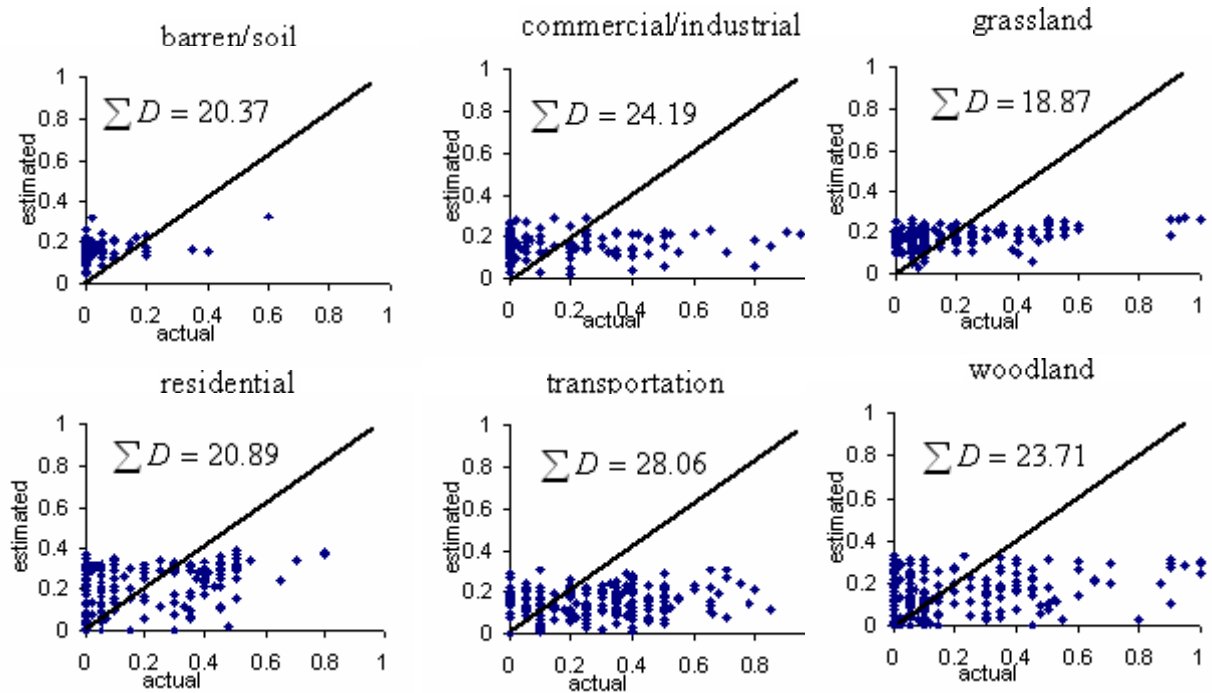

Fig. 22. Regression relationships for the 30 test samples between the estimated fraction using Linear SMA and the "actual" fraction digitized from the IKONOS image
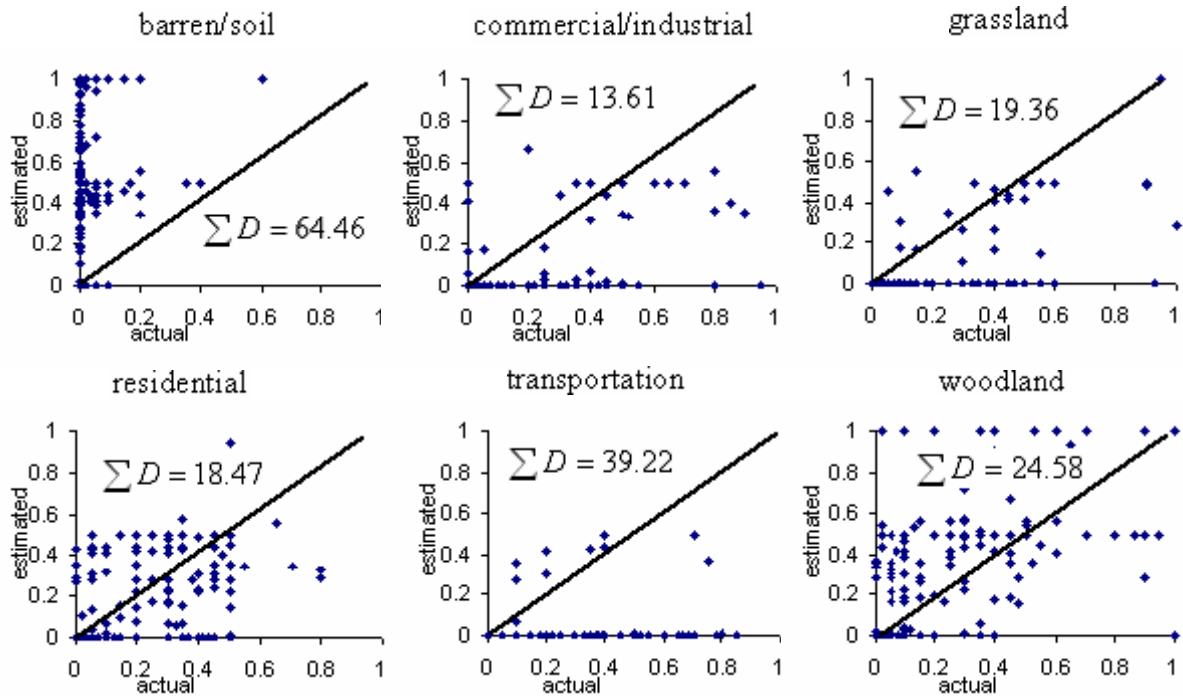
Fig. 23. Regression relationships for the 30 test samples between the estimated fraction using Partial-Fuzzy and the "actual" fraction digitized from the IKONOS image

Compared to the MLC, Linear SMA, and Partial-Fuzzy, Fuzzy-SMA has achieved a promising result with the smallest overall distance to the standard line (Figure 24). The best classification result using Fuzzy-SMA was observed in the barren/soil and residential area, with total distances as 1.80 and 6.60, respectively. The test samples were much closer to the standard line in the Fuzzy-SMA, indicating that the Fuzzy-SMA method gives the most accurate estimation of the landscape composition in this study area.
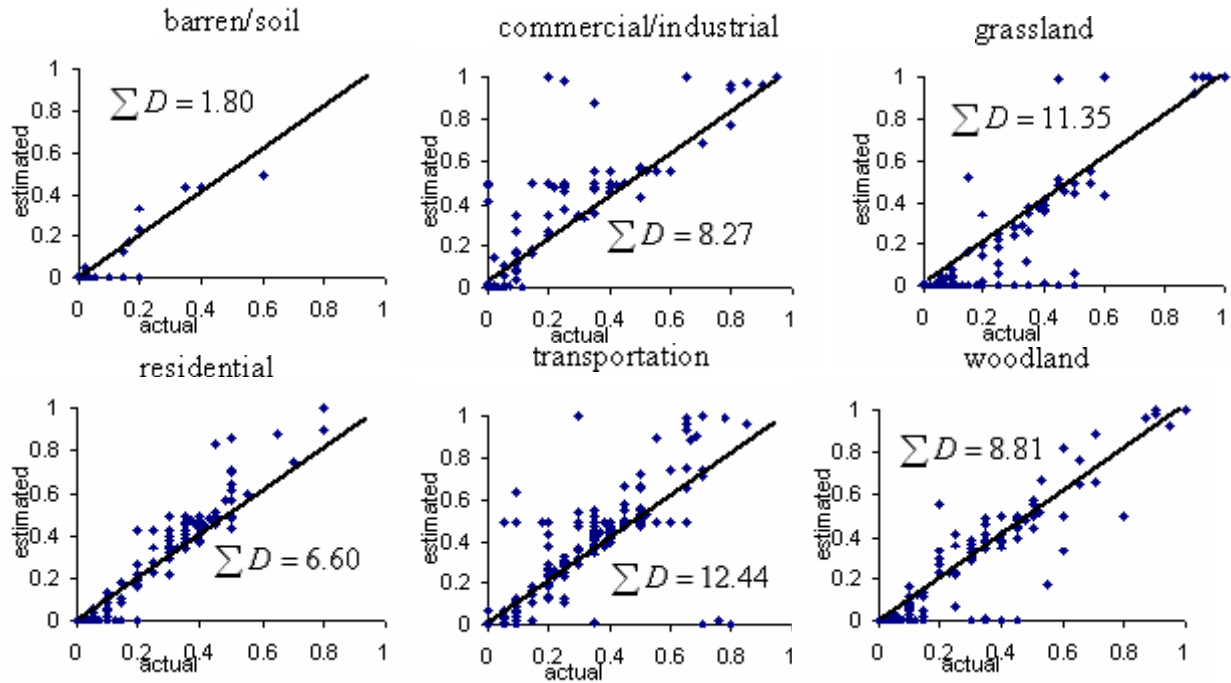
Fig. 24. Regression relationships for the 30 test samples between the estimated fraction using Fuzzy-SMA and the "actual" fraction digitized from the IKONOS image

Conclusion

Using moderate resolution satellite images, traditional "hard" classification is usually inappropriate for urban landscape analysis since multiple class memberships exist within one pixel. In this dissertation, we developed a Fuzzy-SMA method to estimate the subpixel fractions for urban landscape and the performance was compared to Linear SMA, Partial-Fuzzy, and MLC methods. The same sets of training and test samples were used in these methods based on IKONOS data. Previous studies proved that the SMA and

Partial-Fuzzy were effective in the urban classification, especially when addressing

fuzziness in the training and testing samples. However, the straightforward application of

Linear SMA was not satisfied when the number of endmembers goes over four using TM

images. Conversely, we propose to carry out SMA in the first stage and serve its result in

the calculation of fuzzy mean and fuzzy covariance, followed up with a fuzzy

classification to derive the final fractions. It turns out that this Fuzzy-SMA performs

consistently better than the MLC, Linear SMA, and Partial-Fuzzy.

For most subpixel classifications, endmember selection is still a critical step

towards the final success. Various unmixture methods are vulnerable with an

inappropriate identification of pure endmembers. This is particularly true without having

a higher spatial resolution reference image. Moreover, most SMA studies only choose

three or four endmembers, i.e. VIS models developed by Ridd (1995) and Wu and

Murray's SMA models (2003). This circumvents a finer characterization of the urban

landscape since it usually has various surface types.

Shade, caused by tall buildings or trees, is an inevitable part of urban area,

especially in the developed area. In this research, we classified it into barren and soil

instead of treating it as a separate endmember. This simplification adversely influences

modeling results, e.g., barren and soil is overestimated and commercial/industrial area is

underestimated. In the future research, we will incorporate the shade as a single

endmember to reduce the error within other classes.

Although the Fuzzy-SMA in this study achieved considerable improvements in

the urban landscape classification, the exact location of each endmember within one pixel

is still unresolved. To locate each endmember, we could incorporate the context

information from its surrounding pure pixels. How to combine this knowledge in a fuzzy classification to develop a more sophisticated soft method is still an interesting research topic.

CHAPTER VI

SPATIAL-TEMPORAL URBAN MODELING

Introduction

Increasing awareness about the importance of urban development and its effect on the environment is stimulating an improvement in the current methods to better understand and predict the evolution of urban landscapes (Turner 1987). One of the greatest challenges in designing effective models is that their performances are often limited by the availability of high-quality data. Modern remote sensing techniques provide rich and efficient data, however, the capability to interpret and use these data has not kept the pace with our ability to generate them. Moreover, considerable uncertainty continues to exist in choosing data sources with the appropriate spectral and spatial resolutions. In other words, a fundamental problem confronted by urban researchers is the difficulty in finding an effective model with the appropriate data to represent urban changes and predict its future patterns.

The motivation to model urban landscape dynamics arises from the process of examining where, what, and to what extent landscape change has occurred, and furthermore, the need to understand how and why the changes can occur (Weng 2002; Yang and Lo 2002). The Cellular Automata (*CA*) model, introduced by Tobler in 1979, is one of the most powerful spatial dynamics techniques used to simulate a complex urban

system (Batty and Xie 1994). The CA model allows researchers to view the city as a self-organizing system in which the basic land parcels are developed into various land use types. The model begins with a homogeneous cell-based grid and adjusts itself through the transition rules derived from a local spatiotemporal neighborhood. These make the CA model suitable to simulate complex and hierarchical structures since more unknown, immeasurable spatiotemporal variables can be incorporated and manipulated in this model. Wu (1998) combined the multicriteria evaluation (MCE) and GIS into the CA model to define the transition rules in a visualized environment. Li and Yeh (2000) extended the CA model to a constrained CA model within a grid-GIS system. Cecchini and Viola (1990) applied simple decision rules in the CA model to predict the complex, large-scale structure in the urban growth process. The advantages of the CA model in simulating urban spatial process and dynamics (Hillier and Hansen 1984; White and Engelen 1993) have been widely documented because the theoretical abstraction of the CA model and the practical constraints in the real world can be easily related (Batty and Xie 1994; Clarke and Hoppen 1997; Wu and Martin 2002).

Another critical advantage in CA simulation is the ability of the model to incorporate proper parameters or weights to model the alternative socioeconomic states in the model development (Clarke and Gaydos 1998; Li and Yeh 2000). With better computer techniques, the CA model is also able to explore more complex human behavior through defining different transition rules (Li and Yeh 2000; Wu and Martin 2002). However, the tension, between the simple local transition rule in CA models and the complex, unpredicted sociopolitical changes in urban landscapes, still remains. The

ability of most CA models to correlate socioeconomic factors with the urban
development process is still weak.

Modeling cities using CA is virtually impossible without using large-scale data
sources such as historical maps (Clarke and Hoppen 1997), historical land use records
(Batty and Xie 1994), urban land use maps (White and Engelen 1993), and remote
sensing images (Wu and Webster 1998). In this context, integrating high quality data into
models becomes important. Unfortunately, researchers gave more attention to the model
itself than the choice of appropriate data sources for the model. In this chapter, we
developed two sets of typical CA landscape models. One is based on the classification
result from the traditional Maximum Likelihood Classification, and the other is based on
the fuzzy classification result from the Fuzzy-SMA (Chapter V). Daqing's simulation is
only based on the hard classification result given the data availability and its practicality.
For Houston, the fuzzy membership will be incorporated into the CA model to represent
the urban development under the pixel level and to test whether the fuzzy logic function
can improve the defining transition rules in an urban CA model.

<u>Data Preparation</u>

Multi-temporal Hard Classification and Fuzzy Classification

The landscape maps for the model's development and calibration came from the
same data source as Chapter II. For Daqing City, only the hard classification results
(Figure 9B) are used in the model prediction. For Houston, we assembled landscape maps
from hard classification (MLC) and soft classification (Fuzzy-SMA) from 1976 to 2000.

Figure 25 shows the soft classification results using Fuzzy-SMA from 1976 to 2000 for Houston.
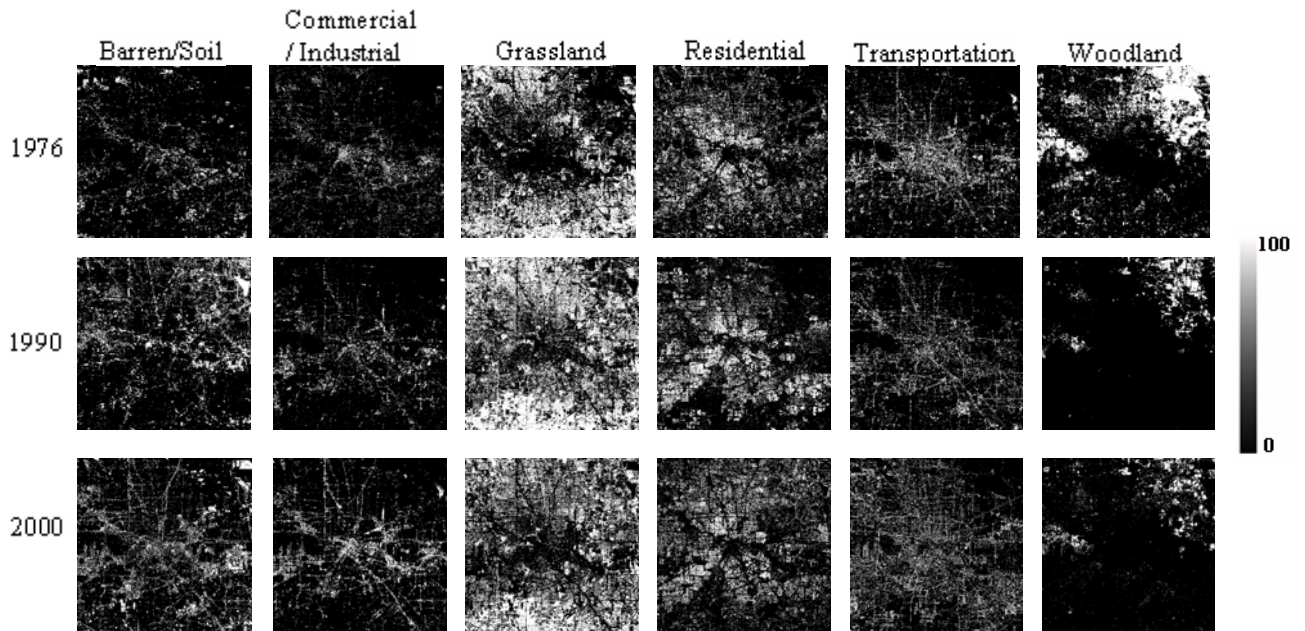
Fig. 25. Fraction images of Houston using Fuzzy-SMA in 1979 1990, and 2000

Ancillary Socioeconomic Data

We collected the socioeconomic data for Houston on the block level. Four socioeconomic variables were used: population density, house density, road density, and distance to highways. All data were collected from the official website of the U.S. Census Bureau (U.S. Census Bureau 2000).

Methodology

General Definitions of the CA Model

A CA model was developed to investigate the scenarios of future urban land transformations in two cities, Houston and Daqing. This model started on a 15-meter grid, initially rescaled from landscape maps for cities. The transition rules were applied to

all cells at the same time, and then the whole grid is updated at the annual iteration.

Transition rules and time are the real engines of change in the CA, which specify the

cell's behavior between time-step evolutions to determine the future status of cells. Four

factors control the behavior of the system: diffusion factor $N_{i,j}$, transition coefficient $M_{i,j}$,

socioeconomic factor $SE_{i,j}$, and current state of cell $S_{i,j}$. To determine the state of a cell

in a certain time period, the simulation function can be written as:

(6.1) $$S_{i,j}^{t+1} = a_N \times N_{i,j}^t + a_M \times M_{i,j} + a_{SE} \times SE_{i,j} + a_S \times S_{i,j}^t$$

Where $N_{i,j}^t$ denotes the diffusion factor regarding its neighborhoods, $M_{i,j}$ denotes

the Markov transition rules, $SE_{i,j}$ denotes the socioeconomic status of the cell and its

neighborhoods, and $S_{i,j}^t$ represents the cell's state at time t at the location (i, j). The

coefficients for these variables are calibrated through the Genetic Algorithm. The

calibration will be discussed in the next section.

For the self-organizing CA model, the first step is to define a way to represent the

neighborhood status in a two-dimensional grid. In this research, we adopted a

conventional 3×3 Moore's neighborhood (Figure 26) to identify and calculate the

diffusion factor $N_{i,j}^t$. The diffusion factor of the observed cell, therefore, directly relates

to the ratio of the observed class to its total amount of neighbor cells. The effect of

neighbors can be calculated as:

(6.2) $$N_{i,j} = \frac{n_{i,j}}{\sum n_{i,j}}$$

Where n_i is the total number of class i surrounding the observed cell j.
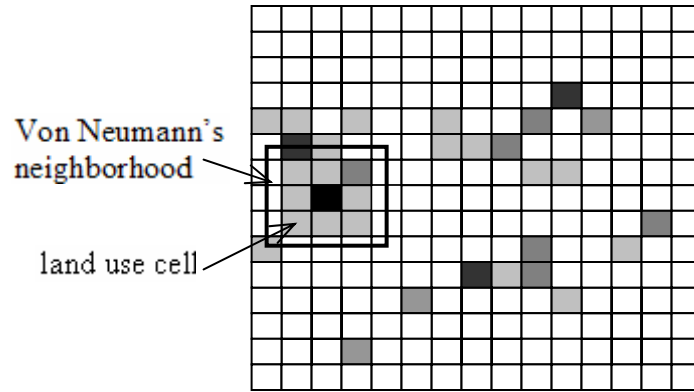
Fig. 26. The cellular space of simulated land use

The Markov transition was used to model landscape changes in understanding and predicting the behavior of complex systems (Baker 1989; Weng 2002; Fortin et al. 2003) using discrete state spaces. In this research, the Markov transition probabilities were derived based on two assumptions. First, we supposed that the landscape change was stochastic, as opposed to deterministic, and that the landscape distribution at a given time was the independent state of the Markov chain. Secondly, we assumed all cells in one block had the same transition probability. The transition probabilities P were derived from the landscape transitions occurring on the census block as:

$$(6.3) \qquad P_m(i, j) = N(i, j) / \sum_{i=1}^{n} n_{ij} \; ; \quad P(i, j) = \sum_{k=1}^{k} \frac{P_m(i, j)}{k * n_m}$$

Where $N(i, j)$ is the observed landscape change during the transition from state i to j, and n_{ij} is the number of years between time step i and time step j, and total years is m.

A third factor, the socioeconomic factor, includes four variables: population density, house density, road pattern, and distance to highways. We calculated the

population density (Figure 28a), house density (Figure 28b), road density (Figure 28c),

and the distance to highways (Figure 28d) for each block (Figure 27), and then assigned

those values to each cell located in the corresponding block. The difference of

socioeconomic values between the observed cell and the neighbors was used to measure

the socioeconomic factor as:

$$(6.6) \qquad SE_{i,j} = \frac{\sum_{n=1}^{n}\left(\dfrac{d_{i,j}^n - \min(d_{i,j}^n)}{\max(d_{i,j}^n) - \min(d_{i,j}^n)} \right)}{n}$$

Where $SE_{i,j}$ is the standardized score at location (i, j), $d_{i,j}^n$ is the different value in

four variables between the observed cell and its neighbors, and n is the total number of
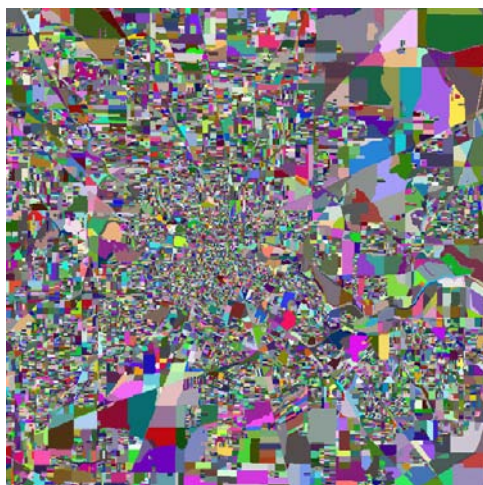
neighborhood cells.

Fig. 27. Census blocks in Houston
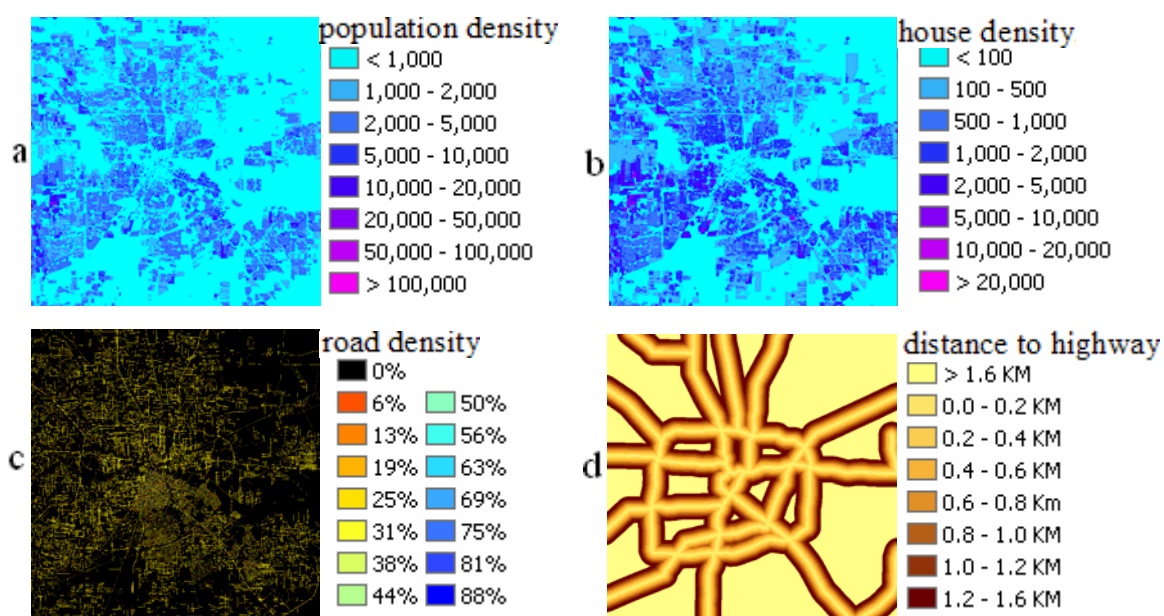
Fig. 28. A Visualization of the socioeconomic value in Houston

Obviously, different socioeconomic factors vary in the importance of their impact on urban land use and land cover change. In order to find the relative importance of each

socioeconomic variable, I invited 20 experts to assign weight to each variable using an

index ranging from 0-10, and then calculated the average value of their ratings (Table 12).

TABLE 12 INDEXES OF WEIGHTED THE SOCIOECONOMIC VARIABLES

Houston	Population Density	Road Density	Distance to Highway	House Density
Barren / Soil	3.67	3.50	3.40	4.00
Industrial / Commercial	8.80	8.17	8.42	7.33
Grassland	3.18	2.75	3.36	4.90
Residential	9.46	8.08	6.25	8.92
Transportation	7.66	9.00	8.95	6.82
Woodland	2.82	2.58	3.18	4.70

Note: The weight value range is from 0-10. The higher the weight, the more affect the socioeconomic variable will have on the urban land use class.

Model Calibration and Validation

A critical issue in the CA model is the provision of proper methods to calibrate

the CA model to find suitable parameter values. In this research, Genetic Algorithms (GA)

was used for the model calibration. The original GA was designed to optimize solutions

based on natural selection and natural genetics (Goldberg 1989). In general, the GA

operates on a set of coded individuals, and each one of them receives a fitness value

using the coding of their genes (Mertens et al. 2003) to produce a new population. The

individuals with a higher fitness value are more likely to be selected over others in the

evolutionary process and the new population is most likely to have a higher average

fitness than the old one (Bornholdt 1998).

Figure 29A depicts how the GA is used to calibrate the CA model. In this research,

the fitness is the discrepancy between the observed data and the model-predicted result.

The observed data is a set of maps that were classified from Landsat TM images on the

following dates: November 5, 1984; January 8, 1985; July 20, 1990; October 27, 1998;

October 6, 1999; and November 9, 2000. In order to calibrate four major factors in our

CA model, a code was obtained for each parameter by randomly selecting from a set of

encoded numbers (Figure 29B). The specific calibration process using the GA is as

follows: (1) randomly select an encoded parameter for each factor; (2) run the CA model

with these parameters; (3) compare the cells simulated in the CA model with the cells

located in the empirical maps; (4) choose the simulated data with the highest fitness as

the highest probability parents to generate the next generation.
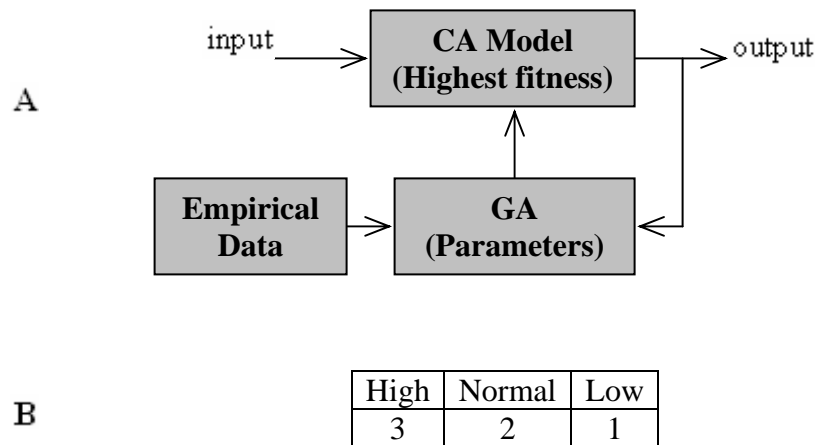
Fig. 29. The calibration for CA model using Genetic Algorithm. A: The calibration
process. B: The parameters values for the variables in the CA model

Validation of a landscape dynamics model is usually carried out by examining the

ability of the model to recreate the spatial pattern of landscape change, preferably at the

pixel level. In order to validate the model, the simulated output is compared to the

empirical map in the same year (Pontius JR et al. 2001). There are two stages in the

validation: a visual inspection and a quantitative evaluation. First, we rasterized the

simulated land use maps and compared them with the empirical maps. Due to the

availability of images and data, we adopted the classified image in 2003 as an empirical

map for Houston and a 2001 map for Daqing, respectively. A black-and-white image was

generated to denote the distribution of error. Meanwhile, the error matrix was built up to

show the accuracy of each class.

To validate the fuzzy model result, the IKONOS acquired in 2002 were utilized as

a ground reference. Two hundred test plots with 90×90 m^2 were selected randomly from

the simulated result and the digitized IKONOS image. Two types of error measurement,

root-mean-square error (RMSE) and systematic error (SE) were used to evaluate the

accuracy of the model's results.

$$(6.7) \qquad RMSE = \sqrt{\frac{\sum\limits_{i=1}^{N}(P_o - P_e)^2}{N}}$$

$$(6.8) \qquad SE = \frac{\sum\limits_{i=1}^{N}|P_o - P_e|}{N}$$

Where P_o is the percentage of each class of the model's simulated output, P_c is the

percentage of each class of the empirical map, and n is the number of classes. A

"successful" simulation occurs when the model's simulated output best matches the

empirical land-use map with the least RMSE and SE.

Results and Discussions

Initial prediction from the Markov Chain model

Although water is one of the most important landscape types in the landscape

pattern analysis, it is unlikely to have a significant change and effect on the overall

landscape pattern change. In this research, all water areas in three periods were masked

out first. Figure 30 shows the mask layer used for Houston and Daqing.
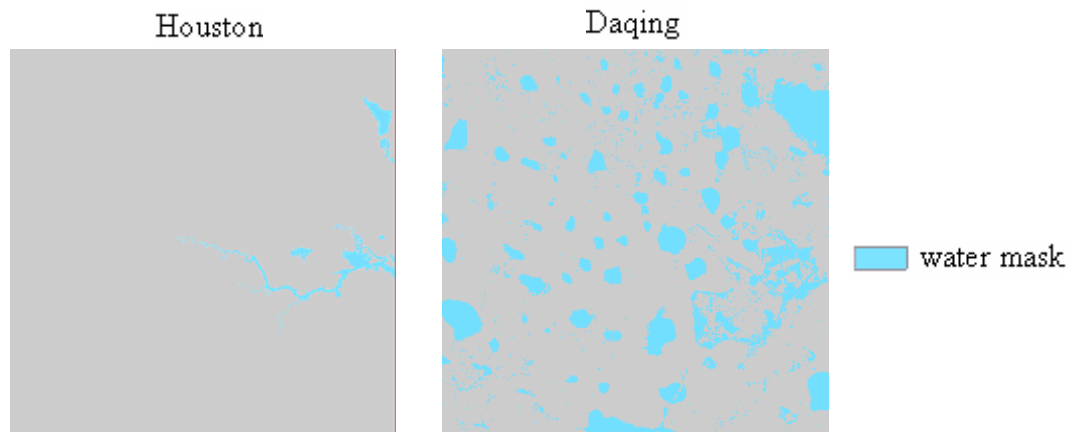
Fig. 30. The layer used to mask out the water for Houston and Daqing

Since our model is based on actual observation from the last 30 years for both

Houston and Daqing, the temporal transition probability matrix is calculated using

equation 6.3, by accumulating the periods 1979 – 1990 and 1990 – 2000 for Houston and

1976 – 1990 and 1990 – 2000 for Daqing. The yearly transition probability matrix is

shown in Table 12.

TABLE 13 YEARLY TRANSITION PROBABILITY (%) MATRIX FOR HOUSTON AND DAQING

Houston (1976 - 2000)	residential	industrial / commercial	grassland	woodland	barren / soil
residential	97.97	0.75	0.71	0.36	0.19
industrial/commercial	1.70	97.55	0.23	0.03	0.40
grassland	2.28	0.55	96.05	0.72	0.38
woodland	1.02	0.24	1.20	97.25	0.26
barren/soil	2.23	2.34	1.36	0.17	93.90

Daqing (1979 - 2000)	urban	agriculture	grassland	woodland	wetland	saline
urban	94.93	1.37	2.31	0.31	0.10	0.71
agriculture	0.70	94.57	3.25	0.83	0.13	0.42
grassland	1.15	2.33	94.55	0.58	0.26	0.86
woodland	0.40	3.69	3.06	92.07	0.41	0.22
wetland	0.40	1.05	1.05	1.29	95.32	0.29
saline	1.81	1.19	3.15	0.20	0.08	92.98

Using the yearly transition probability matrices in Table 12 and equation 1, we predicted the future pattern of Houston and Daqing and compared the simulated landscape maps to the empirical landscape map. From Table 13, we can easily see that the Markov Chain model is valid for predicting the future pattern, especially for the class which has obvious trends, e.g. the residential area in Houston: agriculture, woodland, and wetland in Daqing.

**TABLE 14 THE COMPARISON OF SIMULATED RESULTS WITH THE
EMPIRICAL MAP**

Houston (2003)	Residential	Industrial / Commercial	Grassland	Woodland	Barren/soil	
Empirical results	41.80	16.06	16.19	15.43	9.45	
Predicted results	42.47	17.22	20.34	14.26	5.02	
Daqing (2001)	urban	agriculture	grassland	woodland	wetland	saline
Empirical results	14.47	25.72	27.20	10.11	6.28	8.00
Predicted results	13.69	25.80	32.59	8.93	5.52	8.30

As a demonstration of the change pattern in these two cities, we generated future
landscapes for the years of 2010, 2030, and 2050 (Table 14). A notable trend is
discernible: the sprawl of the cities and oil fields will result in grasslands being cultivated
to agriculture or degraded to barren area. As sprawl continues, many woodlands and
wetlands will be converted into grassland, resulting in a more fragmented landscape.

**TABLE 15 THE PREDICTED RESULTS FROM THE MARKOV CHAIN
MODEL IN 2010, 2030, AND 2050**

Houston	Residential	Industrial / commercial	Grassland	Woodland		Barren/soil
2010	43.70	18.54	18.72	13.60		4.91
2030	45.28	20.96	16.53	12.21		4.80
2050	45.80	22.21	15.78	11.40		4.79
Daqing	Urban	Agriculture	Grassland	Woodland	Wetland	Saline
2010	14.02	24.75	31.53	8.42	5.18	8.28
2030	14.50	24.57	31.48	8.25	5.00	8.41
2050	14.64	24.55	31.49	8.21	4.94	8.44

Although the Markov Chain analysis is able to predict the general development
trends in these two cities, it is unable to simulate the exact location of the changes. The
CA model was then applied after that to detect the relationship between landscape change
and its location.

The CA Model Prediction Using the Hard Classification

This CA model took into account three factors: the Markov transition probability, socioeconomic variables, and each cell's neighbors. For Houston, we parameterized the Markov transition probability and socioeconomic variables on the block level. For Daqing, we only considered the global Markov transition probability and neighbor classes due to a lack of available data for Daqing. The distributions of landscape classes in these two cities are shown in Figure 31 and Figure 32.
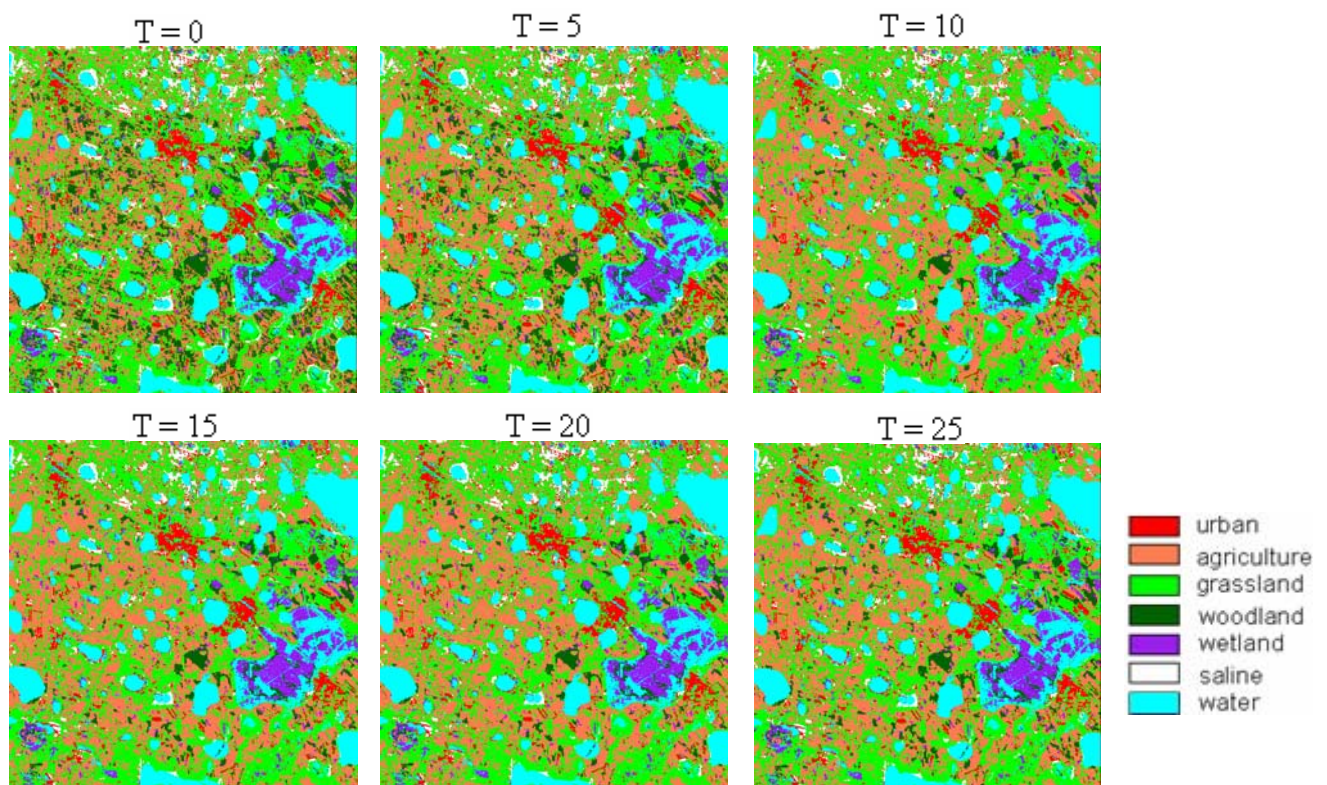
Fig. 31. The simulated landscape pattern for Daqing. Note: T means the number of years since 1979

Compared with the initial status of Daqing (T = 0), its development is not as obvious as it should be, especially in the urban areas. As shown in Figure 31, the future changes of Daqing were characterized by a loss of woodlands due to an increase in

cultivated agricultural lands. Without other ancillary socioeconomic data, the urban area

in Daqing has no observable sprawl. This might be the result of its small area and small

boundary in this class, and further indicates the importance of the behavioral aspect of the

CA model.
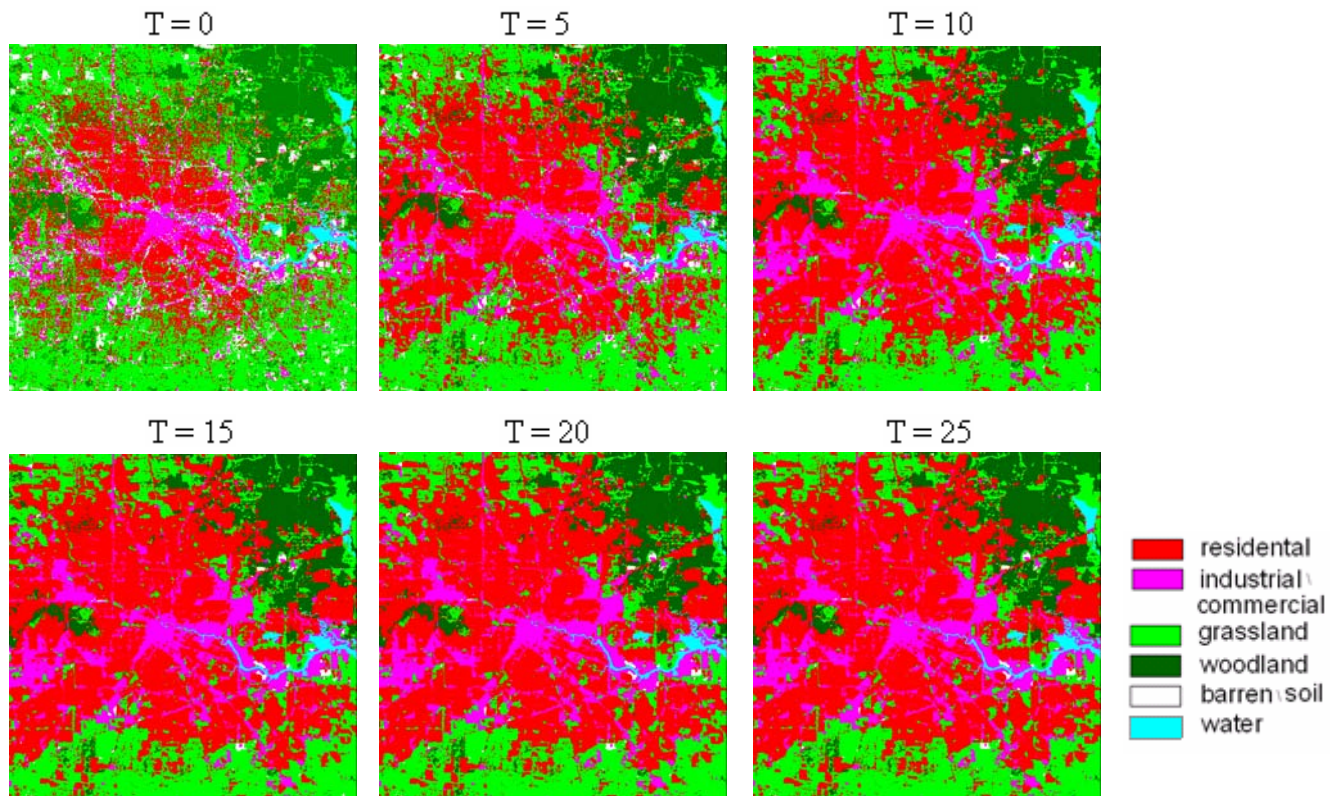
Fig. 32. The simulated landscape pattern for Houston. Note: T means the number of years since 1976

Figure 32 shows the initial state and the simulated patterns of Houston. With the

parameterized socioeconomic variables, Houston's model is much better than Daqing's.

The residential and industrial/commercial area obviously sprawled greatly from the center of city. The evident urbanization process was found in the suburban areas, which was driven by the economic development in Houston. In sum, the Houston results indicate that the ability of the CA spatial model to include the socioeconomic variables makes it especially suitable for simulating the evolutions of urban landscapes.
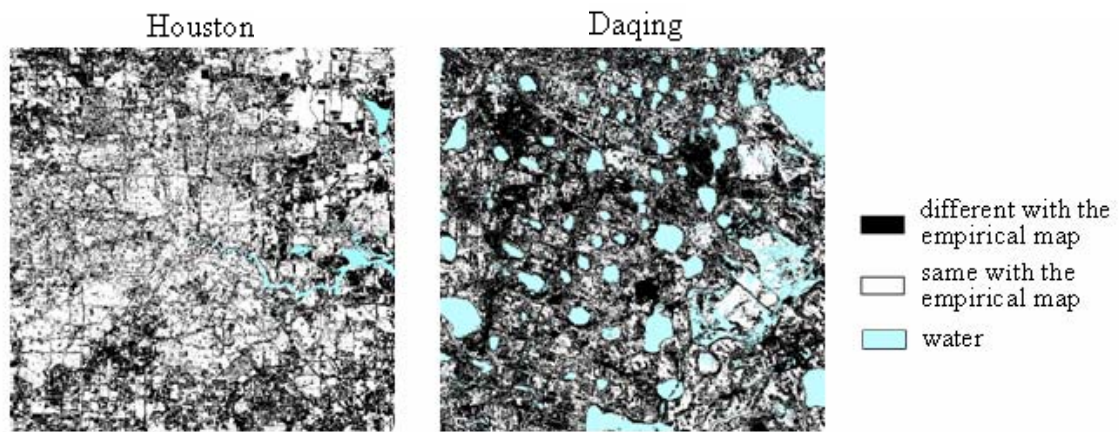
Fig. 33. Maps showing the differences between the predicted map and the empirical map

By comparing our predicted results with the empirical maps, we were able to show the errors found in the predicted map. Figure 33 illustrates the differences between two maps. Obviously, the predicted results for Houston matched the empirical maps much more closely than did the results of Daqing. In Houston, the most accurately predicted classes are residential and industrial/commercial areas. The majority of errors were found in the woodlands and barren/soil classes in the suburban area. It is easy to understand this result since the natural landscape will be least affected by the socioeconomic variable. In Daqing, most of the errors were found in urban areas. Since

only the relationship between neighboring cells was considered in the CA model of Daqing, this model has less feasibility when considering the human effect on the model development.

For further validation of the difference between the model's simulated and predicted results, the confusion matrix was developed and shown in Table 15. The value of user's accuracy and producer's accuracy represents the accuracy for each class. For example, in Houston, the best predicted class is the residential area and the worst predicted class is barren / soil. For Daqing, the agriculture performed best in all classes, while the woodland has the smallest value in accuracy. The analysis of the model validation certifies that the appropriate ancillary parameters are necessary for the CA model to derive a solid result. In fact, the value of the simulation approach lies in its exploratory nature, which enables the improvement of models by the use of additional variables.

TABLE 16 CONFUSION MATRIX AND THE MODEL VALIDATION FOR BOTH HOUSTON AND DAQING

				EMPIRICAL MAP				
	Houston	**Residential**	**Industrial / commercial**	**Grass-land**	**Wood-land**	**Barren / soil**	**User's Accuracy (%)**	**Producer's Accuracy (%)**
P	**Residential**	1756004	257388	230903	201696	175892	66.97	77.32
R	**Industrial/ commercial**	123890	467825	34540	7576	110447	62.86	54.56
E	**Grassland**	320672	109304	518946	209275	185157	38.63	59.60
D	**Woodland**	68802	15960	84838	419194	28620	67.90	50.02
I	**Barren/soil**	1688	6949	1544	357	7258	40.78	1.43
C								
T				Overall Accuracy (%): 59.30; **Kappa**: 0.43				

	Daqing	**Urban**	**Agriculture**	**Grass-land**	**Wood-land**	**Wetland**	**Saline**	**User's Accuracy (%)**	**Producer's Accuracy (%)**
E	**Urban**	125104	57382	67136	29579	4769	25271	40.46	17.21
S	**Agriculture**	246039	769932	494941	221726	29128	88788	41.61	57.05
U	**Grassland**	286168	397967	684850	196925	32807	229077	37.47	49.28
L	**Woodland**	19636	46507	45809	15558	21911	4673	10.10	3.09
T	**Wetland**	17387	58155	56673	25529	101491	10181	37.67	52.69
	Saline	125104	19638	67136	29579	2495	25271	18.77	6.54
				Overall Accuracy (%): 37.89; **Kappa**: 0.16					

CA Model Prediction Using the Fuzzy Classification

In this soft CA model, we calculated the average transition probability for each pixel using the fuzzy classification result for 1979, 1990, and 2000. The results of this fuzzy CA model are given in Figure 34 as proportion maps of each class. One of the innovative features of our soft CA model is the addition of information from the sub-pixel level. It is apparent that the short-term predictions are more reliable than the long term predictions. The difference between hard prediction and fuzzy prediction is primarily related to the transportation-based growth. Obviously, the fuzzy urban growth is visually presented as the expansion of residential areas and transportation. Taking in

road parameters and transportation landscape, most transportation-based growth is captured.
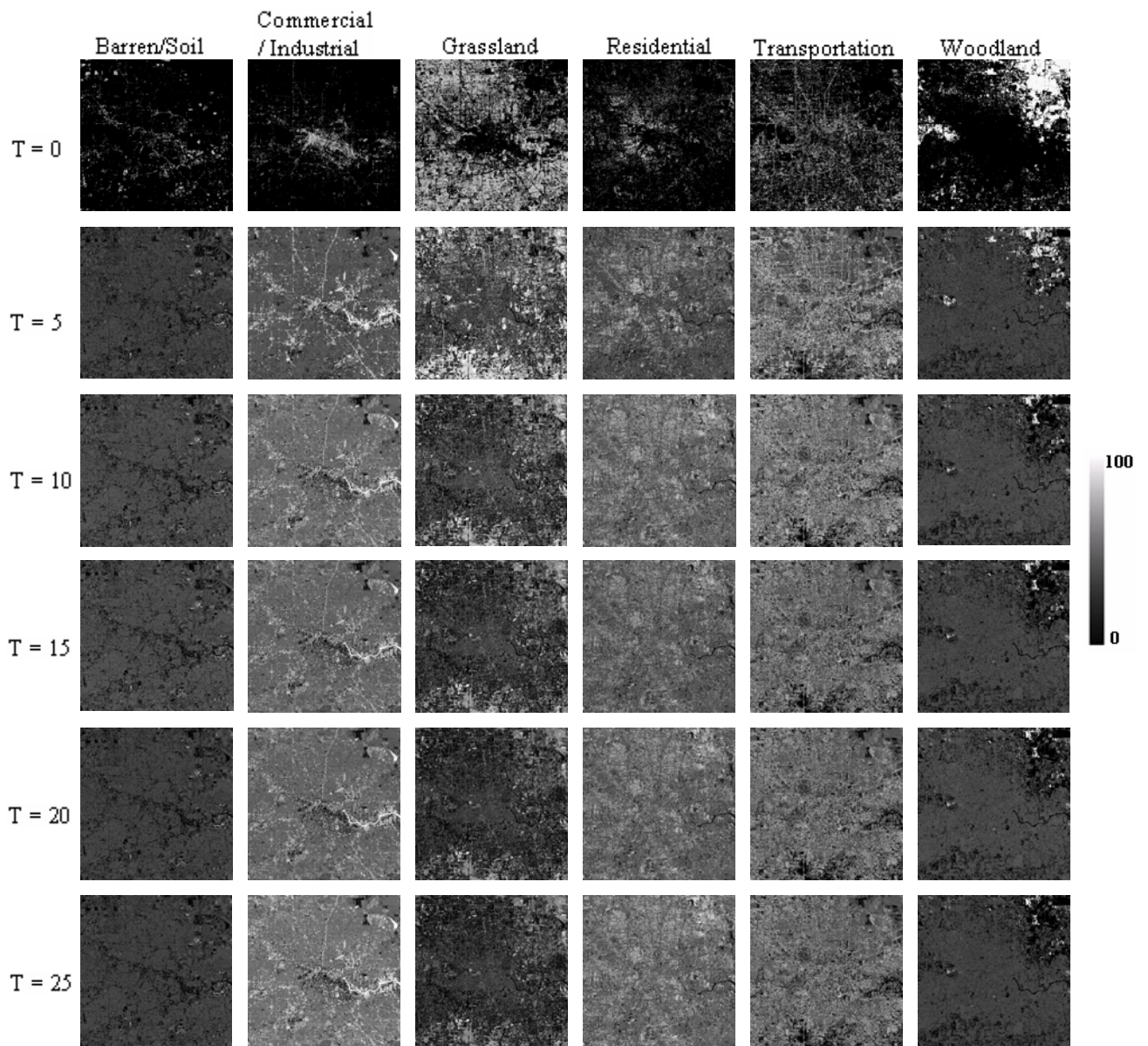
Fig. 34. The simulated landscape pattern of Houston from fuzzy classification

Another obvious difference is the fast shrinkage in grasslands and woodlands, especially the woodlands. Most likely, the outward expansion of residential or industrial/commercial area is the most predictable type of growth (Clarke and Gaydos

1998). Moreover, the homogenous landscapes, such as woodlands or grasslands, have less accuracy than the heterogeneous landscapes in the sub-pixel classification. When a new expansion runs in a repeated model, these classes could easily be turned into "an isolated island", a site gradually shrinking over the time during the urbanization process.
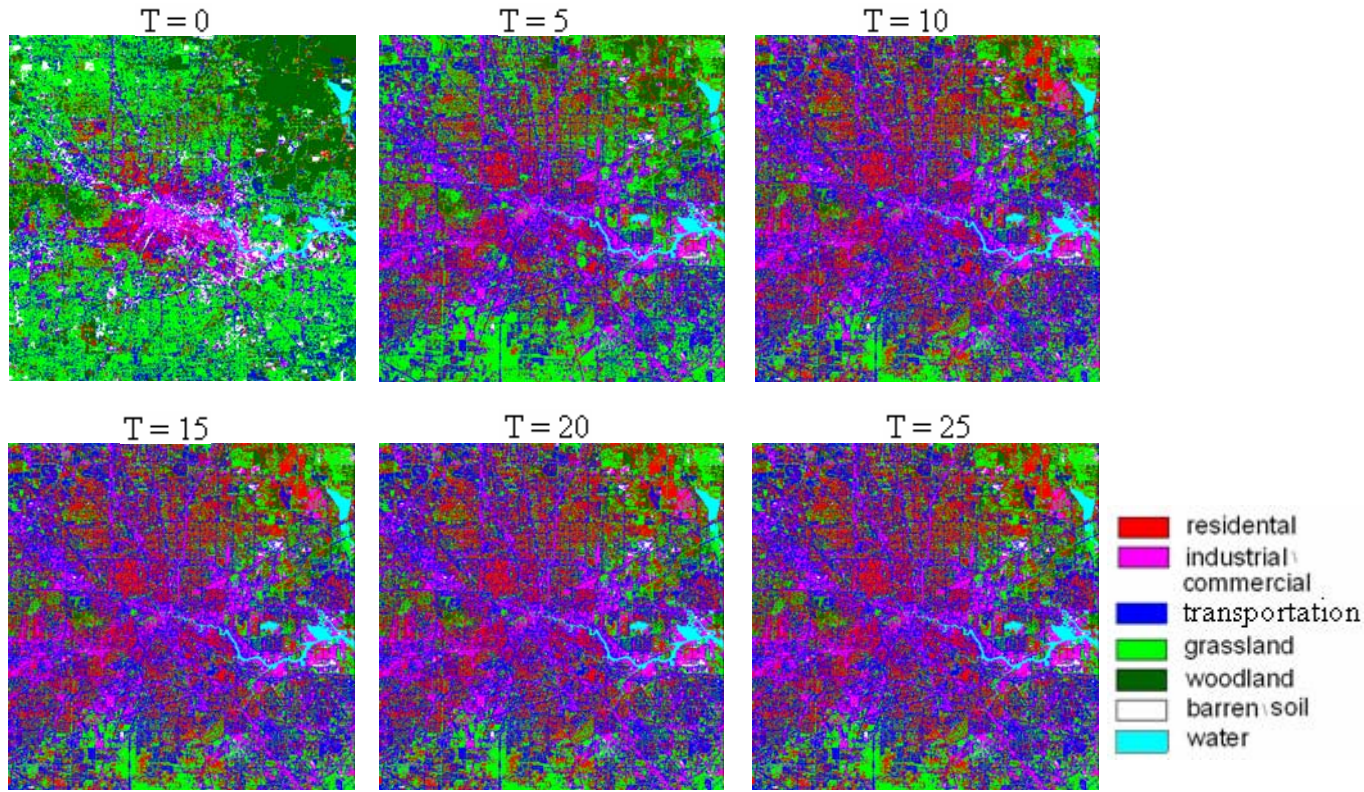
Fig. 35. Hardened map from the fuzzy CA model

The fuzzy prediction results were hardened and compared with the hard CA results. In Figure 35, we can see that the urban pattern is more heterogeneous than the one predicted from the hard classification. Furthermore, we can note that the evolution of urbanization direction in Houston partially followed the direction of the major highways. The woodlands and grasslands are gradually transformed into the residential areas. All these changes turned the downtown area into a more fragmented pattern.

A further comparison between the fuzzy prediction and hard prediction in the error assessment is shown in Table 17. The smaller the error indices are, the more accurate the predicted results. Fuzzy predictions have a smaller value in both SE and RMSE. The most improvement in the fuzzy prediction is in the residential and transportation areas which have a much smaller value in the SE. These results are easy to understand because the fuzzy classification always derives the proportion of the residential area, while the hard classification always classifies one whole pixel into residential areas. In the real world, it is impossible to find the house as big as one pixel of the Landsat image. The fuzzy prediction has a less accurate result in barren/soil and industrial/commercial areas. For the woodland landscape, even though it has a large error in the northeastern corner, the total error of fuzzy prediction is still smaller than the hard prediction. One possible reason for this is that the trees planted around the residential area were classified out as a proportion from the residential area and then this proportion was applied to the model.

TABLE 17 THE COMPARISON OF ERROR ESTIMATION OF FUZZY PREDICTION AND HARD PREDICTION

Error Assessment (%)		barren/soil	industrial / commercial	grassland	residential	transportation	woodland	Overall
Fuzzy prediction	SE	7.99	13.47	20.23	5.23	3.95	10.43	61.3
	RMSE	12.13	18.80	30.94	16.16	19.44	27.19	124.66
Hard prediction	SE	1.93	9.47	24.07	49.36	17.06	19.62	121.51
	RMSE	17.39	26.92	31.34	59.83	24.35	28.70	188.53

Conclusion

We use the spatio-temporal CA model of urban landscape patterns using multi-temporal TM and MSS imagery enabled us to characterize the internal structure of landscapes and monitor the landscape dynamics for both Daqing and Houston. For Houston, we also explored the potential of using socioeconomic variables to detect how human forces affect the urban spatial pattern. Moreover, incorporation of the fuzzy classification results for representing spatial information in a sub-pixel level proved to be a practical effective improvement for the CA model.

The CA model, coupled with the Markov transition probability, has indicated the capability of trend projection for landscape change. This spatio-temporal model provided not only the quantitative description of change in the past but also the direction and magnitude of change in the future. However, based on the experimental results and exploratory analysis, several limitations still exist within the current study:

o Since the modeling process involves the usage of data from multiple sources, the accuracy of prediction result will be closely related to the individual accuracy with in each type of data, especially for the fuzzy classification. The development of a robust method to incorporate data in different spatial resolution is still an interesting issue.

o Although the Markov transition probability is calculated on the census block level, it is stationary and unable to accommodate unpredictable influence variables, such as the climate, policy, and human disturbance. In addition, the pace of landscape change was not usually steady over the entire period of time.

o   In this research, we supposed the relation between socioeconomic factors, neighborhood effect, and Markov transition probability is linear and deterministic during the calibration. Finding an exact dynamic coefficient between them is still an intricate study in urban modeling.

o   For the fuzzy classification result, the exact location of proportion for each class still cannot be simulated in the CA model. An examination on the relationship between landscape change and its location is recommended for future research.

Currently, it is not fully conclusive that the CA model based on sub-pixel classification is inferior to the one based on pixel-level classification. It is still necessary to find more sophisticated methods applying to a series of varied landscapes to verify this new fuzzy model.

Most urban landscapes have been influenced by human disturbance, resulting in a heterogeneous mosaic of natural and human-managed patches that vary in size, shape, and arrangements (Turner 1989). The landscape responses to human disturbances are important: however, they are difficult to assess because the landscape-level simulation involves numerous challenging experiments and hypotheses in the development of models. These hypotheses are always assumed to make the model easier to manipulate, leading to a more homogenous pattern in the predicted result. Thus, it is necessary to relate the homogenous analysis in the model prediction with the heterogeneous analysis in the quantitative landscape method for a comprehensive understanding of the urbanization process. In conclusion, thess urban studies show that by incorporating more

spatial algorithms into the prediction of landscape change, more accurate long-term

landscape changes can be reproduced in the future.

CHAPTER VII

SUMMARY AND FUTURE WORK

Research Summary

The goal of this doctoral research is to develop a comprehensive comparison, both on pattern and process, between two typical economically petroleum-based cities using the extracted geospatial information from the satellite imagery. This study is structured to build a bridge between the remote sensing research, urban pattern characterization, and modeling of spatial processes. Although urban study is a very popular topic, the integrative perspective and methodology make this research unique since relatively little work has been reported in the literature to exploit two cities with similar economic history using both the remote sensing data, spatial analysis method, and urban landscape model.

Specifically, this dissertation began with the research problem, study objectives, and research design in Chapter I. In Chapter II, a variety of background material was presented on the urban geographical research. Given the development of complexity and variability in urban infrastructure, classic urban methods became unrealistic to represent and predict urban patterns and dynamics. The data requirements in the remote sensing application, as well as the classification methods, were discussed. Choosing well-suited imagery and methods for urban research is significant. Following the discussion of urban

remote sensing, a number of relevant quantitative methods on spatiotemporal urban patterns and processed were reviewed. Finally, current research challenges in combining the remote sensing with urban research were summarized.

Chapter III presented the detailed physical environment and socio-economical status of Houston in United States, and Daqing in China. Since the main economical backbones of these two cities are petroleum and petrochemical industries, they have a similar history and economic system even though they are under different socio-political system. Considering the study size and data availability, we collected Landsat imagery from the 1970s to 2000 as our main data sources.

Chapters IV, V, and VI are the core part of this dissertation. To distinguish the difference of landscape patterns between Houston and Daqing, a set of landscape ecology metrics with complementary ecological meaning were chosen in Chapter IV. This comparison of urban landscape patterns is of high importance not only because of the many applications for which they can be used, but also because the further research on the sub-pixel level is based on this pattern analysis. Obviously, Houston is a concentric-zonal pattern based on one central business district (CBD) while Daqing is a multiple-nuclei pattern. Based on the derived indices, a general trend of landscape change was revealed: Houston experienced the urban expansion by gradually replacing the grassland around the suburban area, whereas a mass of grassland and woodland was cultivated and taken over by agriculture and urban area in Daqing.

A combined fuzzy classification and spectral mixture analysis (Fuzzy-SMA) for urban landscape classification in Houston were presented in Chapter V. In addition to the urban land cover classes identified by the pixel-based classifier, the

industrial/commercial and the transportation classes were classified out to further refine the landscape classification in highly dense urban areas. To facilitate fuzzy classification fully, the training sample was decomposed into proportion in the pixel level using spectral mixture analysis (SMA) to calculate the fuzzy mean and fuzzy covariance. This fully-fuzzy classification approach produced a higher accuracy than the maximum likelihood classification, linear spectral mixture analysis, and partial fuzzy.

After the pattern analysis and image classification, we developed a CA model to monitor and predict the future spatial pattern for both Daqing and Houston in Chapter VI. The CA models, especially for the urban land use and land over, require the exploitation of image data in a span of time, at least ten to twenty years. Both the availability and quantity of data limit the feasibility of model development. Considering the feasibility, we only incorporated both the socioeconomic variables and fuzzy classification results in Houson's CA model. Obviously, the sub-pixel classification provides more detailed information for the CA model and also improves the model accuracy, especially for the residential and transportation areas.

<p style="text-align:center;"><u>Future Work</u></p>

A systematic analysis and comparison of two petroleum-based cities from multi-temporal satellite imagery have been developed in this doctoral research. I have shown how Houston and Daqing experienced a remarkable change in the last two decades and what is the possible change trend in the future. My methodology on the urban sprawl analysis, urban remote sensing, and urban modeling is not only applicable to the urban structure, but also to the other natural environments such as savanna or rainforest.

Building on the presented results here, there are a number of areas that can be further explored. In the future, I would like to develop a more advanced technique to combine the data fusion and fuzzy classification. Currently, the sub-pixel classification used only one data source, mostly Landsat images in this research. The fuzzy integral is an important technique for combining supplementary information from multiple remote sensing data sources. As with the traditional classification, the fuzzy classification is only based on the spectral information. More features can be explored in further research, such as spatial, textural, and contextual characteristics. Based on the segmentation techniques, these object-based features can then be used as additional data bands to the supervised fuzzy classification.

The socioeconomic parameters of the urban model deserve additional attention given their importance in governing the model. A more detailed and systematic parameter could provide useful information from the human dimension. My potential research could be an establishment of the site-particular parameters, not only about its current status, but also the change trend which is dominated by the urban dynamic process.

Developing more sophisticated function to model the uncertainty and ambiguity associated with the fuzzy classification and model development would prove quite interesting. Most landscape models lack an easy and accessible technique to perform a convincing model validation. Usually, most errors in the model come from two sources: input data or the model itself. Each of these accurate assessments would provide valuable insight into the influence of the data source on the model prediction. This information will likely have a significant influence on the model calibration and the chosen data for urban landscape models.

LIST OF REFERENCES

Aplin, P., P. M. Atkinson, and P. J. Curran. 1997. Fine spatial resolution satellite sensors for the next decade. *International of Journal of Remote Sensing* 18, no. 18: 3873-82.

Baker, W. L. 1989. A review of models of landscape change. *Landscape Ecology* 2: 111-133.

Bandyopadhyay, S. 2005. An efficient techniques for superfamily classification of Amino acid sequences: feature extraction, fuzzy clustering and prototype selection. *Fuzzy Sets and Systems* 152, no.1: 5-16.

Barr, S. and M. Barnsley. 1997. A region-based, graph-oriented data model for the inference of second order information from remotely-sensed images. *International Journal of Geographical Information Science* 11, no. 6: 555-56.

Barnsley, M. J. and S. L. Barr. 1997. A graph based structural pattern recognition system to infer urban land-use from fine spatial resolution Land-cover data. *Computers, Environment and Urban Systems* 21, no. 3/4: 209-25.

Bateson, C. A., G. P. Asner, and C. A. Wessman. 2000. Endmember bundles: a new approach to incorporating endmember. *IEEE Transactions on Geoscience and Remote Sensing* 38, no. 2: 1083-94.

Batty, M. and P. A. Longley. 1988. The morphology of urban land use. *Environment and Planning B* 15: 461-88.

Batty, M., P. A. Longley, and S. Fotheringham. 1989. Urban growth and form: scaling, fractal geometry, and diffusion-limited aggregation. *Environment and Planning A* 21: 1447-72.

Batty, M. and Y. Xie. 1994. From Cells to Cities, *Environment and Planning B* 21:31-48.

Bell, E. J. 1974. Markov analysis of land use change: an application of stochastic processes to remotely sensed data. *Socio-Economic Planning Sciences* 8: 311-16.

Berry, B. J. L. and E. H. Frank. 1970. *Geographic perspectives on urban systems: with integrated readings.* Englewood Cliff, New Jersey: Prentice-Hall, Inc.

Berry, B. J. L. and W. L. Garrison. 1958. A note on central place theory and the range of a good. *Economic Geography* 34, no. 2: 145-54.

Berry, B. J. L., J. W. Simmons, and R. J. Tennant. 1963. Urban population density: Structure and change. *Geographical Review* 53, no. 3: 389-405.

Berry, M. W., R. O. Flamm, B. C. Hazen, and R. L. MacIntyre. 1996. Lucas: A System for Modeling Land-Use Change. *IEEE Computational Science & Engineering* 3, no. 1: 24-35.

Bezdek, J. C., R. Ehrlich, and F. Full. 1984. FCM: Fuzzy C-means clustering algorithm. *Computers and Geosciences* 10, no.2/3: 191-203.

Blanchard, Raoul. 1917. Flanders. *Geographical Review* 4: 417-433.

Bornholdt, S. 1998. Genetic algorithm dynamics on a rugged landscape. *Physical Review E* 57, no. 4: 3853-60.

Boulding, K. 1956. *The image: Knowledge in life and society*. Ann Arbor, MI: University of Michigan Press.

Bourne, L. S. 1976. Monnitoring change and evaluation the impact of planning policy on urban structure: a marlov chain experiment. *Plan Canada* 16: 5-14.

Bosdogianni, P., M. Petrou, and J. Kittler. 1997. Mixture models with higher order oments. *IEEE Transactions on Geoscience and Remote Sensing* 35, no. 2: 341-53.

Breuste, J., H. Feldmann, and Q. Uhlmann. 1998. *Urban Ecology*. Berlin: Springer.

Brivio, P. A. and E. Zilioli. 2001. Urban pattern characterization through geostatistical analysis of satellite images. In *Remote Sensing and Urban Analysis*, eds. J. Donnay, M. J. Barnsley, and P. A. Longley, 39-54. New York: Taylor & Francis.

Burgess, E. W. 1925. The growth of the city: An introduction to a research project. In *The City*, eds. Park, R. E., Burgess, E. W. and R. D. Mckenzie, 44-62, Chicago: The Chicago University Press.

Carpenter, G. A., S. Gopal, S. Macomber, S. Martens, and C. E. Woodcock. 1999. A neural network method for mixture estimation for vegetation mapping. *Remote Sensing of Environment* 70, no. 2: 138-52.

Cater, P., W. E. Gardner, T. F. Smith, and M. J. Jackson. 1977. An urban management information service using Landsat imagery. *The Photogrammetric Record* 9, no. 50: 151-71.

Cecchini, A. and F. Viola. 1990. Eine Stadtbausimulation. *Wissenschaftliche Zeltschrift der Hochschule fur Architektur und Bauwesen* 36, no.1: 159-62.

Christaller, W. 1933. *Die Zentralen Orte in Sudlentschland*. Jena, E. Germany: G. Fischer.

Chrysoulakis, N. and C. Cartalis. 2002. Thermal detection of plumes produced by industrial accidents in urban areas based on the presence of the heat island. *International Journal of Remote Sensing* 23, no. 14: 2909-16.

Chuvieco, E. 1999. Measuring changes in landscape pattern from satellite images: short-term effects of fire on spatial diversity. *International Journal of Remote Sensing* 20, no. 12: 2331-46.

Clarke, K. C. and S. Hoppen. 1997. A self-modifying cellular automaton model of historical urbanization in the San Francisco Bay area. *Environment and Planning B* 24: 247-61.

Clarke, K. C. and L. J. Gaydos. 1998. Loose-coupling a cellular automata model and GIS: Long-term urban growth prediction for San Francisco and Washington/Baltimore. *International Journal of Geographic Information Science* 12, no. 7: 699-714.

Collins, W. G. and Aly. H. A. El-Beik. 1971. The acquisition of urban land use information from aerial photographs of the city of Leeds (Great Britain). *Photograprammetria* 27, no. 2: 71-92.

Cooley, C. H. 1894. The theory of transportation. *Publication of the American Economic Association* 9, no. 3: 113-48.

Cortijo, F. J. and N. P. De la Blanca. 1998. Improving classical contextual classifications. *International Journal of Remote Sensing* 19, no. 8: 1591-613.

Couclelis, H. 1992. People manipulate objects (but cultivate fields): beyond the raster-vector debate in GIS. In *Theories and methods of spatiao-temporal reasoning in geographic space, Lecture Notes in Computer Science*, eds. Frank, A. U., I. Campari, and U. Formentini. Berling, 65-66. Berlin: Springer.

Crowe, P. R. 1938. On progress in geography. *Scottish Geographical Magazine* 54: 1-19.

Cushnie, J. L. 1987. The interactive effect of spatial resolution and degree of internal variability within land-cover types on classification accuracies, *International Journal of Remote Sensing* 8: 15-22.

De Cola, L. 1989, Fractal analysis of a classified Landsat scene. *Photogrammetric Engineering & Remote Sensing* 55: 601-10.

De Cola, L. and N. N.-S. Lam. 1993. *Introduction to fractals in Geography*. Fractals in Geography, eds. N. N.-S. Lam, and L. De Cola, no. 1. Englewood Cliffs, New Jersey: Prentice Hall.

De Koning, H. J. Gerardus, P. H. Verburg, T. (A.) Veldkamp, and L. O. Fresco. 1999. Multi-scale modelling of land use change dynamics in Ecuador. *Agricultural Systems* 61: 77-93.

Donnay, J., M. J. Barnsley, and P. A. Longley. 2001. Remote sensing and urban analysis. In *Remote sensing and urban analysis*, eds. J. Donnay, M. J. Barnsley, and P. A. Longley, 3-18. New York: Taylor & Francis.

Douglas, I. 1994. Human settlements. In *Changes in land use and land cover: a global perspective*, eds. W. B. Meyer, and B. L. Turner II, 149-70. United Kingdom: Cambridge University Press.

Envi. 2000. *ENVI user's guide*. Boulder, Colorado: Research System Inc.

Erb, R. B. 1974. *ERTS 1 urban land use analysis.* Report for period July 1972 – June 1973, the ERTS-1 Investigation (ER-600), Vol. V, NASA TM X-58121.

Foody, G. M. 1992. A fuzzy sets approach to the representation of vegetation continua from remotely sensed data: an example from lowland health. *Photogrammetric Engineering & Remote Sensing* 58, no. 2: 221-25.

Foody, G. M. and D. P. Cox. 1994. Sub-pixel land cover composition estimation using a linear mixture model and fuzzy membership functions. *International Journal of Remote Sensing* 15, no. 3: 619-31.

Foody, G. M. 1996. Approaches for the production and evaluation of fuzzy land cover classifications from remotely-sensed data. *International Journal of Remote Sensing* 17, no. 7: 1317-40.

Foody, G. M. and M. K. Arora. 1996. Incorporating mixed pixels in the training, allocation and testing stages of supervised classifications. *Pattern Recognition Letters* 17, no. 13:1389-98.

Foody, G. M. 1997. Fully fuzzy supervised classification of land cover from remotely sensed imagery with an artificial neural network. *Neural computing & Applications* 5, no. 3: 238-47.

Forman, R. T. T. and M. Gordron. 1986. *Landscape Ecology*. New York: John Wiley & Sons.

Forster, B. 1983. Some urban measurements from landsat data. *Photogrammetric Engineering and Remote Sensing* 49, no. 12: 1693-707.

Fortin M-J, B. Boots, F. Csillage and T. K. Remmel. 2003. On the role of spatial stochastic models in understanding landscape indices in ecology. *Oikos* 102, no.1: 203-12.

Fox, Karl A. and T. K. Kumar. 1966. Delineating functional economic area. *Research and Education for Regional and Area Development*, eds. R. M. Wilbur and B. J. L. Berry. 1-55. Ames, IA: Iowa State University Press.

FRAGSTATS * ARC, 2004, Fragstats Manual: Definition and description of Class Metrics, Available online at: www.innovativegis.com/products/fragstatsarc/manual/manclass.htm#Patch %20Size%20Standard%20Deviation%20-%20PSSD(Accessed on May 12, 2004).

Frank, A. 1999. Tracing socioeconomic pattern of urban development: issues, problems and methods of spatio-temporal urban analysis. In *Geoinformatic and Socioinformatics*: Proceedings of International Symposium on Geoinformatics and Socioinformatics and Geoinformatcis Held in University of Michigan 19-21 June 1999, edited by B. Li, 1-12. Berkeley: UC Berkeley.

Frohn, R. C. 1998. *Remote sensing for landscape ecology, new metric indicators for monitoring, modeling, and assessment of ecosystems*. Florida: Lewis Publishers.

Fuller, D. O. 2001. Forest fragmentation in Loudoun County, Virginia, USA evaluated with multitemporal Landsat imagery. *Landscape Ecology* 16, no. 7: 627-42.

Galloway, M. 1975. Texture analysis using gray level run lengths. *Computers Graphics and Image Processing* 4, no. 1:172-99.

Gamba, P. and B. Houshmand. 2002. Joint analysis of SAR, LIDAR and aerial imagery for simultaneous extraction of land cover, DTM and 3D shape of buildings. *International Journal of Remote Sensing* 23, no. 20: 4439-50.

Ganas, A., E. Lagios, and N. Tzannetos. 2002. An investigation into the spatial accuracy of the IKONOS 2 orthoimagery within an urban environment. *International Journal of Remote Sensing* 23, no. 17: 3513-19.

Gardner, R. H., B. T. Milne, M. G. Turner, and R. V. O'Neill. 1987. Neutral models for the analysis of broad-scale landscape pattern, *Landscape Ecology* 1, no. 1: 19-28.

Geoghegan, J., L. Pritchard, Y. Orgneva-Himmelberger, R. R. Chowdhury, S. Sanderson, and B. L. Turner II. 1998. "Socializing the pixel" and "pixelizing the social" in land-use and land-cover change. In *People and Pixels-linking remote sensing and social science*, eds. D. Liverman, E. F. Moran, R. R. Rindfuss, and P. C. Stern. pp.51-69. Washing D. C.: National Academy Press.

Gilabert, M. A., F. J. Garcia-Haro, and J. Melia. 2000. A Mixture modeling approach to estimate vegetation parameters for heterogeneous canopies in remote sensing, *Remote Sensing of Environment* 72, no. 3: 328-45.

Goldberg, D. E. 1989. *Genetic Algorithms in Search, Optimization, and Machine Learning*. Addison-Wesley: Mass.

Gong, P. and P. J. Howarth. 1989. Performance analyses of probabilistic relaxation methods for land-cover classification. *Remote Sensing of Environment* 30, no. 1: 33-42.

Gong, P. and P. J. Howarth. 1990. The use of structural information for improving land-cover classification accuracies at the rural-urban fringe. *Photogrammetric Engineering & Remote Sensing* 56, no. 1: 67-73.

Green, N. E. 1957. Aerial photographic interpretation and the social structure of the city. *Photogrammetric Engineering* 23, no. 1: 89-96.

Griffith, J. A., C. C. Trettin, and R. V. O'Neill. 2002. A landscape ecology approach to assessing development impacts in the tropics: a geothermal energy example in Hawaii, *Singapore Journal of Tropical Geography* 23: 1-22.

Grove, J. M. and W. R. Burch. 1997. A social ecology approach and applications of urban ecosystem and landscape analyses: a case study of Baltimore, Maryland. *Urban Ecosystems* 1: 259-75.

Gurney, C. M. 1981. The use of contextual information to improve land cover classification of digital remotely sensed data. *International Journal of Remote Sensing* 2, no. 4: 379-88.

Gustafson, E. J. and G. R. Parker. 1992. Relationships between landcover proportion and indices of landscape spatial pattern. *Landscape Ecology* 7, no. 2: 101-10.

Haig, R. M. 1926. Towards an understanding of the metropolis. *Quarterly Journal of Economics* 40, no. 3: 402-34.

Haralick, R. M. 1979. statistical and structural approaches to texture. *Proceedings of the IEEE* 67, no. 6: 786-804.

Harris, Chauncy D. and Edward L. Ullman. 1945. The nature of cities. *Annals of the American Academy of Political and Social Science* 242: 7-17.

Harris, R. 1985. Contextual classification post-processing of Landsat data using a probabilistic model. *International Journal of Remote Sensing* 6, no. 6: 847-66.

Hassert, Kurt. 1907. Die Stadte: Geographisch Betrachtet. Leipzig: B. G. Teubner. Quoted in M. Aurousseau. *Recent Contributions to Urban Geogrpahy: A Reivew*. Geographical Review 14, 444-455, 1924.

Heckscher, Eli. 1949. *The effect of foreign trade on the distribution of income.* Readings in the Theory of International Trade. Eds. H. S. Ellis, and L. A. Mezler. 272-300. Philadephia: Blakiston Co..

Hepner, G. F., B. Houshmand, I. Kulikow, and N. Bryant. 1998. Investigation of the integration of AVIRIS and IFSAR for urban analysis. *Photogrammetric Engineering and Remote Sensing* 64, no. 8: 813-20.

Herbert, David T. and Colin J. Thomas. 1982. *Urban geography: A first approach*. New York: John Wiley & Sons.

Herbert, David T. and R. J. Johnson. 1979. *Geography and the urban environment: Progress in research and applications*. New York: John Wiley & Sons.

Herold, M., N. C. Goldstein, and K. C. Clarke. 2003. The spatiotemporal form of urban growth: measurement, analysis and modeling. *Remote Sensing of Environment* 86, no. 3: 286-302.

Herold, Martin. 2004. Remote sensing and spatial metrics for mapping and modeling of urban structures and growth dynamics. Ph. D. diss., University of California-Santa Barbara.

Herold, M., D. Roberts, M. Gardner, and P. Dennison. 2004. Spectrometry for urban area remote sensing – Development and analysis of a spectral library from 350 to 2400 nm. *Remote Sensing of Environment* 91, no. 3/4: 304-19.

Hillier, B. and J. Hanson. 1984. *The Social Logic of Space*. Cambridge: Cambridge University Press.

Hoyt, H. 1939. *The structure and growth of residential neighborhoods in American cities*. Washington, D. C.: Federal Housing Administration.

Houston city and meeting planners guide. 2004. Houston tourism. Available at: http://www.houston-guide.com/guide/info/infovisit.html. Accessed on Dec, 26, 2004.

IGBP (International Geosphere-Biophere Program, Committee on Global Change). 1988. *Toward an understanding of global change*. Washington, D.C: National Academy Press.

Imbernon, J. and A. Branthomme. 2001. Characterization of landscape patterns of deforestation in tropical rain forest. *International Journal of Remote Sensing* 22, no. 9: 1753-65.

Jensen, J. R. 1996. *Introductory digital image processing, a remote sensing Perspective*. 2d ed. New Jersey: Prentice Hall.

Johnson, K. 1994. Segment-based land use classification from SPOT satellite data. *Photogrammetric Engineering and Remote Sensing* 60, no. 1: 47-53.

Johnston, R. J. 1984. *City and Society: An outline for urban geography*. London: Hutchinson.

Ju, J.E., D. Kolaczyk, and S. Gopal. 2003. Gaussian mixture discriminant analysis and sub-pixel land cover characterization in remote sensing. *Remote sensing of Environment* 84, no. 4: 550-60.

Key to the city. 2001. Houston, Harris County, Texas. Available at: http://www.usacitiesonline.com/txcountyhouston.htm. Accessed on Dec, 26, 2004.

Klosterman, R. E. 1999. The What if? Collaborative Planning Support System. *Environmental and Planning B: Planning and Design* 26, no. 3: 393-407.

Kontoes, C. C., V. Raptis, M. Lautner, and R. Oberstadler. 2000. The potential of kernel classification techniques for land use mapping in urban areas using 5m-spaital resolution IRS-1C imagery. *International Journal of Remote Sensing* 21, no. 16: 3145-51.

Li, H. and J. F. Reynolds. 1993. A new contagion index to quantify spatial patterns of lanscapes. *Landscape Ecology* 8: 155-62.

Li, X. and A. G. O. Yeh. 2000. Modelling sustainable urban development by the integration of contrained cellular automata and GIS. *International Journal of Geographical Information Science* 14, no.2: 131-52.

Lichtenberg, E. R. 1985. The role of land quality in agricultural diversification. Ph.D. diss., University of California-Berkeley.

Liebrand, W. B. G., A. Nowak, and R. Hegselmann. 1988. *Computer Modeling of Social Process*. London: Sage Publications.

Lillesan, Thomas M., Ralph W. Kiefer, and Jonathan W. Chipman. 2004. *Remote sensing and image interpretation*. New York: John Wiley & Sons.

Linderman, M., J. Liu, J. Qi, L. An, Z. Ouyang, J. Yang, and Y. Tan. 2004. Using artificial neural networks to map the spatial distribution of understorey bamboo from remote sensing data. *International Journal of Remote Sensing* 25, no. 9: 1685-700.

Lo, C. P. and J. Choi. 2004. A hybrid approach to urban land use/cover mapping using Landsat 7 enhanced thematic amper plus (ETM+) images. *International Journal of Remote Sensing* 25, no. 14: 2687-700.

Longley, P. A., M. J. Barnsley, and J. Donnay. 2001. *Remote Sensing and urban analysis: A research agenda*. Remote sensing and urban analysis, ed. J. Donnay, M. J. Barnsley, and P. A. Longley, no.13. New York: Taylor & Francis.

Lopez E., G. Bocco, M. Mendoza, and E. Duhau. 2001. Predicting land cover and land use change in the urban fringe: A case in Morelia city Mexico. *Landcape and Urban Planning* 55, no. 4: 271-85.

Lösch, August. 1954. *The economics of location*. New Haven: Yale University Press.

Lu, D. and Q. Weng. 2004. Spectral mixture analysis of the urban landscape in Indianapolis with Landsat ETM+ imagery. *Photogrammetric Engineering & Remote Sensing*, 70, no. 9: 1053-62.

Macleod, R. D. and R. G. Congalton. 1998. A quantitative comparison of change-detection algorithms for monitoring eelgrass from remotely sensed data. *Photogrammetric Engineering & Remote Sensing* 64, no. 3: 207-16.

MacPhail, D. D. and L. F. Campbell, 1970. The El-Paso (Texas-New Mexico) study area: A comprehensive analysis of Gemini 4 and Apollo 6 and 9 space photography. Paper presented at AAG commission on Graphic Applications of Remote Sensing, East Tennessee State Univeristy, Johnson City.

Macleod, R. D., R. G. Congalton. 1998. A quantitative comparison of change-detection algorithms for monitoring eelgrass from remotely sensed data. *Photogrammetric Engineering & Remote Sensing* 64, no. 2: 207-16.

Madhavan, B. B., S. Kubo, N. Kurisaki, and T. V. L. N. Sivakumar. 2001. Appraising the anatomy and spatial growth of the Bangkok metropolitan area using a vegetation-impervious-soil model through remote sensing. *International Journal of Remote Sensing* 22, no. 5: 789-806.

Mandelbrot, B. B. 1967. How long is the coast of Britain? Statistical self-similarity and fractional dimension. *Science* 156: 636-38.

Marceau, D. J., P. J. Howarth, J. M. M. dubois, and D. J. Gratton. 1990. Evaluation of the gray-level co-occurrence matrix-method for land cover classification using SPOT imagery. *IEEE Transactions on Geoscience and Remote Sensing* 28, no. 3: 513-19.

Markham, B. L. and J. L. Barker. 1987. Thematic mapper bandpass solar exoatmospheric irradiances. *International Journal of Remote Sensing* 8, no. 3: 517-23.

Mas, J.-F. 1999. Monitoring land-cover changes: a comparison of change detection techniques. *International Journal of Remote Sensing* 20, no. 1:139-52.

Meer, F. V. D. 1999. Iterative spectral unmixing. *International Journal of Remote Sensing* 20, no. 17: 3431-36.

Mertens, K. C., L. P. C. Verbeke, E. I. Ducheyne, and R. R. De Wulf. 2003. Using genetic algorithms in sub-pixel mapping. *International Journal of Remote Sensing* 24, no.21: 4241-47.

Mesev, T. V., P. A. Longley, M. Batty, and Y. Xie. 1995. Morphology from imagery: detecting and measuring the density of urban land use. *Environment and Planning A* 27: 759-80.

Mesev, V., B. Gorte, and P. A. Longley. 2001. *Modified maximum-likelihood classification algorithms and their application to urban remote sensing*. Remote Sensing and Urban Analysis, eds. J. Donnay, M. J. Barnsley, and P. A. Longley, editors, p. 71-88. New York: Taylor & Francis Inc.

Mesev, Victor. 2003. *Remotely sensed cities: an introduction*. Remotely Sensed Cities, ed.V. Mesev, no. 1. New York: Taylor & Francis.

Metzger, J. P. and E. Muller. 1996. Characterizing the complexity of landscape boundaries by remote sensing. *Landscape Ecology* 11: 65-77.

Miller, A. B., E. S. Bryant, and R. W. Birnie. 1998. An analysis of land cover changes in the northern forest of new England using multitemporal Landsat MSS data. *International Journal of Remote Sensing* 19, no. 2: 245-65.

Moser, D. C. 1998. Diane Moser Properties. Abailable online at: http://www.texasbest.com/houston/geograph.html. Accessed on Dec, 26, 2004.

Muller, M. R. and J. Middleton. 1994. A markov model of land-use change dynamics in the Niagara Region, Ontario, Canada. *Landscape Ecology* 9: 151-57.

Myint, S.W. 2003. Fractal Approaches in Texture Analysis and Classification of Remotely Sensed Data: Comparisons with Spatial Autocorrelation Techniques and Simple Descriptive Statistics. *International Journal of Remote Sensing* 24, no. 9: 1925-47.

Nelson, R. F. 1983. Detecting forest canopy change due to insect activity using Landsat Mss. *Photogrammetric Engineering & Remote Sensing* 49, no. 9: 1303-14.

Ohlin, Bertil. 1933. *Interregional and international trade*. Cambridge, Mass: Harvard University Press.

Olsen, E. R., R. D. Ramsey, and D. S. Winn. 1999. A modified fractal dimension as a measure of landscape diversity. *Photogrammetric Engineering & Remote Sensing*, 59, no. 10: 1517-20.

O'Neill, R. V., J. R. Krummel, R. H. Gardner', G. Sugihara, B. Jackson, D. L. DeAngelis, B. T. Milne, M. G. Turner', B. Zygmunt, S. W. Christensen', V. H. Dale', and R. L. Graham. 1988. Indices of landscape pattern. *Landscape Ecology* 1: 153-62.

O'Neill, R. V., K. H. Riitters, J. D. Wichham, and K. B. Jones. 1999. Landscape pattern metrics and regional assessment. *Ecosystem Health* 5: 225-33.

Orville, R. E., G. Uffines, J. Nielsen-Gammon, R. Zhang, R. Ely, S. Steiger, S. Phillips, S. Allen, and W. Read, 2000. Enhancement of Cloud-to-Ground lightning over Houston, Texas. *Geophysical Research Letter* 28: 2597-600.

Palmquist, R. B. 1989. Land as a Differentiated Factor of Production: A Hedonic Model and its Implications for Welfare Measurement. *Land Economics* 65, no.1: 23-8.

Patton, D. R. 1975. A diversity index for quantifying habitat "edge". *Wildlife Socitey Bulletin* 3, no. 1: 171-3.

Petit, C., T. Scudder, and E. Lambin. 2001. Quantifying processes of land-cover change by remote sensing: resettlement and rapid land-cover changes in south-eastern Zambia. *International Journal of Remote Sensing* 22, no. 17: 3435-56.

Phinn, S., M. Stanford, P. Scarth, A. T. Murray, and P. T. Shyy. 2002. Monitoring the composition of urban environments based on the vegetation-impervious surface-soil (VIS) model by sub-pixel analysis techniques. *International Journal of Remote Sensing* 23, no. 20: 4131-53.

Pijanowski, B. C., D. T. Long, S. H. Sage, and W. E. Cooper. 1997. A land transformation model: conceptual elements, spatial object class hierarchies, GIS command syntax and an application to Michigan's Saginaw Bay Watershed. Sioux Fall, South Dakota: Land use modeling workshop, June 3-5, 1997.

Pontitus JR, R. G., J. D. Cornell, and C. A. S. Hall. 2001. Modeling the spatial pattern of land-use change with GEOMOD2: application and validation for Costa Rica. *Agriculture, Ecosystems and Environment* 85, no.1-3: 191-203.

Pontius JR, R. G., M. L. Cheuk. 2006. A generalized cross-tabulation matrix to compare soft-classified maps at multiple resolutions. *International Journal of Geographical Information Science* 20, no. 1: 1-30.

Priestnall, G., J. Jaafar, and A. Duncan. 2000. Extracting urban features from LIDAR digital surface models. Computers. *Environment and Urban System* 24, no. 2: 65-78.

Puissant, A., J. Hirsch, and C. Weber. 2005. The utility of texture analysis to improve per-pixel classification for high to very high spatial resolution imagery. *International Journal of Remote Sensing* 26, no. 4: 733-45.

Quattrochi, D. A. and M. K. Ridd. 1994. Measurement and analysis of thermal energy responses from discrete urban surfaces using remote sensing data. *International Journal of Remote Sensing* 15, no. 10: 1991-2022.

Quattrochi, D. A. and J. C. Luvall. 1999. Thermal infrared remote sensing for analysis of landscape ecological processes: methods and application. *Landscape Ecology* 14: 577-98.

Radeloff, V. C., D. J. Mladenoff, and M. S. Boyce. 1999. Detecting jack pine budworm defoliation using spectral mixture analysis: separating effects from determinants. *Remote Sensing of Environment* 69, no. 2: 159-69.

Read, J. M. and N. S-.N. Lam. 2002. Spatial methods for characterizing land cover and detecting land-cover changes for the tropics. *International Journal of Remote Sensing* 23, no. 12: 2457-74.

Richards, J. A. 1993. *Remote sensing digital image analysis: an introduction*. Berlin: Springer-Verlag.

Richard, J. A. and X. Jia. 1999. *Remote Sensing Digital Image Analysis: An Introduction*. 3d ed. Berlin: Springer.

Ridd, M. K. 1995. Exploring a V-I-S (vegetation-imprevious surface-soil) model for urban exosystem analysis through remote sensing: comparative anatomy for cities. *International Journal of Remote Sensing* 16, no. 12: 2165-85.

Roy, P. S. and S. Tomar. 2001. Landscape cover dynamics pattern in Meghalaya. *International Journal of Remote Sensing* 22, no. 18: 3813-25.

Schumaker, N. H. 1996. Using landscape indices to predict habitat connectivity. *Ecology* 77, no. 4: 1210-25.

Seto, K. C. and W. Liu. 2003. Comparing ARTMAP neural network with the maximum-likelihood classifier for detecting urban change. *Photogrammetric Engineering & Remote Sensing* 69, no. 9: 981-90.

Settle, J. J. and N. A. Drake. 1993. Linear mixing and the estimation of ground cover proportions. *International Journal of Remote Sensing* 14, no. 6: 1159-77.

Shaban, M. A. and O. Dikshit. 2001. Improvement of classification in urban areas by the use of textural features: the case study of Lucknow city, Utter Pradesh. *International Journal of Remote Sensing* 22, no. 4: 565-93.

Shimabukuro, Y. E. and J. A. Smith. 1991. The lease squares mixing models to generate fraction images derived from remote sensing multispectral data. *IEEE Transactions on Geoscience and Remote Sensing* 29, no. 1: 16-20.

Singh, A. 1989. Digital change detection techniques using remotely-sensed data. *International Journal of Remote Sensing* 10, no. 6: 989-1003.

Small, C. 2001. Estimation of urban vegetation abundance by spectral mixture analysis. *International Journal of Remote Sensing* 22, no. 7: 1305-34.

Small, C. 2003. High spatial resolution spectral mixture analysis of urban reflectance. *Remote Sensing of Environment* 88, no. 1/2: 170-86.

Small, C. 2004. The Landsat ETM+ spectral mixing space. *Remote sensing of Environment* 93, no. 1/2: 1-17.

Smith, R. H. T. 1965. Method and purpose in functional town classification. *Annals, Association of American Geographers* 55, no. 3: 539-48.

Song, C. 2005. Spectral mixture analysis for subpixel vegetation fractions in the urban environment: how to incorporate endmember variability? *Remote sensing of Environment* 95, no. 2: 248-63.

Statistic Bureau of Daqing. 2001. *Daqing Statistical Yearbook in 2001*. Heilongjiang: Heilongjiang Statistic Bureau.

Stefanov, W., L., M. S. Ramsey, and P. R. Christensen. 2001. Monitoring urban land cover change: an expert system approach to land cover classification of semiarid to arid urban center. *Remote Sensing of Environment* 77, no. 2: 173-85.

Stewart, W. 1994. *Introduction to the numerical solution of Markov Chains*. Princeton, New Jersey: Princeton University Press.

Tanaka, S. and T. Sugimura. 2001. A new frontier of remote sensing from IKONOS images. *International Journal of Remote Sensing* 22, no. 1: 1-5.

Tang, J. and S. Zhang. 2002. Application research of MODIS data in monitoring Landuse change. *Remote Sensing Technology and Application* (in Chinese) 17, no. 2: 104-7.

Tang, J., L. Wang, and S. Zhang. 2005. Investigating landscape pattern and its dynamics in Daqing, China. *International Journal of Remote Sensing* 26, no. 11: 2259-80.

Texas State Historical Association. 2002. Handbook of Texas online. Available at: http://www.tsha.utexas.edu/handbook/online/articles/view/HH/hdh3.html, Assessed on Dec, 26, 2004.

Theseira, M. A., G. Thomas, and C. A. D. Sannier. 2002. An evaluation of spectral mixture modeling applied to a semi-arid environment. *International Journal of Remote Sensing* 23, no. 4: 687-700.

Thompson, See Wilbur. 1965. *A preface to Urban Economics*. New York: John Wiley & Son, Inc.

Thunen, J. H. von. 1826. *Der isolierre staat in eziehung auf landwirtschaft und nationalokomie* (The Isolated State). Translated by C. M. Wartenburg. Oxford: Oxford University Press.

Tobler, W. 1979. *Cellular geography*. Philosophy in geography, eds. G. Gale, and S. Olsson. p. 379-86. Reidel: Dordrecht.

Tompkins, S., J. F. Mustard, C. M. Pieters, and D. W. Forsyth. 1997. Optimization of endmembers for spectral mixture analysis. *Remote Sensing of Environment* 59, no. 3: 472-89.

Turner, M. G. 1987. Spatial simulation of landscape changes in Georgia: a comparison of 3 transition models. *Landscape Ecology* 1, no. 1: 29-36.

Turner, M. G. 1989. Landscape ecology: the effects of pattern on process. *Annual Review of Ecology and Systematics* 20: 171-97.

Turner, M. G. 1990. Landscape changes in nine rural counties in Georgia. *Photogrammetric Engineering & Remote Sensing* 56, no. 4: 379-86.

Turner, M. G. and R. H. Gardner. 1990. Quantitative method in landscape ecology: an introduction. *Ecological Studies* 82, no. 1: 3-14.

U.S. Census Bureau. 2000. Your gateway to census 2000. Available at: http://en.wikipedia.org/wiki/Urbanization. Accessed on August 16, 2005.

Viedma, O. and J. Melia. 1999. Global change and plant diversity: Monitoring temporal changes in the spatial patterns of a Mediterranean shrubland using Landsat TM image. *Diversity & Distribution* 5: 275-93.

Waddell, P. 2002. UrbanSim: Modeling urban development for land use, transportation, and environmental planning. *APA Journal* 68, no. 3: 297-313.

Wang, F. 1990. Improving remote sensing image analysis through fuzzy information representation. *Photogrammetric Engineering & Remote Sensing* 56, no. 8: 1163-69.

Ward, D., S. R. Phinn, and A. T. Murray. 2000. Monitoring growth in rapidly urbanizing areas using remotely sensed data. *The Professional Geographer* 52, no. 3: 371-86.

Weber, A. F. 1899. *The growth of cities in the Nineteenth century: A study in statistics*, New York: Macmillan.

Welch, R. 1982. Spatial resolution requirements for urban studies. *International Journal of Remote Sensing* 3, no. 1: 139-46.

Wellar, B. S. 1968. *Generation of housing quality data from multiband aerial photographs.Technical Letter NASA-119*. Houston: NASA Manned Spacecraft Center.

Weng, Q. 2002. Land use change analysis in the Zhujiang Delta of China using satellite remote sensing, GIS and stochastic modeling. *Journal of Environmental Management* 64: 273-84.

White R. and G. Engelen. 1993. Cellular automata and fractal urban form:a cellular modeling approach to the evolution of urban land-use patterns. *Environment and Planning A* 25, no. 8: 1175-99.

Wikipedia, 2006. *Urbanization*. Available at: http://en.wikipedia.org/wiki/Urbanization. Accessed on August 16, 2006.

Willmott, C. J. and K. Matsuura. 2006. On the use of dimensioned measures of error to evaluate the performance of spatial interpolators. *International Journal of Geographical Information Science* 20, no. 1: 89-102.

Woodcock, C. E. and A. H. Strahler. 1987. The factor of scale in remote sensing. *Remote Sensing of Environment* 21, no. 3: 311-32.

Wu, C. and A. T. Murray. 2003. Estimating impervious surface distribution by spectral mixture analysis. *Remote Sensing of Environment* 84, no. 4: 493-505.

Wu, C. A. 2004. Normalized spectral mixture analysis for monitoring urban composition using ETM+ imagery. *Remote Sensing of Environment* 93, no. 4: 480-92.

Wu, F. 1998. Simulating urban encroachment on rural land with fuzzy-logic-controlled cellular automata in a geographical information system. *Journal of Environmental Management* 53, no. 4: 293-308.

Wu, F. and Webster C.J. 1998. Simulation of natural land use zoning under free-market and incremental development control regimes. *Computers Environment and Urban Systems* 22, no. 3: 241-56.

Wu, F. and D. Martin. 2002. Urban expansion simulation of Southeast England using population surface modelling and cellular automata. *Environment and Planning A* 34, no.10:1855-76.

Xu, B., P. Gong, E. Seto, and R. Spear. 2003. Comparison of gray-level reduction and different texture spectrum encoding methods for land-use classification using a panchromatic IKONOS image. *Photogrammtric Engineering & Remote Sensing* 69, no. 5: 529-36.

Yagoub, M. M. 2004. Monitoring of urban growth of a desert city through remote sensing: A1-Ain, UAE, between 1976-2000. *International Journal of Remote Sensing* 25, no. 6: 1063-76.

Yang, X. and C. P. Lo. 2002. Using a time series of satellite imagery to detect land use and land cover changes in the Atlanta, Georgia metropolitan area. *International Journal of Remote Sensing* 23, no. 9: 1775-98.

Yeates, M. 1965. Some factors affecting the spatial distribution of Chicago land values, 1910-1960. *Economic Geography* 41, no. 1: 55-70.

Yeh, A. G. and X. Li. 1997. An integrated remote sensing and GIS approach in the monitoring and evaluation of rapid urban growth for sustainable development in the pearl river delta, China. *International Planning Studies* 2, no. 2: 193-211.

Yuan, D. and C. Elvidge. 1998. NALC land cover change detection pilot study: Washington DC data experiments. *Remote Sensing of Environment* 66, no. 2: 166-78.

Zadeh, L. 1965. Fuzzy sets. *Information and contral* 8, no.3: 338-53.

Zha, Y., J. Gao, and S. Ni. 2003. Use of normalized difference built-up index in automatically mapping urban areas from TM imagery. *International Journal of Remote Sensing* 24, no. 3: 583-94.

Zhang, J. and G. M. Foody. 2001. Fully-fuzzy supervised classification of sub-urban land cover from remotely sensed imagery: statistical and artificial neural network approaches. *International Journal of Remote Sensing* 22, no. 4: 615-28.

Zhang, Q., J. Wang, X. Peng, P. Gong, and P. Shi. 2002. Urban built-up land change detection with road density and spectral information from multi-temporal Landsat TM data. *International Journal of Remote Sensing* 23, no. 15: 3057-78.

Zhao, Y., Z. Liu, and L. Xu. 1996. Changes of landscape pattern and its influence on environment in Dongling district, Shenyang city, China. *Journal of Environmental Sciences* 8, no. 1: 166-73.

Zheng, D., D. O. Wallin, and Z. Hao. 1997. Rates and patterns of landscape change between 1972 and 1988 in the Changbai Mountain area of China and North Korea. *Landscape Ecology* 12: 241-54.

Zhou, G., C. Song, J. Simmers, and P. Cheng. 2004. Urban 3D GIS From LiDAR and digital aerial images. *Computers & Geosciences* 30, no. 4: 345-53.

VITA

Junmei Tang was born in Jian City, Jiangxi province in China on October 3, 1978. She graduated from No. 1 high school of Jian, Jiangxi in 1995, and then entered Jiangxi Normal University. There she completed her Bachelor of Science degree in Geography Education. In 1999, she attended the graduate school at Changchun Geography Institution of Chinese Academic Science at Changchun, Jilin in China, where she completed a Master degree in Cartography and Geography Information Science. During this time, Junmei worked at the Institute as a graduate assistant and participated in some national research projects on the application of Remote Sensing & GIS in the environment monitor and resource management. Upon completion of her master's work in 2002, Junmei entered Texas State University-San Marcos in 2003, where she conducted the research for her Ph.D. She has been active in urban remote sensing and urban model for several years. Her doctoral research focused on the urban sub-pixel classification and the urban process model based on the fuzzy theory.

Permanent Address: #165 Jinggangshan Rd.

Jian, Jiangxi Province 343000

P. R. China

This dissertation was typed by Junmei Tang.